論文 / 著書情報
Article / Book Information

題目(和文)	ドーパミンの電気化学的研究
Title(English)	Electrochemistry of dopamine
著者(和文)	イリヤニ イスマイル
Author(English)	Iryane Binti Ismail
出典(和文)	学位:博士（工学）, 学位授与機関:東京工業大学, 報告番号:甲第10333号, 授与年月日:2016年9月20日, 学位の種別:課程博士, 審査員:北村 房男,菅野 了次,冨田 育義,稲木 信介,平山 雅章,大坂 武男
Citation(English)	Degree:, Conferring organization: Tokyo Institute of Technology, Report number:甲第10333号, Conferred date:2016/9/20, Degree Type:Course doctor, Examiner:,,,,,
学位種別(和文)	博士論文
Type(English)	Doctoral Thesis

Electrochemistry of Dopamine

Department of Electronic Chemistry

Tokyo Institute of Technology, Japan

Iryane Binti Ismail

Electrochemistry of Dopamine

CHAPTER 1

GENERAL INTRODUCTION

1.1 Introduction to dopamine (DA)

DA is an organic molecule that plays an important role in the brain and body. DA can also be found in plants and multicellular animal. In human, it is synthesized in the brain from its precursor, L-3,4-dihydroxyphenylalanine (L-DOPA) as shown in Fig. 1.1. DA acts as one of the main neurotransmitters in the central nervous system which consist of the brain and spinal cord. DA is also the precursor of other neurotransmitter such as norepinephrine (NE) [1]. DA, NE and also epinephrine (E) make up the catecholamine group where their basic molecular structures are the catechol and the monoamine moieties.

Research in DA is important since DA and its oxidation products have been studied due to their roles in the Parkinson's and Alzheimer's diseases [2]. In addition, the various possibilities of oxidation of catecholamine may be related to the biochemical theories of mental illness, particularly schizophrenia [3]. Due to the important roles of DA, we chose to investigate and clarify the electrochemical and chemical reactions of DA since the present studies on electrochemical reactions of DA are scarce. Besides that, the similarities of the structures (amino side chain and catechol) among L-DOPA, DA and NE will make it possible for the results of this study to be applied to the studies of L-DOPA or NE as has been done by other previous studies.

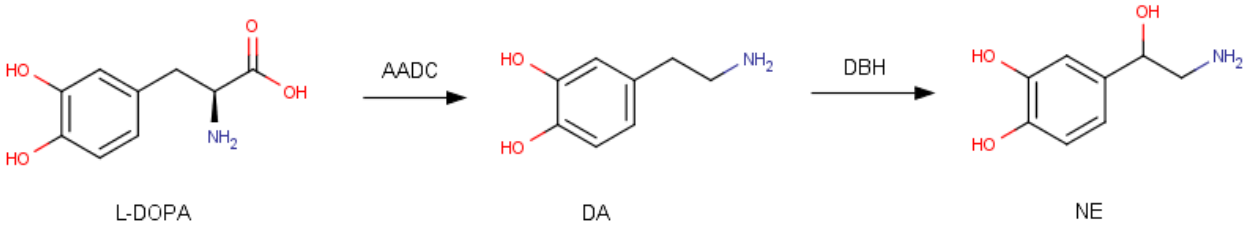

Fig. 1.1. Biosynthesis pathway of DA (AADC =Aromatic L-amino acid decarboxylase; DBH = Dopamine β-hydroxylase).

Previous research topics on DA can be divided into five general categories: (1) electrochemical behaviour of DA [2-5], (2) electrochemical behavior of DA on modified electrodes [6-13], (3) computational studies of DA [14-15], (4) electrode modification with DA [16-18] and (5) polymerized DA [19-20]. Some of these studies are also combined depending on purposes of study. Every research category was done based on their goals. Category (1) studies were done to investigate the DA oxidation effect of the disease related to the brain. The common goals of Category (2) studies are selective determination of DA or prevention from electrode fouling. Research in Category (3) provides data for comparison to experimental results. DA is used as electrode modifier in Category (4) and finally, Category (5) involves the polydopamine material research.

Since there are limitless data in the study of DA reaction on modified electrodes and also DA polymerized film study, in this research, we will focus on the electrochemical behavior of DA, specifically the electrooxidation pathways of DA. Then, DA will be covalently bound to the electrode surface. The study will be divided into 3 major parts; (1) Electrochemical study of DA and 5-MDA on bare electrodes, (2) Electrochemical study of DA and 5-MDA incorporated in

Nafion film and (3) Electrochemical study of DA and DA-PQQ composite covalently bound on chemically modified electrodes.

1.2 Background of research

1.2.1 Electrochemistry of DA

DA is known to react differently and produce different oxidation products based on the solution's pH it contained. Besides that, different concentrations of DA also affect the electrochemical reaction of DA where at high concentration of DA, faster chemical reactions (such as dimerization, polymerization) may occur which will affect the DA reaction [4,9,19]. Hence, more studies need to be conducted to understand the electrochemistry of DA and also the intracyclization reaction (ICR) of its oxidation product (dopamine o-quinone) in various pH.

In this study, the experimental results will be supported by the results obtained from the theoretical calculations where the HOMO/LUMO energies, Gibbs free energies of the electrochemical and chemical reactions (can be used to estimate the redox potential of electrochemical reaction) and natural charges of DA will be done. These data will be supporting the electrooxidation pathway of DA model we are proposing besides giving insights on the electrochemistry of DA.

The key reaction in electrooxidation pathway of DA is the intracyclization reaction of DA. Even though this reaction has an important effect on the reaction of DA, not much of this chemical reaction is known. To understand this, an analog of DA called 5-Methyldopamine (5-MDA) was synthesized in order to further confirm the intracyclization and its effects on the DA reaction. The name of 5-MDA is based on the nomenclature by IUPAC (Fig. 1.2). 5-MDA was

chosen as the DA analog in this study since there has been no report on 5-MDA and previous researches have dealt with 5-OHDA, 5-FDA and 4-MC (Fig. 1.3).

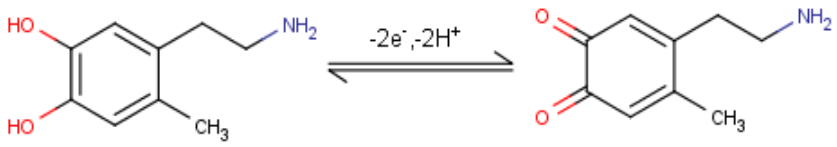

Fig. 1.2. Redox reaction of 4-(2-aminoethyl)-5-methylbenzene-1,2-diol (or 5-MDA).

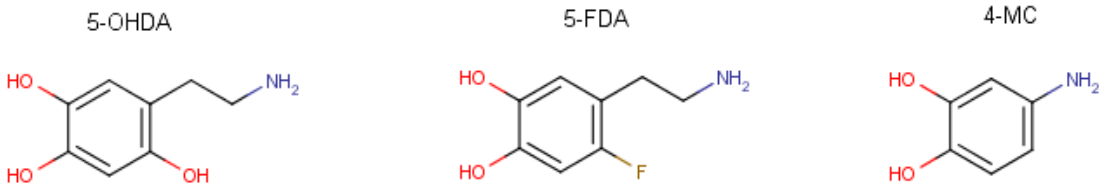

Fig. 1.3. Analogs of DA.

1.2.2 Electrochemical reaction of DA on Nafion-modified electrode

Nafion is a perfluorinated ion-exchange polymer material (Fig. 1.4). It is thermally and chemically very stable and insoluble in water. The dissociable proton allows incorporation of positively charged redox species via ion-exchange [21]. Due to these properties of Nafion, it is an attractive choice for selective determination of DA using modified electrodes. This is due to the electrostatic attraction between the negatively charged Nafion and positively charged DA. Thus, Nafion repels the negatively charged molecules which coexist in the biological sample (eg.,

extracellular brain fluid) such as ascorbic acid (AA). Besides that, Nafion film on electrode surface could protect the electrode from becoming insensitive due to the oxidation products of DA strongly adsorbed on the electrode surface (i.e, fouling).

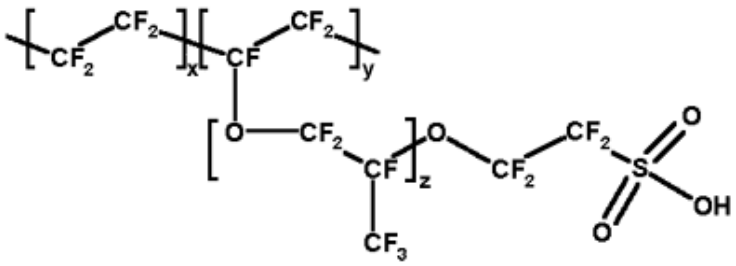

Fig. 1.4. Chemical structure of Nafion.

1.2.3 DA covalently bound to the electrode surface through diazonium reduction

Electrode modification through reduction of diazonium cation is a popular technique due to its simplicity of the technique and stability of the modified electrode [22]. The technique used in this study involves the in situ generation of diazonium cation by mixing aqueous acidic solution or acetonitrile with amine. Then, the aryl radical formed is reduced on the electrode surface through electrochemical reduction. This technique provides formation of strong bond between the surface and the bound molecule. In the post-functionalization step, the terminal groups of the stably attached organic layer can be functionalized further by attaching biomolecules, enzymes or neurotransmitters [23] for various applications. Thus, in this study, this technique will be used to attach *p*-benzoic acid (PABA) on the electrode surface and then DA will be attached to the PABA through amide bond coupling.

1.2.4 Electrohemical oxidation of ascorbic acid (AA)

In biological sample, DA coexists with other interference molecules such as AA (Fig. 1.5). Selective determination of DA is very important since AA can affect the measurement of DA in the sample. The AA oxidation peak potential is near to that of DA which made the two peak currents overlap and leads to difficulty in accurately quantifying DA. After the electrode modification, the peak potential could be shifted thus separating both peak currents [8,10,11]. Besides that, AA oxidation on bare electrode could result in the fouling of electrode and results in an inaccurate AA measurement. Also, it is expected that the oxidized form of DA (i.e, dopamine o-quinone) oxidizes AA. Thus, in this study, application of DA-modified electrode for AA measurement will be attempted.

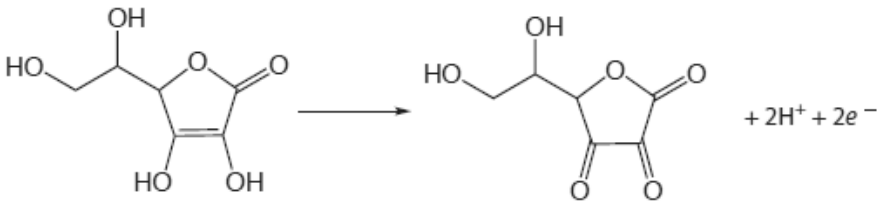

Fig. 1.5. Redox reaction of ascorbic acid (AA).

1.3 Objectives

There are two main objectives of this research:

1- To propose an extended DA electrooxidation pathways

2- To investigate electrochemistry of DA bound on chemically modified electrodes

1.4 Thesis outline

Chapter 1 briefly introduces DA and explains the current research on DA being studied by other researchers. The significance and aims of this research is also stated.

In Chapter 2, electrooxidation pathways of DA are researched. Electrochemistry of DA is studied through experimental and theoretical calculations. For the experimental part, effect of pH of solutions, time duration of holding oxidation potential, continuous potential cycles, potential scan rates and also concentrations on the redox reactions of DA is investigated. Calculations of Gibbs free energy, HOMO/LUMO energies and natural charges of DA are done. The results obtained from this chapter support the model of oxidation pathways of DA.

In Chapter 3, the electrochemical behavior of analogue of DA, 5-MDA is studied. The results of experiments and calculations obtained are slightly different from those obtained for DA due to the methyl group at C5 position of benzene ring of 5-MDA blocked the intracyclization reaction from occurring. The results from this chapter also supported the oxidation pathways of DA and the intracyclization reaction has been clarified.

Electrochemical reactions of DA and 5-MDA on Nafion modified electrode are examined in Chapter 4. DA and 5-MDA are incorporated into the Nafion film at acidic and neutral pH through electrostatic attraction between the negatively charged sulfonate groups in Nafion and positively charged amino groups in DA and 5-MDA. The comparison between incorporation behavior at different pH solutions and effect of methyl group in 5-MDA are discussed.

Electrodes are chemically modified with *p*-aminobenzoic acid (PABA) and DA through diazonium reduction technique and amide bond coupling in Chapter 5. Modification of GC and EPPG electrodes is done to compare the diazonium reduction on different carbon electrodes.

Electrochemistry of DA covalently bound to PABA-modified electrode was examined. Due to the DA strongly bound to the electrode, AA oxidization study is done with the modified electrodes.

Since the reduction of diazonium and amide bond coupling technique (as in Chapter 5) successfully bound DA stably on chemically modified electrodes, the same technique is applied in Chapter 6. However, the PABA is changed to *p*-phenylenediamine (PDA) and another redox active molecule is added which is pyrolloquinoline quinone (PQQ). In this chapter, PDA was attached on the electrode surface first. Next, carboxyl group of PQQ reacted with the amino group of PDA forming amide bond. Finally, amino group of DA formed amide bond with another carboxyl group of PQQ. This modified electrode's electrochemistry is studied in various pH, and the modified electrode is applied to AA oxidation.

In Chapter 7, all the results obtained from Chapters 2 to 6 are summarized.

1.5 References

[1] K.J. Broadley, *Pharmacology and Therapeutics* **125** (2010) 363-375.

[2] E. Herlinger, R.F. Jameson and W. Linert, *J. Chem. Soc. Perkin Trans*. **2** (1995) 259-263.

[3] D.C.S. Tse, R.L. McCreery and R.N. Adams, *J. Med. Chem*. **19** (1) (1976) 37-40.

[4] M.D. Hawley, S.V. Tatawawadi, S. Piekarski and R.N. Adams, *J. Am. Chem. Soc*. **89** (2) (1967) 447-450.

[5] J.A. Stamford and J.B. Justice, Jr., *Anal. Chem. News and Feat*. (1996) 359A-363A.

[6] S.H. DuVall and R.L. McCreery, *Anal. Chem*. **71** (1999) 4594-4602.

[7] H. Zhao, Y. Zhang and Z. Yuan, *Anal. Chim. Acta* **441** (2001) 117-122.

[8] C.R. Raj, K. Tokuda and T. Ohsaka, *Bioelectrochem*. **53** (2001) 183-191.

[9] S. Chen and K. Peng, *J. Electroanal. Chem*. **547** (2003) 179-189.

[10] C.R. Raj, T. Okajima and T.Ohsaka, *J. Electroanal. Chem*. **543** (2003) 127-133.

[11] P.R. Roy, T. Okajima and T. Ohsaka, *Bioelectrochem*. **59** (2003) 11-19.

[12] C.A Martinezz-Huitle, M. Cerro-Lopez and M.A. Quiroz, *Mat. Res*. **12** (4) (2009) 375-384.

[13] J. Huo, J. Li and Q. Li, *Mat. Sci. Eng*. **C33** (2013) 507-511.

[14] Y. Song, Y. Song, W. Xie and D. Shi, *Russian J. Phy. Chem*. **80** (9) (2006) 1467-1474.

[15] H. Mohammad Shiri, M. Ghaemi, S. Riahi and A. Akbari-Sehat, *Int. J. Electrochem. Science* **6** (2011) 317-336.

[16] J. Sun, J. Xu, H. Fang and H. Chen, *Bioelectrochem. Bioenerg*. **44** (1997) 45-50.

[17] B.D. Bath, H.B. Martin, R.M. Wightman and M.R. Anderson, *Langmuir* **17** (2001) 7032-7039.

[18] J. Ghilane, F. Hauquier and J. Lacroix, *Anal. Chem*. **85** (2013) 11593-11601.

[19] Y. Li, M. Liu, C. Xiang, Q. Xie and S. Yao, *Thin Solid Films* **497** (2006) 270-278.

[20] Y. Liu, K. Ai and L. Lu, *Chem. Rev*. **114** (2014) 5057-5115.

[21] C.R. Martin, I. Rubinstein and A.J. Bard, *J. Am. Chem. Soc*. **104** (1982) 4817-4824.

[22] S. Baranton and D. Belanger, *J. Phys. Chem*. B **109** (2005) 24401-24410.

[23] D. Belanger and J. Pinson, *Chem. Soc. Rev*. **40** (2011) 3995-4048.

CHAPTER 2

ELECTROCHEMICAL BEHAVIOUR OF DOPAMINE (DA)

2.1 Introduction

Electrochemical behavior of DA has been extensively studied due to its role in the Parkinson's and Alzheimer's diseases [1]. On the other hand, DA has also been studied extensively due to the versatile properties of the polymerized DA which can be applied in energy, environmental and biomedical fields [2]. In both fields, neuroscience and the non-neuroscience, the information about oxidation mechanism of DA is very important. However, the fundamental studies regarding the oxidation mechanism from DA to the polymerized DA are few, and more researches are needed to understand the oxidation mechanism in depth.

The DA oxidation mechanism is very complicated and has been proposed to follow an ECC (electron transfer-chemical reaction-chemical reaction) pathway [3]. This means that spontaneous chemical reaction will occur after the electrochemical reaction (oxidation reaction) takes place. The spontaneous chemical reaction such as intracyclization will lead to the formation of new molecules such as leucodopaminechrome and the DA oxidation products finally polymerized to form a melanin-like compound. In this chapter, we aim to clarify the intracyclization reaction (ICR) since no research has been done yet to understand this chemical reaction.

Many studies have been done on the redox reaction of DA and it is well known that it is a pH dependent reaction [3][4]. This means that any reaction of DA or its oxidation product will

occur depending on the solution's pH which leads to shift in the potential. Besides that, fast scan voltammetry technique (potential scan rate: $v \sim 400$ Vs^{-1}) has been employed when using carbon fiber electrode since the smaller the size of the electrode used, the faster it will take for the chemical reaction to take place [5] due to bigger surface area. The electrochemical measurement will take only 20 ms and the measurement can be repeated continuously without any interference from the DA oxidation products.

Hence, in this chapter, the DA redox reaction was examined under various experimental conditions: various pH solutions (pH 1-11), potential scan rates (200 - 10 mVs^{-1}), number of potential scans (up to 100^{th} scan) and concentrations (0.1, 1, 5 mM) to clarify their effects on the electrochemical behavior of DA. Quantum chemical calculations regarding DA and its related compounds was also done to further confirm the reactions of DA and to determine the accurate molecular structures of each molecules involved in the DA oxidation process. Finally, we aim to propose the oxidation pathways of DA.

2.2 Materials and methods

2.2.1 Materials

Dopamine hydrochloride (DA, 4-(2-aminoethyl) benzene-1,2-diol, hydrochloride salt), citric acid monohydrate, and trisodium phosphate dodecahydrate ($Na_3PO_4 \cdot 12H_2O$) were purchased from Kanto Chem. Co., Inc., Japan. Boric acid (H_3BO_3), hydrochloric acid (HCl) and sodium chloride (NaCl) were commercially available from Wako Pure Chem. Ind., Ltd., Japan. All the reagents were of analytical grade and used without any further purification. Universal buffer solutions (pH range from 3.25 to 10.41) containing 0.1 M (1 M = 1 mol dm^{-3}) NaCl were

composed of 0.005 or 0.050 M H_3BO_3 - citric acid - Na_3PO_4 three-component solutions. The solution of pH 1.69 was composed of 0.05 M HCl and 0.1 M NaCl. All the aqueous solutions were prepared using water purified by a Millipore Milli-Q system (MILLIPORE, Japan).

2.2.2 Electrochemical measurements

Electrochemical measurements were done with a three electrode system: Glassy carbon (GC) with 3 mm diameter was used as working electrode, platinum wire as counter electrode and $Ag|AgCl|KCl_{(sat)}$ as reference electrode. GC electrodes were polished on a polishing pad with 1 and 0.06 μm alumina powders and Milli-Q water. The polished electrode was sonicated in Milli-Q water for 10 min before any electrochemical measurements.

Cyclic voltammetry was carried out in Ar saturated aqueous electrolyte solution at room temperature (25 ± 1 °C) under various experimental conditions: pH from 1 to 11, DA concentrations at 0.1, 1 and 5 mM, potential scan rates from 500 to10 mVs^{-1}, potential scan number up to 100 cycles, potential scan direction towards positive or negative directions and potential holding time from 2 sec to 40 min.

2.2.3 Quantum chemical calculations

All quantum chemical calculations for optimized molecular structures of the most stable conformers regarding dopamine and its derivatives were carried out using the Gaussian 09 (revision D. 01) program package [6]. The structures of reactants and products involved in chemical and electrode processes in aqueous solution (Fig. 2.14, Tables 2.1 and 2.2, and Scheme 2.2) were optimized by the ωB97X-D [7] long-range corrected density functional calculation

including empirical dispersion with the 6-311G (d, p) basis set [8, 9], where the solvent effect on the structures of the reactants and products was taken into account using the reaction field calculation with the integral equation formalism of the polarizable continuum model (IEFPCM) [10] which is default of the used version of Gaussian program. The tight self consistent field (SCF) convergence criterion was used (this is default) and the ultrafine integration grid was specified (keyword is int=ultrafine) throughout the calculations. The molecular structures were optimized at closed shell singlet ground state and they were verified to be true minima by Hessian index. Gibbs free energies were used without scaling the frequencies. We select the ωB97X-D functional for this study because it often gives better results close to ab initio coupled-cluster with single and double (triple) excitations (CCSD(T)) among many functionals including B3LYP, CAM-B3LYP, M11, LC-BLYP, LC-ωPBE, LC-PBEPBE and so on for molecular structures and reaction energetics of small molecules (unpublished results). Including explicit water molecules is expected to improve the calculation of ionic state dopamine molecules, but the position and number of the water molecules about dopamines are arbitrary. Therefore, we decided to treat the water molecules implicitly in this study. Natural charges were calculated using NBO 6.0 program [11].

2.3 Results and discussion

2.3.1 pH dependence

Redox reaction of DA is dependent on pH as shown in Fig. 2.1(A). As pH increased, the $E°'$ decreased. $E_p{}^a{}_1$ ranges from +0.69 V (pH 1.69) to +0.08 V (pH 10.41) while $E_p{}^c{}_1$ ranges from +0.26 V (pH 1.69) to +0.16 V (pH 6.97). This is the redox reaction of dopamine / dopamine o-

quinone. There is no cathodic peak of DA at pH 8. This can be explained by the reaction between the o-quinone and anionic forms of catechol at pH 8 forming new compounds [12]. The possible reaction of DA at alkaline pH is shown in Scheme 2.2. Besides that, hydroxide attacks on the catechols are also possible [13]. The values of $I_p{}^a{}_1$ and $I_p{}^c{}_1$ are quite similar at pH below 7. The values of ΔE_p decreased with increasing pH meaning that electron transfer of the DA redox reaction become slower at acidic pH and redox reaction of DA becomes irreversible.

At low pH (pH < 3), the amine group of DA is protonated (Eqs. (1) and (2) in Scheme 2.1), so intracyclization reaction (ICR) does not occur. However, at high pH (pH > 3), the amine group of DA is not protonated, so ICR occurs. This means the amine group binds to the C5 position of the catechol group (Eq. 3 in Scheme 2.1) producing a new redox couple peaks which is the reaction of leucodopaminechrome / dopaminechrome (Eq. 4 in Scheme 2.1) at $E_p{}^c{}_2$ from -0.2 V to -0.44V (Fig. 2.1(B)). The pathway of DA oxidation has been proposed to be an ECC mechanism [3] rather than ECE mechanism since ECE mechanism cannot be determined experimentally (Amatore and Saveant, 1978). The $I_p{}^c{}_2$ value of leucodopaminechrome also increased as pH increased where the highest $I_p{}^c{}_2$ values are at pH 8.85 and 10.41. The $I_p{}^a{}_2$ of the dopaminechrome can only be seen clearly at pH 10.41 which was contributed by the fast chemical oxidation reaction as soon as the DA was dissolved in the alkaline solution. The plot of $E°'$ against pH for the redox couples of dopamine / dopamine o-quinone and leucodopaminechrome / dopaminechrome are shown in Fig. 2.2. The $E°'$ decreased with increasing pH. The slopes of the lines are near to 60 mV/pH which is expected for a 2e and $2H^+$ process (for pH lower than 7).

ICR do not occur at pH 5.11 according to Fig. 2.1(A) and 2.1(B). This is due to no leucodopaminechrome / dopminechrome redox couples peaks observed. However, Fig. 2.3

(curve b) shows that ICR can occur even at pH 5.11 after long potential holding time (i.e., 40 min). The redox peaks at about -0.1 V are due to the redox reaction of leucodopaminechrome / dopaminechrome couple. Furthermore, at pH 5.11, ICR was observed after continuous potential cycle as shown in Fig. 2.5. The redox peaks can be observed clearly at the 100^{th} cycle compared to the 1^{st} cycle. This means that ICR occurs at slower rate compared to at pH 6.97. At pH 6.97, the redox peaks of leucodopaminechrome / dopaminechrome couple became higher compared to the main redox peaks (i.e., the redox peaks of dopamine / dopamine o-quinone couple) (Fig. 2.3).

ICR would proceed largely when oxidative potential was hold at longer time (Fig. 2.4). When the oxidative potential is hold at long time, the DA is continuously being oxidized at the electrode surface thus ICR also occurs continuously forming leucodopaminechrome. At holding time of 1 min and above, the leucodopaminechrome / dopaminechrome peaks increased largely. This means that long potential holding allows longer time of chemical reactions to take place, forming higher amount of the oxidation products on the electrode surface. After 15 min, the leucodopaminechrome / dopaminechrome and dopamine / dopamine o-quinone peaks stabilized even when the holding time was increased to 30 min. This may be due to the dopamine and leucodopaminechrome adsorbed on the electrode surface thus blocking any possible reaction to take place. This is indicated by the same peaks height at longer potential holding time.

2.3.2 Potential scan dependence

The I_p and ΔE_p of DA depend on the potential scan rate as shown in Figs. 2.6(A) and 2.7(A). At pH 3.25, the higher the scan rate, the higher the I_p. Redox reaction of DA at pH 3.25 is irreversible where the ΔE_p value increased from 336 mV to 495 mV with increasing in scan

rates. However, the $E°'$ value does not depend on scan rates and remains constant at 0.43 V. The plot of I_p against $v^{1/2}$ show straight lines indicating that the electrode reaction of DA is diffusive behavior (Fig. 2.6(B)). Besides that, the ratio of I_p^c / I_p^a is in the range of 0.50 to 0.54 meaning that only half of the oxidized DA are being reduced to the reduced form of DA.

At pH 6.97 also, the higher the scan rate the higher the I_p. Redox reaction of DA at pH 6.97 also is irreversible. However, compared to the redox reaction of DA at pH 3.25, the ΔE_p at pH 6.97 is lower ranging from 186 to 82 mV with decreasing scan rates. The $E°'$ changed a little bit from 0.221 to 0.213 V for scan rates 500 to 10 mVs^{-1}. Plot of I_p against $v^{1/2}$ show straight lines indicating electrode reaction of DA is diffusive behavior (Fig. 2.7(B)). The I_p^c / I_p^a ratio is near to 1 at 500 mVs^{-1}. This indicates nearly all of the oxidized DA changed to reduced DA (Fig. 2.8(A)). However, at lower scan rate, the I_p^c / I_p^a ratio changes from 0.97 (at 500 mVs^{-1}) to 0.40 (at 10 mVs^{-1}). At low scan rate, the measurement time is longer. Hence, after the oxidation of DA, chemical reaction such as ICR may occur and most of the oxidized DA undergoes ICR forming leucodopaminechrome leading to low I_p^c of DA (Fig. 2.8(B)). This can be observed from the I_p^c of leucodopaminechrome / dopaminechrome peak is bigger than the I_p^c of dopamine / dopamine o-quinone at low scan rate (i.e., 10 mVs^{-1}).

Potential scan rate dependence was also examined at pH 5.11. Only the peak of dopamine / dopamine o-quinone can be observed from Fig. 2.9(A). No leucodopaminechrome / dopaminechrome peak observed meaning that no ICR occurs. However, at pH 5.11 as shown in Fig. 2.9(B), the peak of leucodopaminechrome / dopaminechrome was observed at low scan rates (i.e., 20 and 10 mVs^{-1}). At higher scan rates (500 to 50 mVs^{-1}), the leucodopaminechrome / dopaminechrome peak is not visible at all (Fig. 2.9(A)). Thus, it was found that ICR occurs from pH 5.11 and above.

2.3.3 Concentration dependence

The increase of DA concentration leads to increase of I_p^a and I_p^c as shown in Figs. 2.10a, 2.11a and 2.12a. Comparing only the 1st scan, the $E°'$ shifted positively from 0.24 V at 0.1 and 1 mM DA to 0.26 V at 5 mM DA. This means that 1 mM concentration did not affect the value of $E°'$ but at 5 mM concentration, the $E°'$ was affected since the $E°'$ values at 0.1 and 1 mM are the same (0.24 V). At low concentration of DA (0.1 mM), the CVs do not change much after 100th scan. The I_p^a and I_p^c of dopamine / dopamine o-quinone decreased a little bit but the I_p^a and I_p^c of leucodopaminechrome / dopaminechrome increased as can be seen from Fig. 2.10. At 1 mM DA, the I_p^a and I_p^c values of the dopamine / dopamine o-quinone redox couple decreased during the potential cycling and no clear I_p^a peak can be observed at the 100th scan. The E_p^c of leucodopaminechrome / dopaminechrome shifted negatively. At 5 mM concentration, no peak can be seen after 100th scan. The higher the concentration of DA, the more changes of CV can be observed. This may be because at higher DA concentration, polymerization and dimerization reactions are faster compared to lower DA concentration. That is why concentration of 0.1 mM was recommended to reduce the dimerization effect on the DA redox reaction [3].

After the continuous potential scans in solutions containing the dissolved DA, the scanned electrodes were washed with deionized water and scanned in a new buffer solution (pH 6.97) without any DA (Fig. 2.13). At 0.1 mM DA, negligible amount of DA adsorbed on the electrode surface (Fig. 2.12a). However, at 1 mM and 5 mM DA, broad peak were observed (Fig. 2.13(B), 2.13(C)) due to the adsorption of the polymerized products from DA.

2.3.4 Quantum chemical calculations

Comparison between the experimental and calculated $E°'$ values is shown in Table 2.1. Even though the calculated values differs a little compared to the experimental values, it confirms the intracylization reaction has taken place after the DA oxidation reaction from the calculated values of leucodopaminechrome / dopaminechrome at approximately -0.167 V. The values of HOMO for DA, leucodopaminechrome and 5,6-dihydroxyindole are higher than its LUMO energy indicating that they are nucleophiles. However, DA has higher HOMO energies compared to other compounds suggesting its tendency to donate electron, hence the intracyclization occurs, giving rise to the new and more stable compound called dopaminechrome. Furthermore, the negative value of ΔG confirms the spontaneity of chemical reactions such as intracyclization reaction at -23.71 kcal/mol and rearrangement at -13.74 kcal/mol (Table 2.2). Intracyclization will not occur if the amine group is protonated (at pH 3.25) since high energy ($\Delta G > 0$) is needed for the intracyclization reaction to occur. The natural charge shown in Fig. 2.14 shows the possible position for the amine group (electron rich) to attach to the benzene ring (electron deficient). Since the C5 position has lower charge, the higher charge of amine group bind to the C5 in a process which is called the Michael addition reaction.

2.4 Conclusion

Dopamine undergoes an ECC reaction where dopamine is oxidized into dopamine o-quinone leading to spontaneous chemical reactions producing leucodopaminechrome which then oxidized into dopaminechrome. The leucodopaminechrome may also react with the oxidized dopamine regenerating dopamine and forming dopaminechrome. This reaction pathway occurs at

pH 6 and above. At pH 5, different DA behavior was observed where leucodopaminechrome was formed after longer time (low potential scan rate or continuous potential scan) since the intracyclization reaction rate is slower at pH 5 than pH 7. At pH 4 and below, no intracyclization occur meaning no leucodopminechrome was form. The polymerization of dopamine is faster at higher concentrations due to faster chemical reaction rate.

2.5 References

[1] E. Herlinger, R.F. Jameson and W. Linert, *J. Chem. Soc. Perkin Trans*. **2** (1995) 259-263.

[2] Y. Liu, K. Ai and L. Lu, *Chem. Rev*. **114** (2014) 5057-5115.

[3] M.D. Hawley, S.V. Tatawawadi, S. Piekarski and R.N. Adams, *J. Am. Chem. Soc*. **89** (2) (1967) 447-450.

[4] Y. Li, M. Liu, C. Xiang, Q. Xie and S. Yao, *Thin Solid Films* **497** (2006) 270-278.

[5] J.A. Stamford and J.B. Justice, *Anal. Chem. News and Features* (1996) 359A-363A.

[6] Gaussian 09, Revision D.01, M. J. Frisch, G. W. Trucks, H. B. Schlegel, G. E. Scuseria, M. A. Robb, J. R. Cheeseman, G. Scalmani, V. Barone, B. Mennucci, G. A. Petersson, H. Nakatsuji, M. Caricato, X. Li, H. P. Hratchian, A. F. Izmaylov, J. Bloino, G. Zheng, J. L. Sonnenberg, M. Hada, M. Ehara, K. Toyota, R. Fukuda, J. Hasegawa, M. Ishida, T. Nakajima, Y. Honda, O. Kitao, H. Nakai, T. Vreven, J. A. Jr. Montgomery, J. E. Peralta, F. Ogliaro, M. Bearpark, J. J. Heyd, E. Brothers, K. N. Kudin, V. N. Staroverov, R. Kobayashi, J. Normand, K. Raghavachari, A. Rendell, J. C. Burant, S. S. Iyengar, J. Tomasi, M. Cossi, N. Rega, N. J. Millam, M. Klene, J. E. Knox, J. B. Cross, V. Bakken, C. Adamo, J. Jaramillo, R. Gomperts, R. E. Stratmann, O. Yazyev, A. J. Austin, R. Cammi, C. Pomelli, J. W. Ochterski, R. L. Martin, K. Morokuma, V. G. Zakrzewski, G. A. Voth, P. Salvador, J. J. Dannenberg, S. Dapprich, A. D. Daniels, Ö. Farkas, J. B. Foresman, J. V. Ortiz, J. Cioslowski, D. J. Fox, Gaussian, Inc., Wallingford CT, 2009.

[7] J.-D. Chai, M. Head-Gordon, Long-range Corrected Hybrid Density Functionals with Damped Atom-atom Dispersion Corrections, *Phys. Chem. Chem. Phys*. **10** (2008) 6615-6620.

[8] A. D. McLean, G. S. Chandler, Contracted Gaussian-basis sets for molecular calculations. 1. 2nd row atoms, Z=11-18, *J. Chem. Phys*. **72** (1980) 5639-5648.

[9] G. A. Petersson, M. A. A. Al-Laham, Complete basis set model chemistry. II. Open-shell systems and the total energies of the first-row atoms, *J. Chem. Phys*. **94** (1991) 6081-6090.

[10] G. Scalmani, M. J. Frisch, Continuous surface charge polarizable continuum models of solvation. I. General formalism, *J. Chem. Phys*. **132** (2010) 114110/1-114110/15.

[11] NBO 6.0. E. D. Glendening, J. K. Badenhoop, A. E. Reed, J. E. Carpenter, J. A. Bohmann, C. M. Morales, C. R. Landis, and F. Weinhold (Theoretical Chemistry Institute, University of Wisconsin, Madison, WI, 2013); http://nbo6.chem.wisc.edu/.

[12] M.D. Ryan, A. Yueh, and W. Chen, J. Electrochem. Soc. 127 (7) (1980) 1489-1495.

[13] J. Sun, J. Xu, H. Fang and H. Chen, *Bioelectrochem. Bioenerg*. **44** (1997) 45-50.

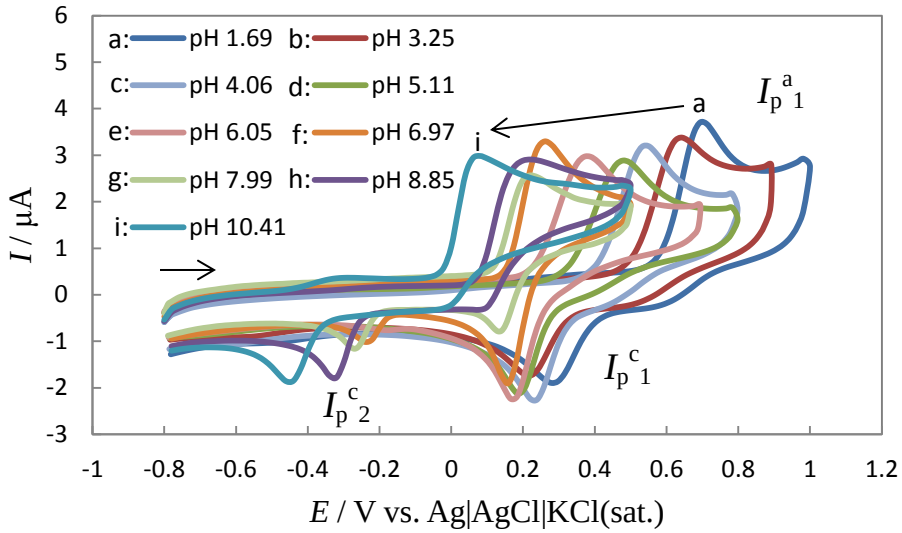

(A)

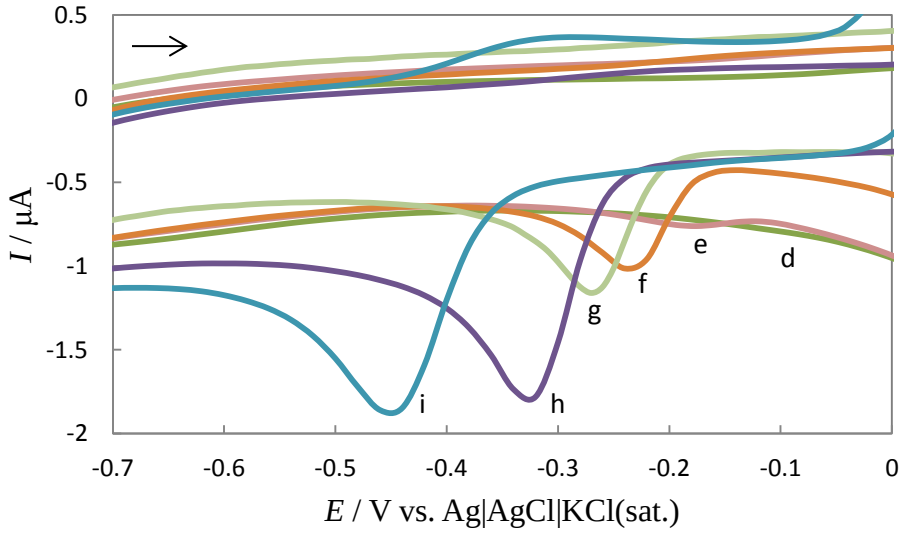

(B)

Fig. 2.1 (A). Cyclic voltammograms (CVs) of 0.1 mM DA at GC electrodes in 0.1 M NaCl solution containing 5 mM universal buffers. (B) CVs obtained in the potential range from 0 to -0.7 V in Fig. 2.1 (A). Potential scan rate: 100 mVs^{-1}.

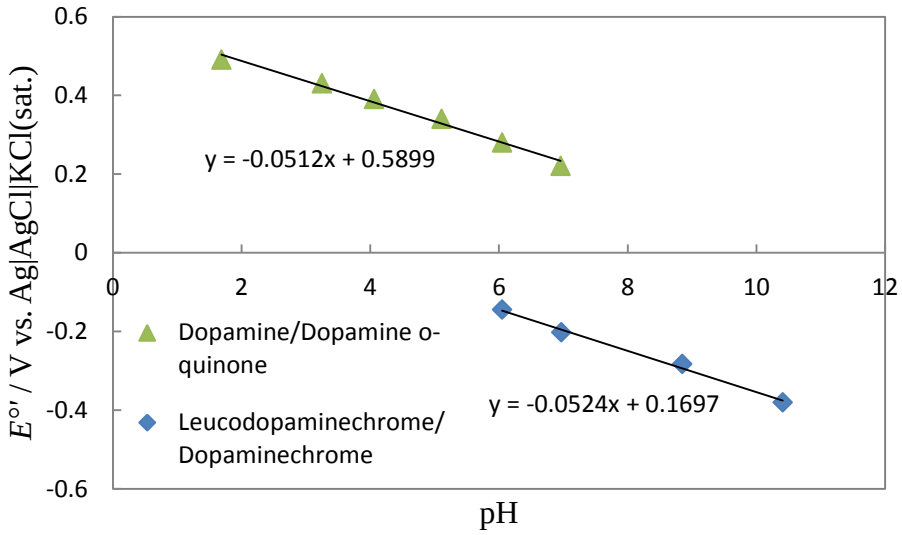

Fig. 2.2. Plots of $E°'$ vs pH for dopamine/dopamine o-quinone and leucodopaminechrome/dopaminechrome redox couples.

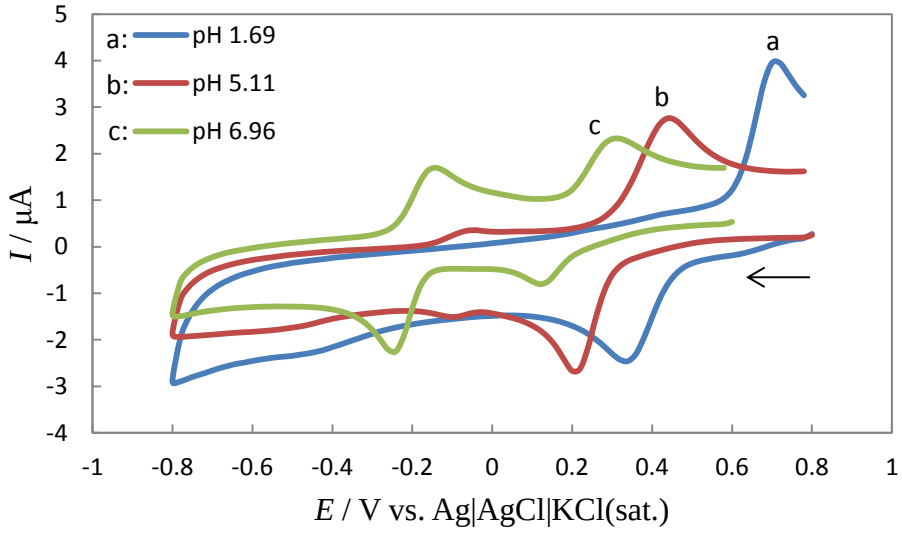

Fig. 2.3. CVs of 0.1 mM DA at GC electrodes in 0.1 M NaCl solution containing 5 mM universal buffers. All CVs were recorded after 40 min of holding time at (a and b) 0.8 V and (c) 0.6 V. Potential scan rate: 100 mVs^{-1}.

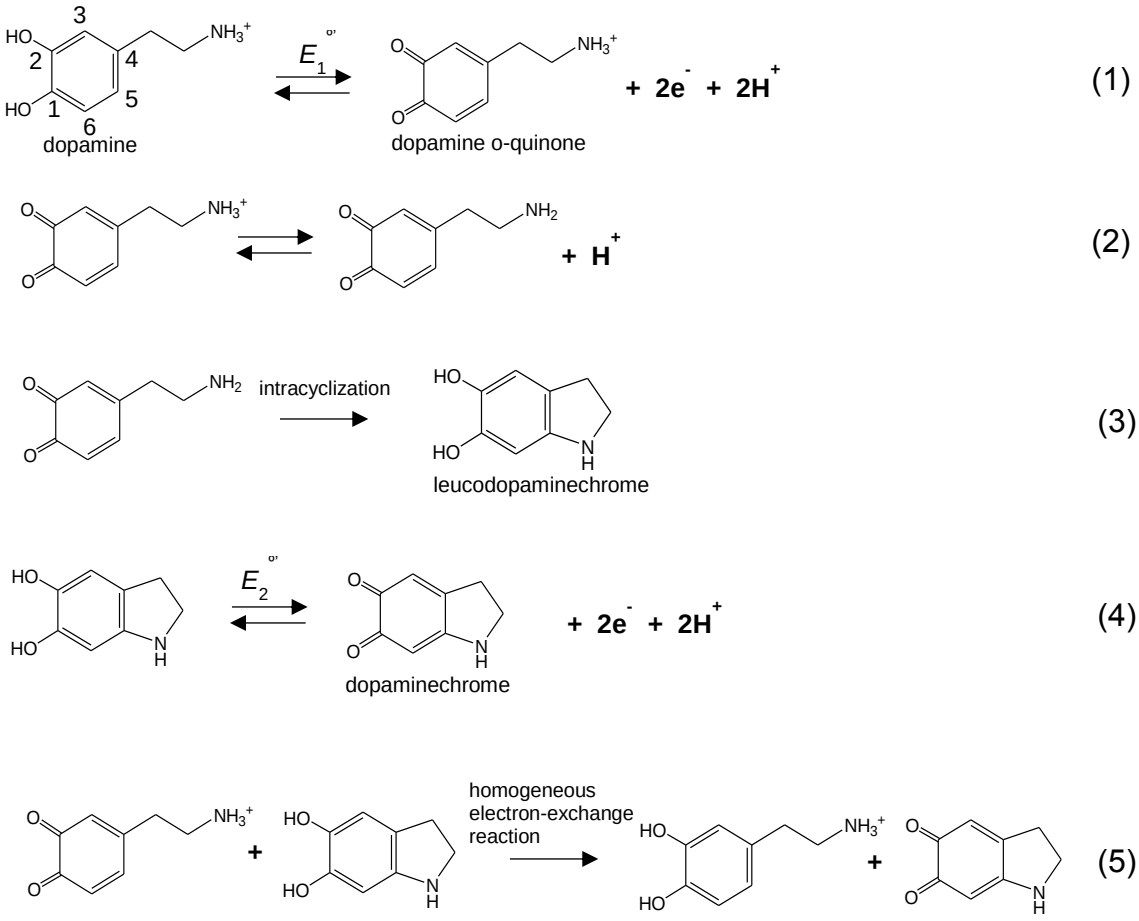

Scheme 2.1. Possible oxidative pathways of dopamine (*e.g.*, at pH 7.5).
$E_1^{o'}$ (formal potential of electrode reaction (1)) > $E_2^{o'}$ (formal potential of electrode reaction (4))
ECE mechanism : (1)→(2) →(3) →(4)
ECC mechanism : (1)→(2) →(3) →(5)

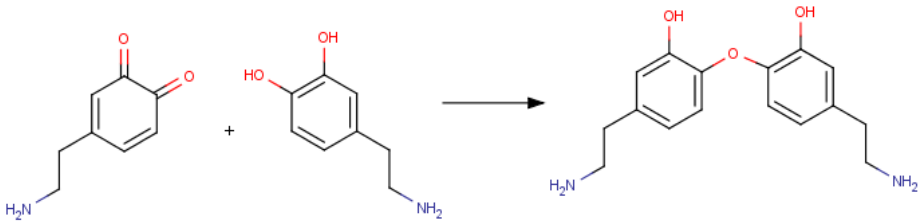

Scheme 2.2. Possible reaction of dopamine at pH 8.

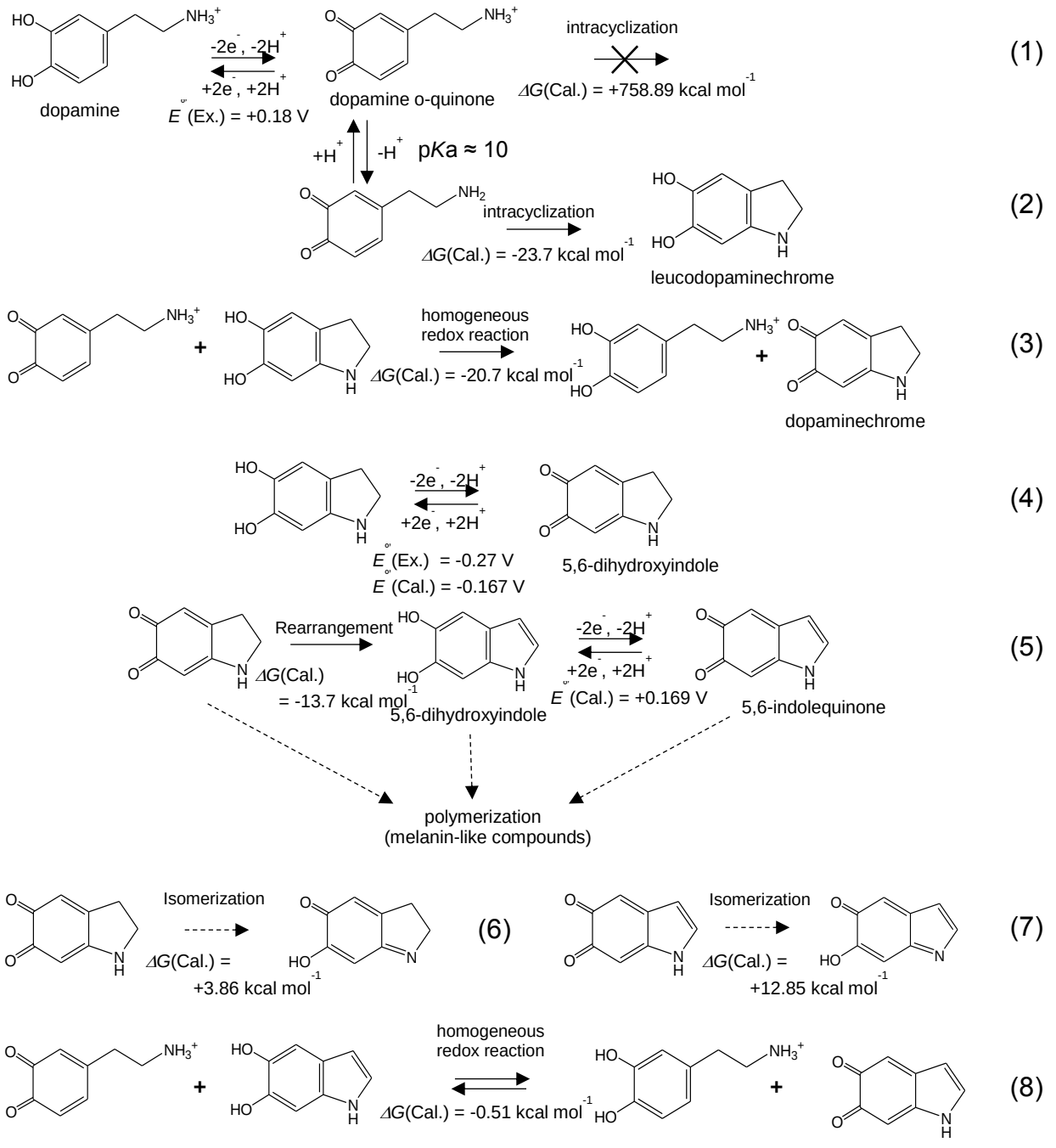

Scheme 2.3. Oxidative pathways of dopamine (at pH 7.5).

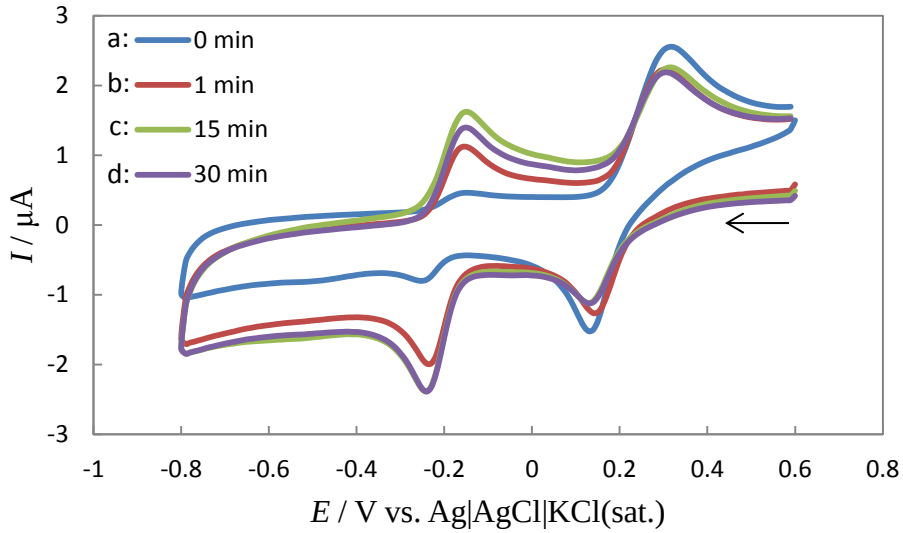

Fig. 2.4. CVs of 0.1 mM DA at GC electrodes in 0.1 M NaCl solution containing 5 mM universal buffer (pH 6.97). CVs were measured after holding the potential at 0.6 V for (a) 0, (b) 1, (c) 15 and (d) 30 min. Potential scan rate:100 mVs^{-1}

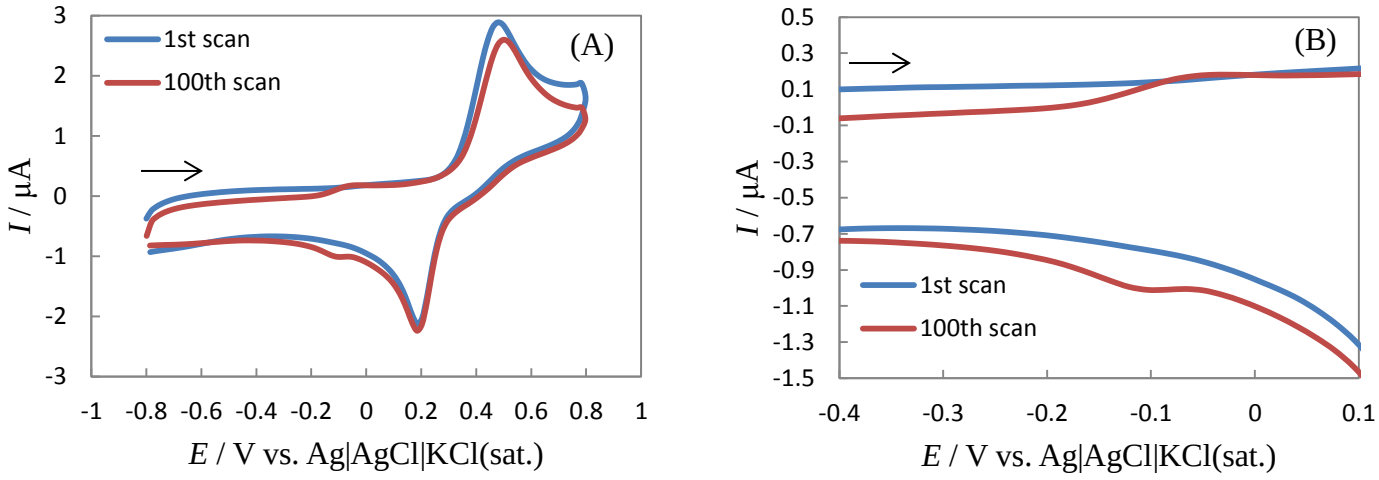

Fig. 2.5 (A) CVs of 0.1 mM DA at GC electrodes in 0.1 M NaCl solution containing 5 mM universal buffers (pH 5.11). (B) CVs partially enlarged in the potential range from 0.1 to -0.4 V in the CVs of Fig 2.5(A). Potential scan rate: 100 mVs^{-1}

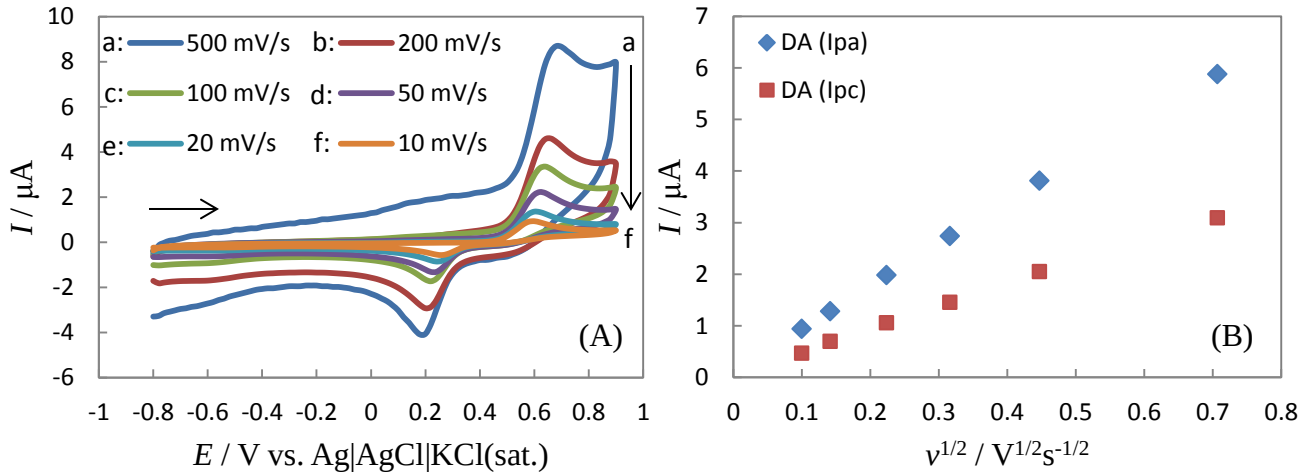

Fig. 2.6 (A) CVs of 0.1 mM DA at GC electrodes in 0.1 M NaCl solution containing 5 mM universal buffer (pH 3.25) at various scan rates. (B) Plots of I_p vs $v^{1/2}$, Data were taken from Fig. 2.6(A).

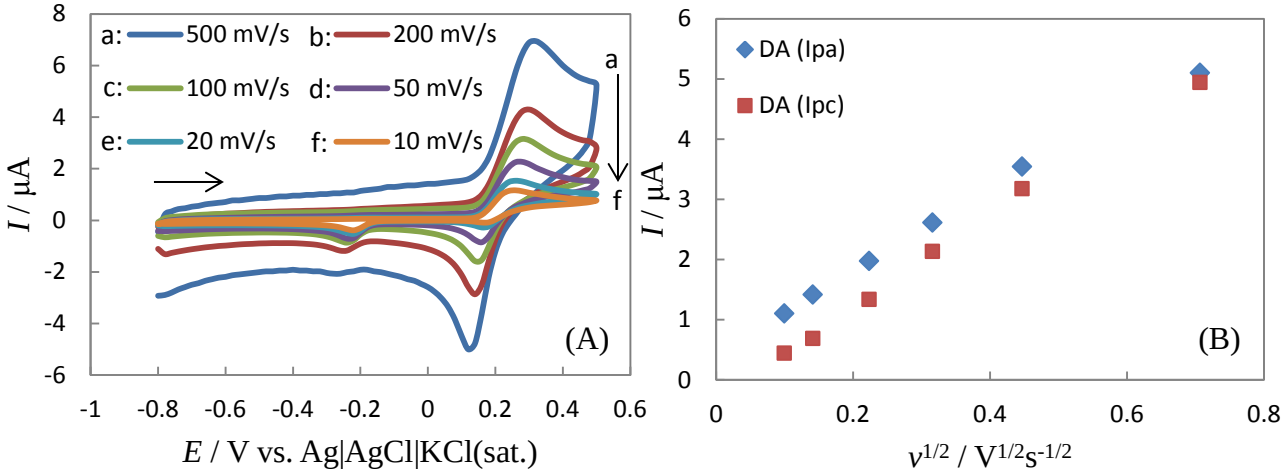

Fig. 2.7 (A) CVs of 0.1 mM DA at GC electrodes in 0.1 M NaCl solution containing 5 mM universal buffer (pH 6.97) at various scan rates. (B) Plots of I_p vs $v^{1/2}$, Data were taken from Fig. 2.7(A).

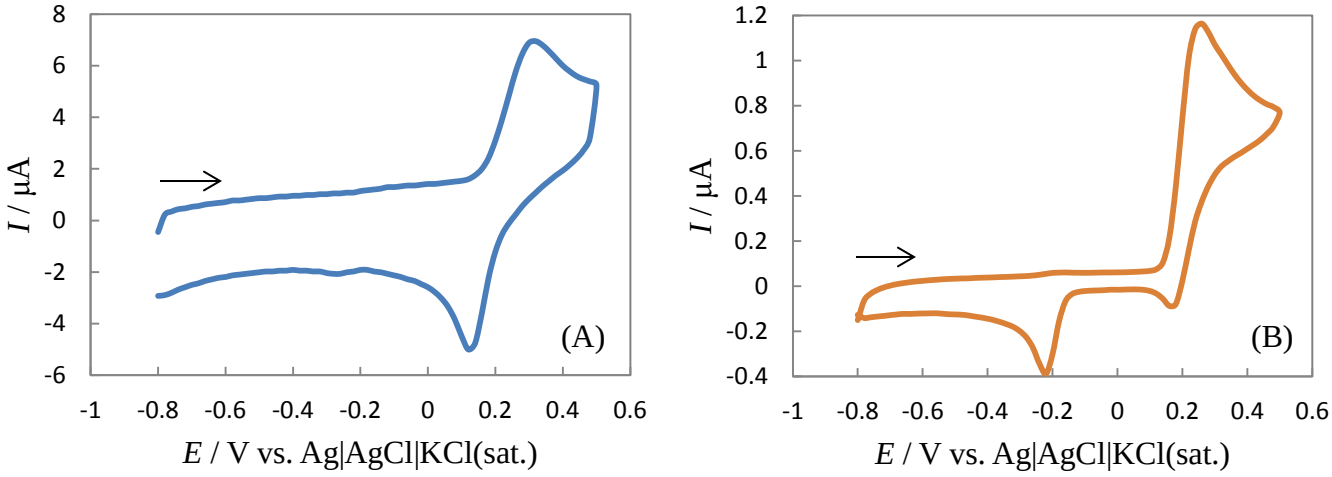

Fig. 2.8 (A) CV at scan rate of 500 mVs^{-1}. (B) CV at scan rate of 10 mVs^{-1}. Data were taken from Fig. 2.7(A).

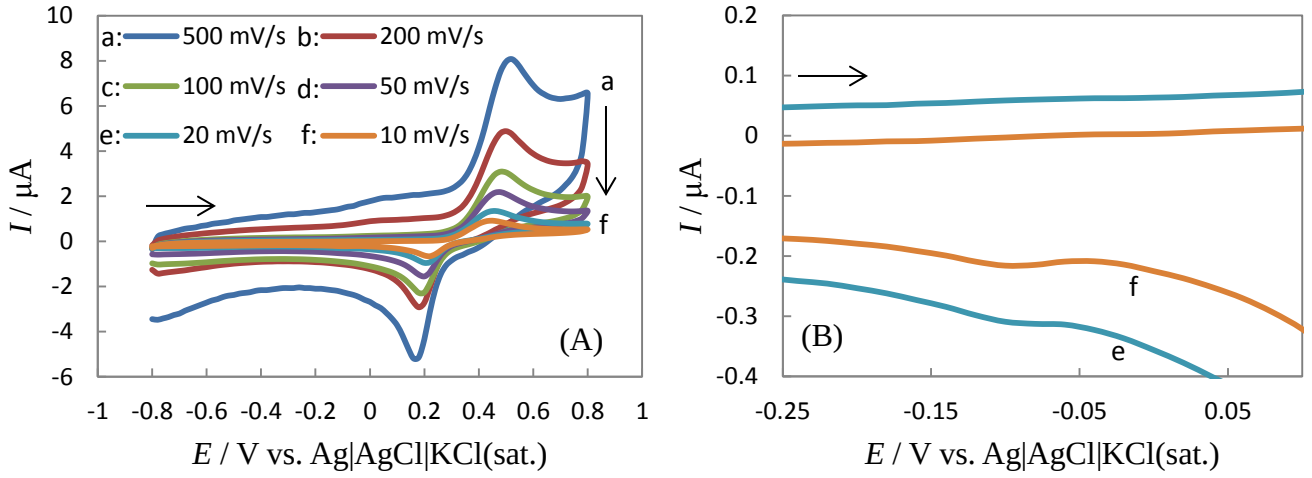

Fig. 2.9 (A) CVs of 0.1 mM DA at GC electrodes in 0.1 M NaCl solution containing 5 mM universal buffer (pH 5.11) at various scan rates. (B) CVs obtained in the potential range from 0.1 to -0.25 V in Fig 2.9(A).

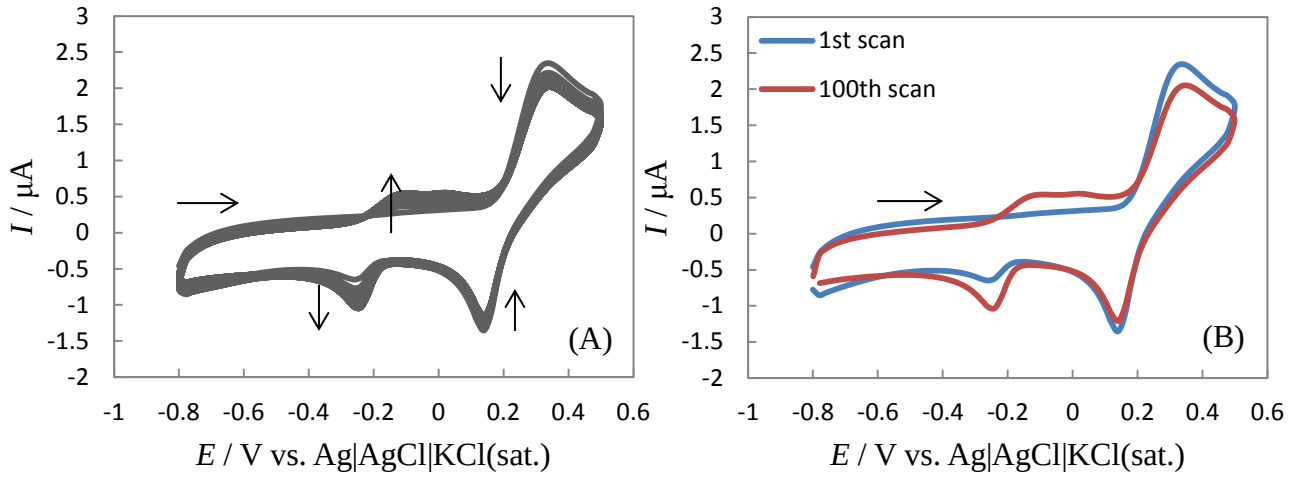

Fig. 2.10 (A) CVs of 0.1 mM DA at GC electrodes in 0.1 M NaCl solution containing 50 mM universal buffer (pH 6.97) from the 1st to 100th potential cycles. (B) The 1st and 100th CVs were taken from Fig. 2.10(A). Potential scan rate: 100 mVs^{-1}.

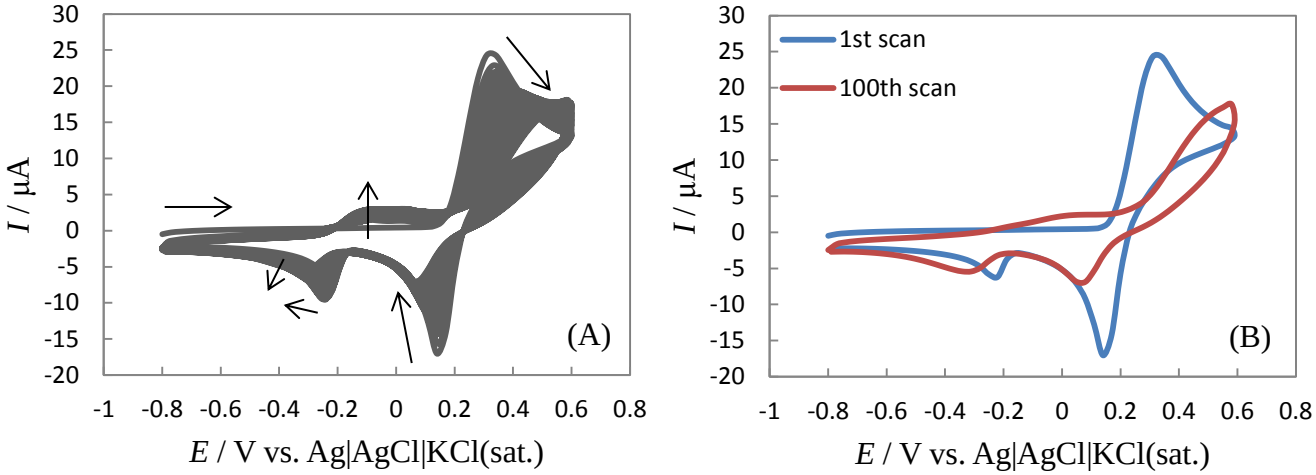

Fig. 2.11 (A) CVs of 1 mM DA at GC electrodes in 0.1 M NaCl solution containing 50 mM universal buffer (pH 6.97) from the 1st to 100th potential cycles. (B) The 1st and 100th CVs were taken from Fig. 2.11(A). Potential scan rate: 100 mVs^{-1}.

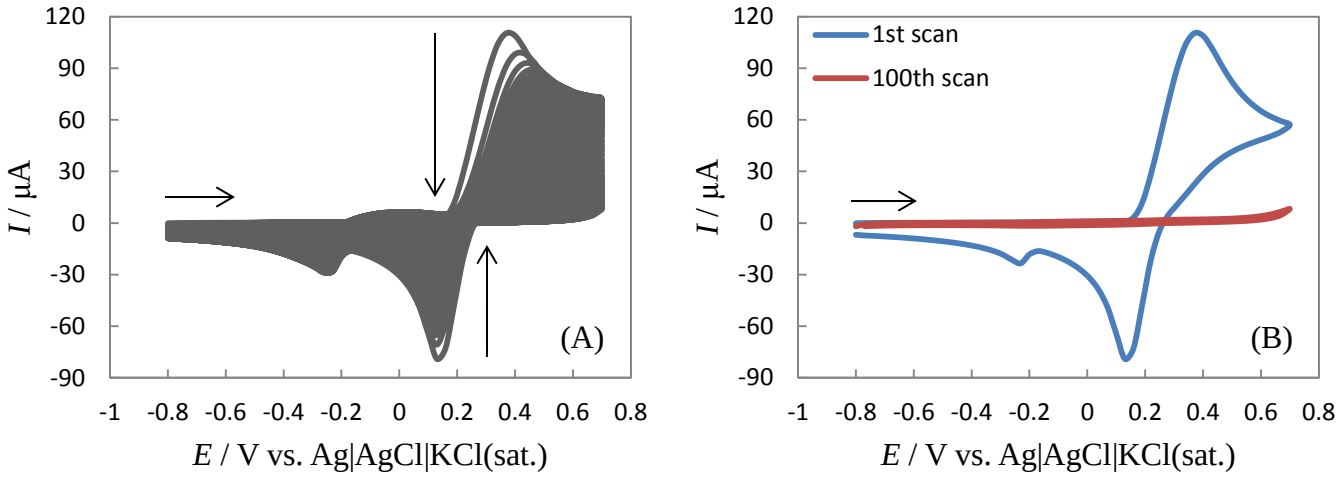

Fig. 2.12 (A) CVs of 5 mM DA at GC electrodes in 0.1 M NaCl solution containing 50 mM universal buffer (pH 6.97) from the 1st to 100th potential cycles. (B) The 1st and 100th CVs were taken from Fig. 2.12(A). Potential scan rate: 100 mVs^{-1}.

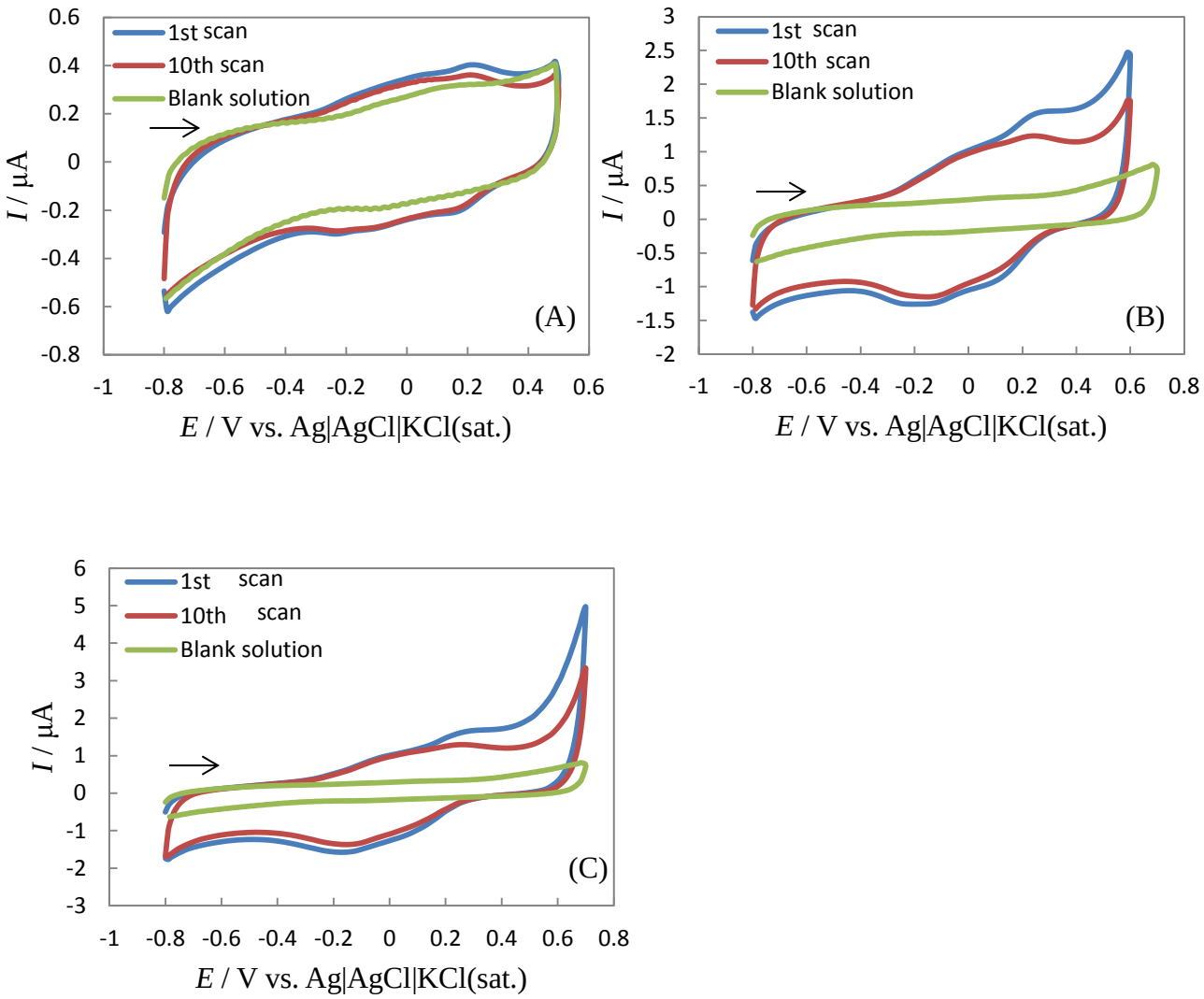

Fig. 2.13. CVs of DA at GC electrodes in 0.1 M NaCl solution containing 50 mM universal buffer (pH 6.97) from the 1st to 10th potential cycles. Concentration of DA: (A) 0.1, (B) 1 and (C) 5 mM. Blank solution means the CV obtained at 100 mVs^{-1} in the same electrolyte solution containing no DA. Potential scan rate: 100 mVs^{-1}

Table 2.1 Formal redox potentials of DA estimated from electrochemical experiments and quantum chemical calculations.

Reactions	$E^{\circ\prime}_1$(Ex.) [a] / V	$E^{\circ\prime}_1$(Cal.) [b] / V	εHOMO		εLUMO	
			Red / eV	Ox / eV	Red / eV	Ox / eV
Dopamine $\longrightarrow$ Dopamine o-quinone + $2H^+$ + $2e^-$ (Eq. (1) in Scheme 2.3)	+0.18	+0.18	-7.715	-8.987	1.833	-1.663
Indoline-5,6-diol $\longrightarrow$ Dopaminechrome + $2H^+$ + $2e^-$ (Eq. (4) in Scheme 2.3)	-0.27	-0.167	-6.918	-8.259	1.849	-1.028
5,6-dihydroxyindole $\longrightarrow$ Indole-5,6-quinone + $2H^+$ + $2e^-$ (Eq. (5) in Scheme 2.3)	-	+0.169	-7.153	-7.921	1.614	-1.602
Catechol $\longrightarrow$ o-quinone + $2H^+$ + $2e^-$	+0.20	+0.229	-7.860	-9.156	1.824	-1.843

a) Based on the cyclic voltammetric measurements at pH = 7.5.

b) Based on the quantum chemical calculations for compounds in water at ωB97X-D/6-311G(d,p). The formal redox potentials for their redox reactions in water were estimated using the experimental formal redox potential of dopamine as a standard (+0.18 V vs. Ag|AgCl|KCl(sat.)).

Table 2.2 Heats of reactions in water at ωB97X-D/6-311(d,p)

Reactions	**ΔG / kcal / mol** [a)]
Dopamine o-quinone $\longrightarrow$ Leucodopaminechrome (Indoline-5,6-diol) (Intracyclization: Eq. (2) in Scheme 2.3)	-23.71
Dopaminechrome $\longrightarrow$ 5,6-dihydroxyindole (Rearrangement: Eq. (5) in Scheme 2.3)	-13.74
Dopaminechrome (Isomerization: Eq. (6) in Scheme 2.3)	+3.86
Indole-5,6-quinone (Isomerization: Eq. (7) in Scheme 2.3)	+12.85
Dopamine o-quinone ($-NH_3^+$) $\longrightarrow$ Leucodopaminechrome ($-NH_2^+$) (Intracyclization: Eq. (1) in Scheme 2.3)	+758.89

a) Based on Gibbs free energy at 298.15 K (25 ℃).

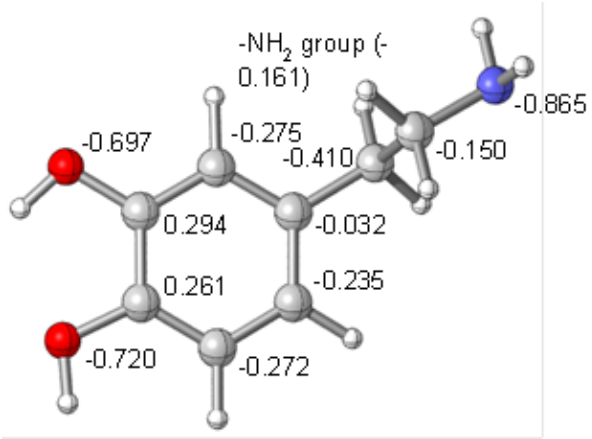

(A)

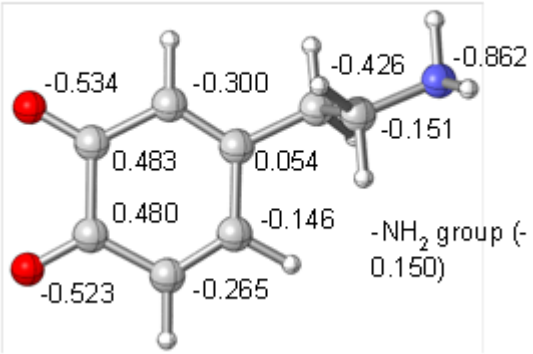

(B)

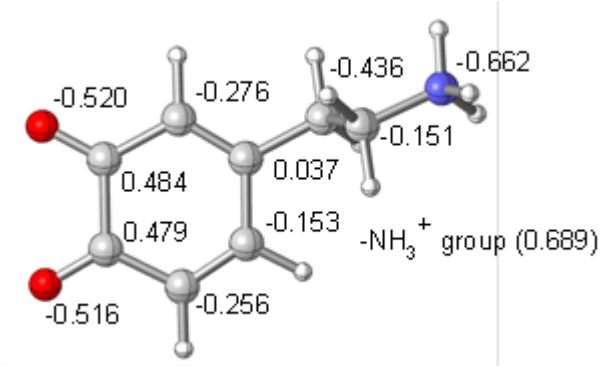

(C)

Fig. 2.14. Natural charges of (A) dopamine and (B and C) dopamine o-quinone.

CHAPTER 3

ELECTROCHEMICAL BEHAVIOUR OF 5-METHYLDOPAMINE (5-MDA)

3.1 Introduction

5-MDA is an analog of DA. In this chapter, the electrochemical behavior of 5-MDA will be studied in comparison to DA to investigate the intracyclization reaction. 5-MDA has methyl group at the C5 position of its benzene ring. This group can block the intracyclization from occurring and then further study regarding the effect of intracyclization can be investigated in depth. In addition, 5-MDA serves as the model compound in this research since it cannot undergo intracyclization.

In previous research on DA, particularly in the study on its intracyclization reaction, 4-methylcatechol (4-MC) has been used as the model compound [1]. However, this model compound may not reflect the complete structure of DA. Some researchers studied 5-hydroxydopamine (5-OHDA) [2][3] in their research related to neurotransmitters that gave some information regarding intracyclization. These researchers investigated the 5-OHDA that exists naturally in the brain which interferes the norepinephrine nerve terminals. Meanwhile, other researcher used 5-fluorodopamine (5-FDA) [4] in studying the oxidation pathway of fluorine substituted catecholamines.

Intracyclization reaction is one of the main chemical reactions which occur in the DA oxidation pathway, and information such as the effect of intracyclization on the electrochemical behavior of DA is needed. Hence, studiy of 5-MDA is very important in

understanding the DA electrochemical behavior of DA. In this chapter, similar studies of DA will be done on 5-MDA, and comparisons of the electrochemical behavior were made between the two compounds. The effects of the substitution of methyl group at the C5 position in the benzene ring to the formal potential, peak separation and reversibility of 5-MDA will be studied. Through this study, we aim to clarify the factors affecting the intracyclization reaction.

3.2 Materials and methods

3.2.1 Materials

5-methyldopamine (4-(2-aminoethyl)-5-methylbenzene-1,2-diol, hydrochloride salt) was supplied by Otava Ltd., Canada. Other reagents such as components of universal buffer solutions are the same as those shown in Section 2.2.1 in Chapter 2 (page 11).

3.2.2 Electrochemical measurements

See Section 2.2.2 in Chapter 2 (page 12).

3.2.3 Quantum chemical calculations

See Section 2.2.3 in Chapter 2 (page 18).

3.3 Results and discussions

3.3.1 pH dependence

Redox reaction of 5-MDA showed pH dependence as shown in Fig. 3.1. As pH increased, the $E^{\circ\prime}$ value decreased. 5-MDA is easily oxidized at higher pH (pH 10.41). Only small anodic and cathodic peak currents of 5-MDA can be observed since it undergoes fast chemical reaction at this pH that could be due to oxidation of 5-MDA by the trace amount of oxygen dissolved in the buffer solution. Even under air atmosphere, the solution containing 5-MDA changed color faster than DA. Solution containing 5-MDA turned into brownish color while solution containing DA turned into grey color.

Plot of $E^{\circ\prime}$ vs pH shows a linear relationship with near 60 mV/pH slope indicating a 2e and $2H^+$ process (Fig. 3.2). At any pH, 5-MDA gives only one redox peak in the potential range from +0.6 to 0 V. This means that intracyclization (ICR) did not occur after the oxidation of 5-MDA because the methyl group at the C5 position prevent the ICR from occurring. Hence, the redox reaction of 5-MDA is a simple redox reaction without any chemical reaction as summarized in Scheme 3.1. Similar anodic and cathodic peak current heights can be observed from pH 3.25 to 6.96. However, decreased in cathodic peak current height is observed at pH 8.85. This could be due to the chemical reaction between the o-quinone and the anionic form of catechol [5] as summarized in Scheme 2.2. Besides that, hydroxides in the solution might attack catechols leading to the electroinactivity of 5-MDA [6]. Only small anodic and cathodic peak currents observed (at ~ 0 V) at pH 10.41. At this pH, 5-MDA may undergo a fast chemical reaction before the electrochemical reaction occurs at 0 V.

The methyl group stably attached at the C5 position of 5-MDA is also confirmed through the potential holding for a long time at oxidative potential (i.e., 0.6 V). Even after 40 min of holding time, only one redox couple peak was observed at various pH meaning that the methyl group did not detach from the C5 position of 5-MDA and the ICR did not occur (Fig. 3.3). However, obvious reduction of anodic and cathodic peak current (I_p^a and I_p^c) is observed as the solution pH increased as can be seen from the CV at pH 6.97.

If we compare the electrochemical behavior of 5-MDA to that of DA at all pH, 5-MDA is more easily oxidized electrochemically since its $E°'$ value is less positive compared to that of DA (Figs. 2.2 and 3.2). For example, at pH 4.06, $E°'$ value of 5-MDA is 0.39 V while that of DA is 0.34 V. This may be due to the methyl group as an electron donor which made the aromatic compound more easily to oxidize. From our study, we observed decreasing value of $E°'$ based on the increasing number of groups attached to the benzene ring. The more groups attached on the benzene ring, the more negative the value of $E°'$. For example, catechol's value of $E°'$ (0.2 V) is less negative compared to that of DA (0.18 V) (Table 2.1) because catechol has no ethylamine group attached to the benzene ring. DA's value of $E°'$ is less negative than 5-MDA (0.14 V) (Table 3.1) because DA has no methyl group attached to the benzene ring.

Laurila et al. also obtained similar result where the value of ΔE_p decreased with increasing number of groups attached to the benzene ring [7]. They observed that value of ΔE_p of DA (0.062 V) is smaller than 4-methylcatechol (0.078 V) and catechol (0.092 V) because DA has ethylamine group attached to the benzene ring. 4-methylcatechol's value of ΔE_p is smaller than catechol because of the methyl group attached to its benzene ring.

3.3.2 Potential scan rate dependence

Potential scan rate dependence of 5-MDA are shown in Figs. 3.4(A) and 3.5(B). From Fig. 3.4(B) at pH 3.25, the ratio of I_p^c / I_p^a are not near to unity (~1) and the ratio is in the range from 0.72 (at 500 mVs^{-1}) to 0.75 (at 10 mVs^{-1}). This indicates that only about 70% of the oxidized 5-MDA has been reduced. Nevertheless, at pH 6.96, the ratio of I_p^c / I_p^a varies widely from 1.15 (at 500 mVs^{-1}) to 0.69 (at 10 mVs^{-1}) as can be seen from Fig. 3.5(B). ΔE_p values of 5-MDA at pH 3.25 are bigger compared to at pH 6.96. As potential scan rate decreased, the value of ΔE_p at pH 3.25 decreased from 0.37 to 0.23 V while at pH 6.96, ΔE_p value decreased from 0.16 to 0.07 V. The variety of potential scan rates did not affect the $E°'$ values in CVs for both pH 3.25 (0.38 V) and at pH 6.96 (0.17 V).

After the oxidation reaction (at pH 1.69), about 70% of the oxidized 5-MDA was reduced while only 50% of oxidized DA was reduced. These show that the methyl group in 5-MDA may enhanced its electron transfer thus increased the rate of reduction reaction compared to DA even though intracyclization reaction did not occur. At pH 6.96 and at lowest scan rate (10 mVs^{-1}), at least 70% of oxidized 5-MDA has been reduced but for DA, at least 40% of oxidized DA was reduced. This means that the presence of methyl group in 5-MDA enhanced the reduction reaction (5-MDA become easier to reduce) and it is not affected by pH since both pH (pH 1.69 and 6.96) gave similar I_p^c / I_p^a value of at least 0.7. However, due to the intracyclization reaction, it reduced the I_p^c / I_p^a value of DA from 0.5 (at pH 1.69) to 0.4 (at pH 6.96).

3.3.3 Concentration dependence

5-MDA reacts differently at different concentrations (Figs. 3.6, 3.7 and 3.8). At low concentration (0.1 mM), the continuous potential scan did not change the $E^{\circ\prime}$ value much where the average value is 0.17 V. However the anodic and cathodic peak current (I_p^a and I_p^c) heights decreased and the ΔE_p increased (0.07 to 0.09 V) with increasing number of potential scan. On the other hand, if the concentration is increased to 1mM, the CV changed largely where the I_p^a and I_p^c values decreased, but value of ΔE_p increased from 0.1 to 0.28 V and $E^{\circ\prime}$ shifted positively from 0.18 to 0.21 V as the number of scan increased. Furthermore, big changes can be observed if the concentration is increased to 5 mM. In this concentrated solution, the cathodic peak largely decreased and no clear anodic peak can be seen. Changes of ΔE_p and $E^{\circ\prime}$ values cannot be estimated due to the broad anodic peak. At 5 mM, only the change of E_p^c value can be determined where it shifted negatively from 0.1 to 0 V.

If we compare the 1st CVs of each concentration, similar $E^{\circ\prime}$ values are obtained at 0.1 mM (0.17 V) and 1 mM (0.18 V) concentrations. The $E^{\circ\prime}$ value at 5 mM positively shifted to 0.22 V compared to the $E^{\circ\prime}$ value at 0.1 and 1 mM concentrations. Continuous potential scan gave bigger impact on the values of $E^{\circ\prime}$ at1 and 5 mM concentrations as can be observed from the 100th CV compared to the 0.1 mM concentration. It seems that with continuous potential scan, the 5-MDA is adsorbed on the electrode surface (Figs. 3.9(A), 3.9(B), 3.9(C)) leading to decreased I_p^a and I_p^c height. This means that the 5-MDA adsorbed on the electrode surface leads to electrode passivation and became less sensitive to 5-MDA. We can also see that bigger amount of 5-MDA is adsorbed on electrode surface

if high concentration (5 mM) of 5-MDA were used instead of low concentrations. This means that electrode passivation will be faster if high concentration is used.

In comparison to DA, high concentrations (1 mM and 5 mM) gave less changes on the CVs of 5-MDA since clear cathodic peaks can still be seen even at 100^{th} scan. This means that DA adsorbed on the electrode surface more easily compared to 5-MDA because we can see bigger current from Fig. 2.12(B) compared to Fig. 3.9(B). The adsorbed DA on electrode surface led to faster passivation of electrode compared to 5-MDA since intracyclization reaction of DA may also contributes to the fast electrode passivation.

3.3.4 Quantum chemical calculations

The calculated $E°'$ value (0.134 V) is quite similar to the experimental value (0.14 V) as seen in Table 3.1. Hence, the calculation method is acceptable for comparison to the experimental values. HOMO energies of oxidized and reduced 5-MDA are higher than their LUMO energies meaning that 5-MDA has tendency of donating electron (an electron donor or nucleophile) rather than accepting electron. This also means that 5-MDA is more easily oxidized. In Fig. 3.10, the natural charges of oxidized and reduced forms of 5-MDA are shown. The methyl groups are uncharged (0.033 for reduced 5-MDA and 0.065 for oxidized 5-MDA) indicating that the methyl group are stable whether the 5-MDA is in oxidized or in reduced forms.

In comparison to DA, 5-MDA has more positive value of HOMO energy meaning that 5-MDA has higher tendency of donating electron (more nucleophilic) rather than accepting electron (less electrophilic) compared to DA. This could be due to the methyl

group stabilizing the 5-MDA. Hence, this is why 5-MDA is more easily oxidized which leads to its more negative $E^{\circ'}$ value compared to DA. The LUMO energy of DA is less positive compared to that of 5-MDA indicating that DA has better tendency to accept electron.

3.4 Conclusion

Redox reaction of 5-MDA is a simple 2e and $2H^+$ process. 5-methyldopamine is a good analog model of dopamine to confirm the intracyclization reaction since the methyl group stably attached at C5 position of the benzene ring. The methyl group blocks the amine group from attaching to the C5 position of benzene ring, hence intracyclization cannot occur at any pH. The substitution of methyl group as electron donor to the benzene ring of 5-MDA decreased the formal potential making it easier to oxidize. As the number of substitution on the benzene ring increased (such as methyl group and ethylamine group) the formal potential decreased and the electron transfer increased.

3.5 References

[1] D.C.S. Tse, R.L. McCreery and R.N. Adams, *J. Med. Chem*. **19** (1) (1976) 37-40.

[2] R.N. Adams, E. Murrill, R. McCreery, L. Blank and M. Karolczak, *Eur. J. Pharm*. **17** (1972) 287-292.

[3] C.L. Blank, P.T. Kissinger and R.N. Adams, *Eur. J. Pharm*. **19** (1972) 391-394.

[4] M.E. Rice, B. Moghaddam, C.R. Creveling and K.L. Kirk, *Anal. Chem*. **59** (1987) 1534-1538.

[5] M.D. Ryan, A. Yueh, and W. Chen, *J. Electrochem. Soc*. **127** (7) (1980) 1489-1495.

[6] J. Sun, J. Xu, H. Fang and H. Chen, *Bioelectrochem. Bioenerg*. **44** (1997) 45-50.

[7] T. Palomaki, S. Chumillas, S. Sainio, V. Protopopova, M. Kauppila, J. Koskinen, V. Climent, J.M. Feliu and T. Laurila, *Diamond and Related Materials* **59** (2015) 30-39.

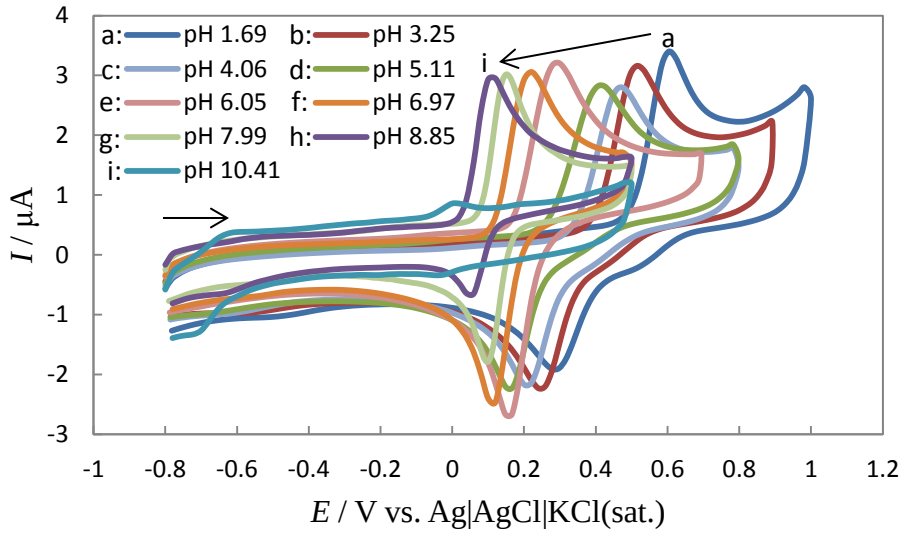

Fig. 3.1. Cyclic voltammograms (CVs) of 0.1 mM 5-MDA at GC electrodes in 0.1M NaCl containing 5 mM universal buffers. Potential scan rate: 100 mVs^{-1}.

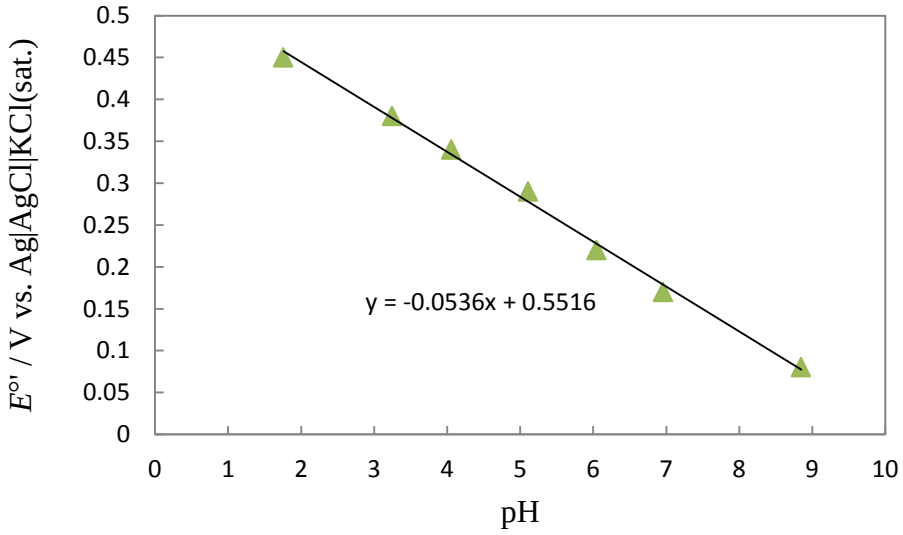

Fig. 3.2. Plot of $E°'$ vs pH for 5-MDA. Data were taken from Fig. 3.1.

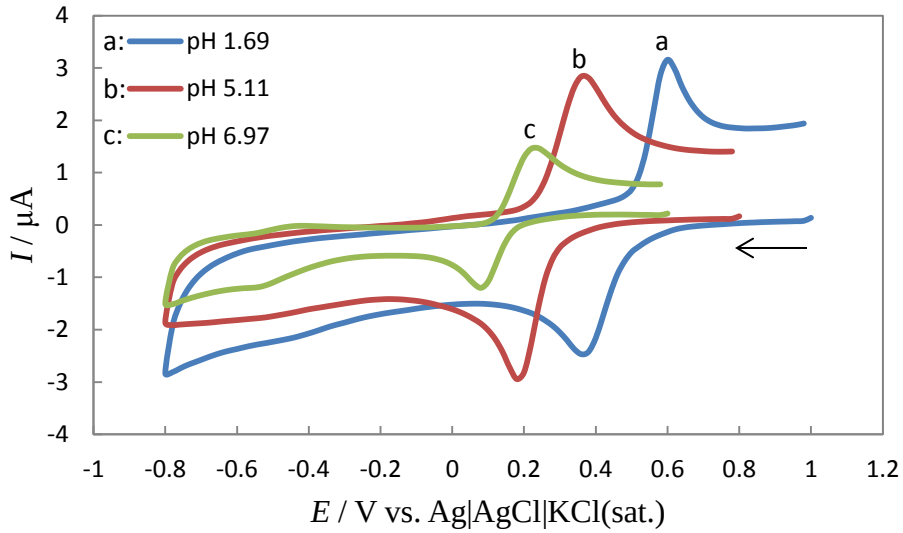

Fig. 3.3. CVs of 0.1 mM 5-MDA at GC electrodes in 0.1 M NaCl containing 5 mM universal buffers. All CVs were recorded after 40 min of holding time at (a) 1, (b) 0.8 and (c) 0.6 V. Potential scan rate: 100 mVs^{-1}.

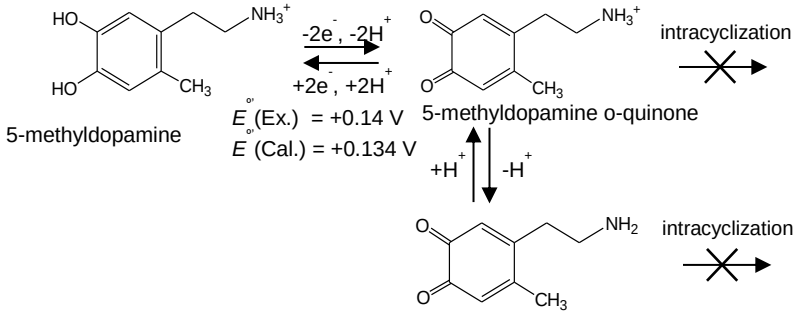

(1)

Scheme 3.1. Oxidative pathways of 5-methyldopamine (at pH 7.5).

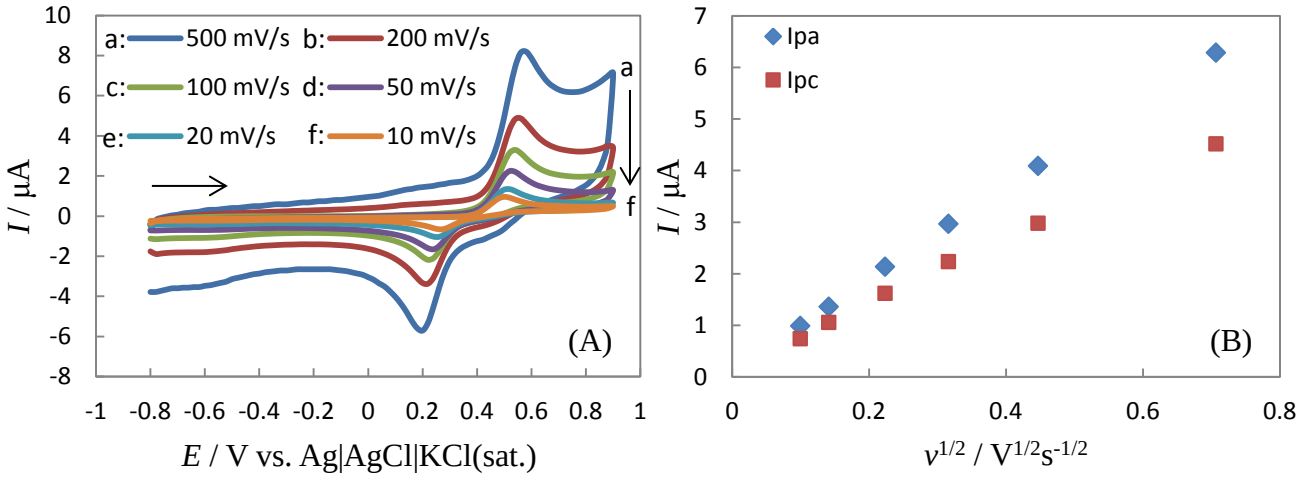

Fig. 3.4 (A) CVs of 0.1 mM 5-MDA at GC electrodes in 0.1 M NaCl containing 5 mM universal buffer (pH 3.25) at various scan rates. (B) Plots of I_p vs $v^{1/2}$, Data were taken from Fig. 3.4(A).

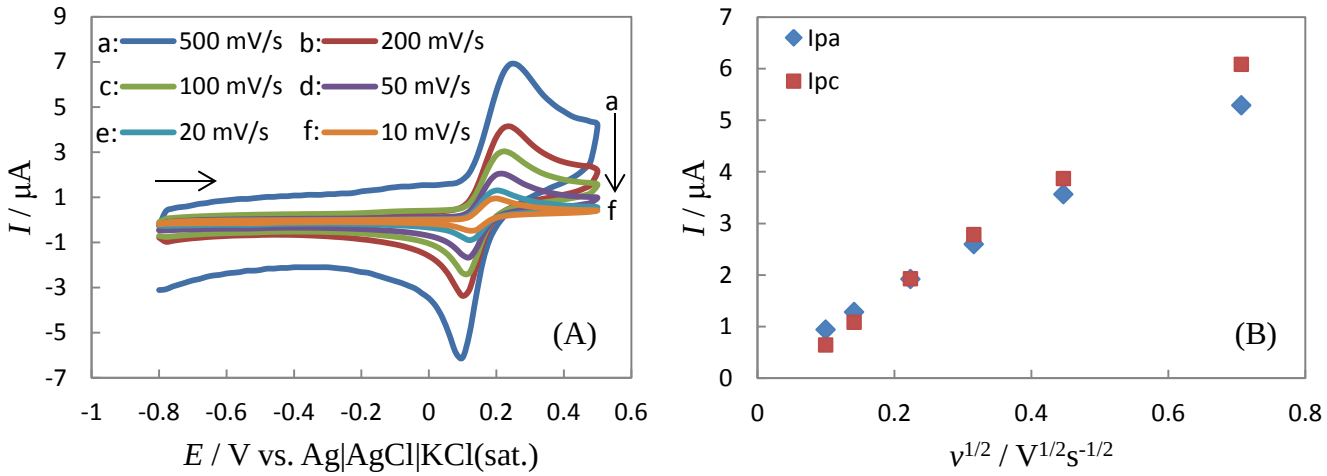

Fig. 3.5 (A). CVs of 0.1 mM 5-MDA at GC electrodes in 0.1 M NaCl containing 5 mM universal buffer (pH 6.97) at various scan rates. (B) Plot of I_p vs $v^{1/2}$, Data were taken from Fig. 3.5(A).

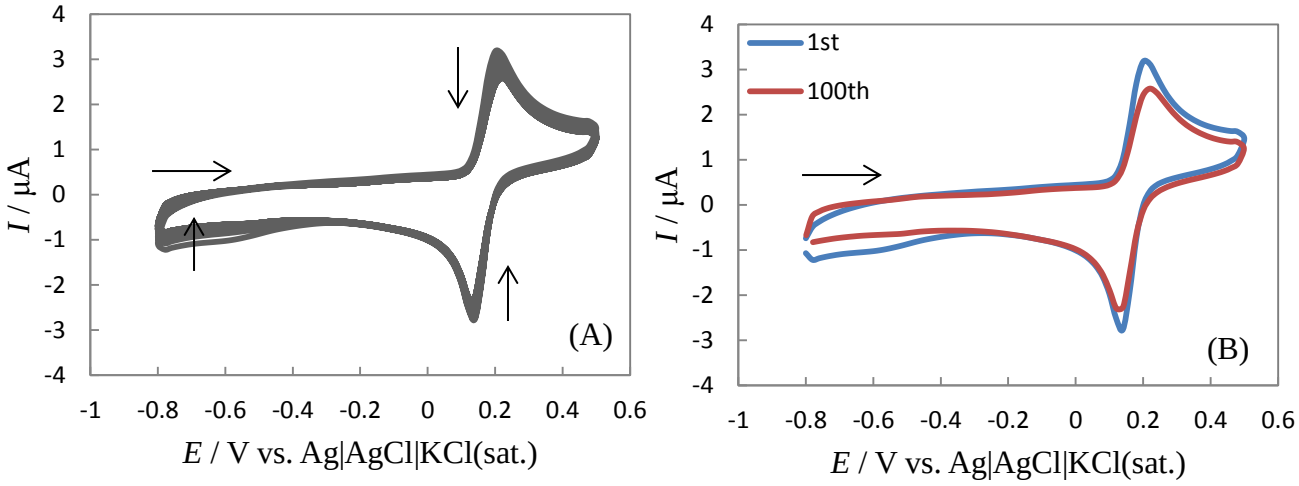

Fig. 3.6 (A) CVs of 0.1 mM 5-MDA at GC electrodes in 0.1 M NaCl containing 50 mM universal buffer (pH 6.97) from the 1st to 100th potential cycles. (B) The 1st and 100th CVs shown in Fig. 3.6(A). Potential scan rate: 100 mVs^{-1}.

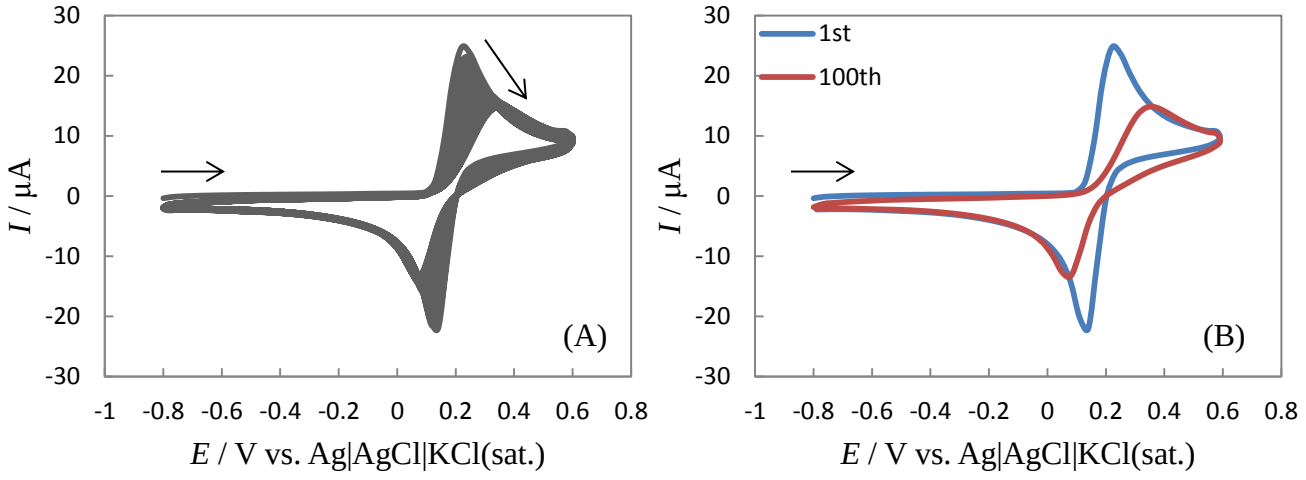

Fig. 3.7 (A) CVs of 1 mM 5-MDA at GC electrodes in 0.1 M NaCl containing 50 mM universal buffer (pH 6.97) from the 1st to 100th potential cycles. (B) The 1st and 100th CVs shown in Fig. 3.7a. Potential scan rate: 100 mVs^{-1}

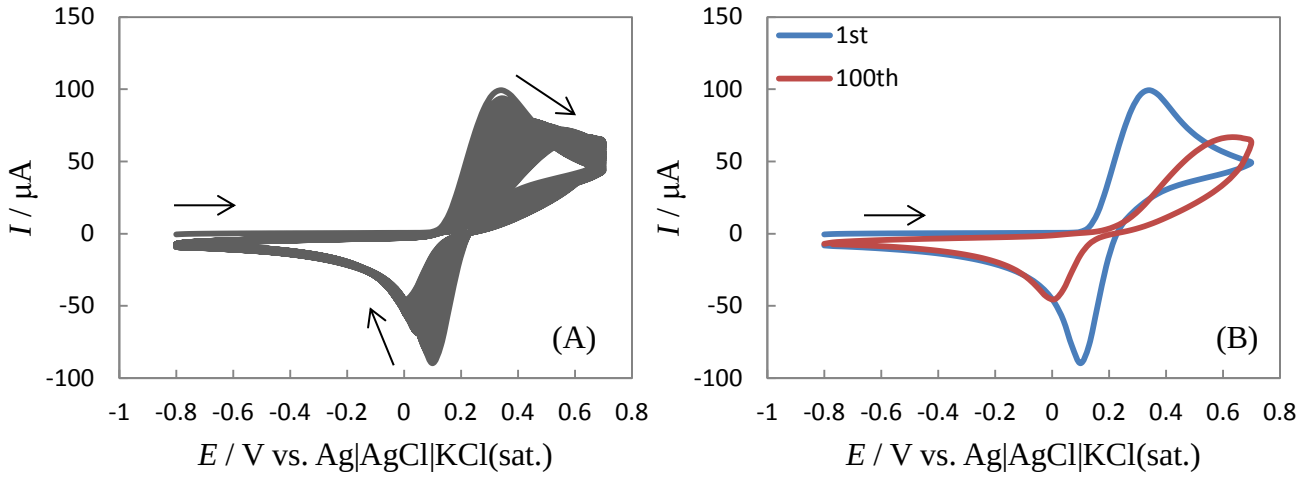

Fig. 3.8 (A) CVs of 5 mM 5-MDA at GC electrodes in 0.1 M NaCl containing 50 mM universal buffer (pH 6.97) from the 1st to 100th potential cycles. (B) The 1st and 100th CVs shown in Fig. 3.8(A). Potential scan rate: 100 mVs^{-1}.

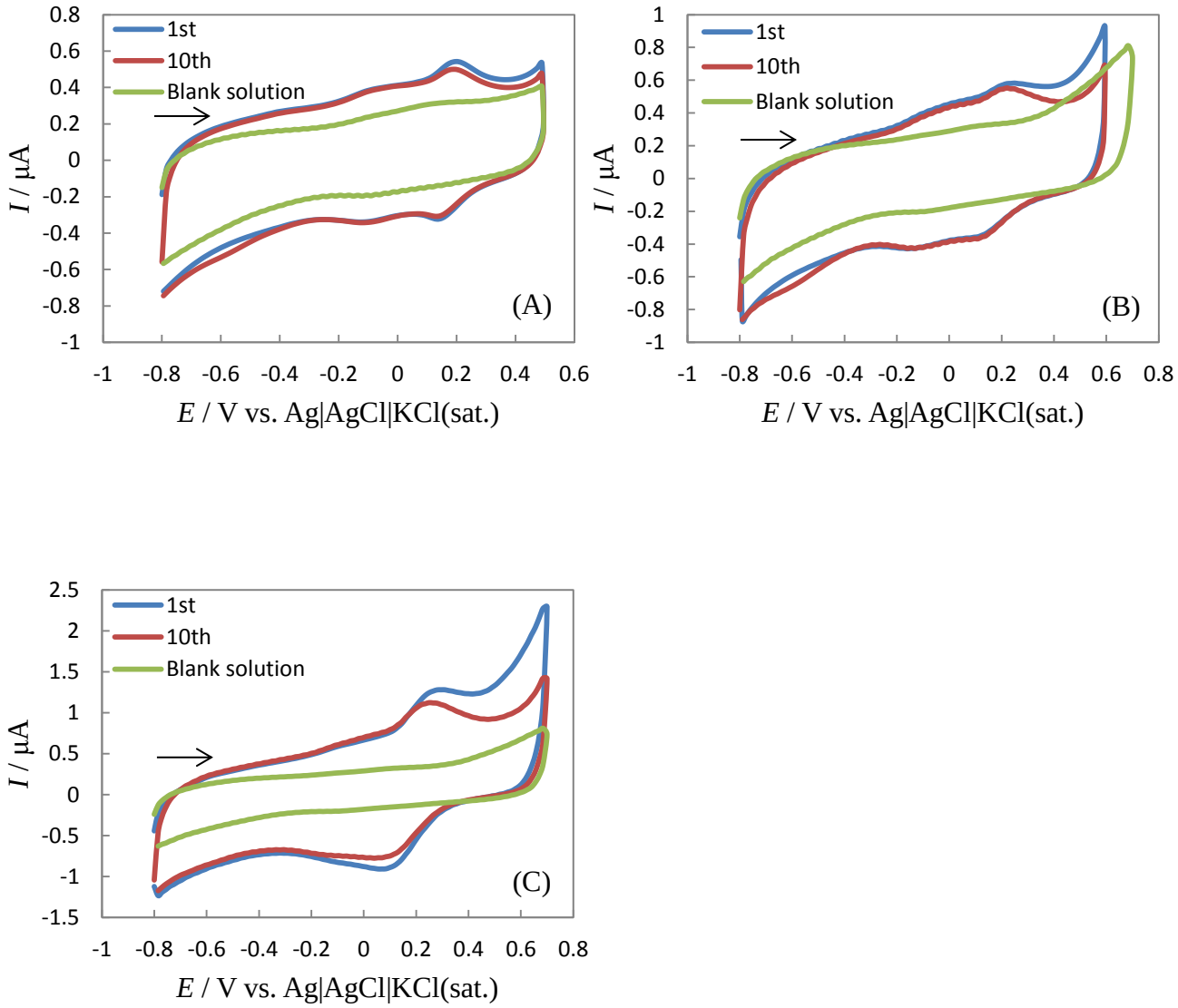

Fig. 3.9. CVs of 5-MDA at GC electrodes in 0.1 M NaCl containing 50 mM universal buffer (pH 6.97) at100 mVs^{-1} from the 1^{st} to 10^{th} potential cycles. Concentration of 5-MDA: (A) 0.1, (B) 1 and (C) 5 mM 5-MDA. Blank solution means the CV obtained at100 mVs^{-1} in the same electrolyte solution containing no 5-MDA.

Table 3.1. Formal redox potentials of 5-MDA estimated from electrochemical experiments and quantum chemical calculations

Reactions	$E^{\circ'}_1$(Ex.) [a)] / V	$E^{\circ'}_1$(Cal.) [b)] / V	εHOMO		εLUMO	
			Red / eV	Ox / eV	Red / eV	Ox / eV
5-methyldopamine $\longrightarrow$ 5-methyldopamine o-quinone + $2H^+$ + $2e^-$	+0.14	+0.134	-7.528	-8.869	1.924	-1.536

a) Based on the cyclic voltammetric measurements at pH = 7.5.

b) Based on the quantum chemical calculations for compounds in water at ωB97X-D/6-311G(d,p). The formal redox potential for the redox reactions in water was estimated using the experimental formal redox potential of dopamine as a standard (+0.18 V vs. Ag|AgCl|KCl(sat.) at pH 7.5).

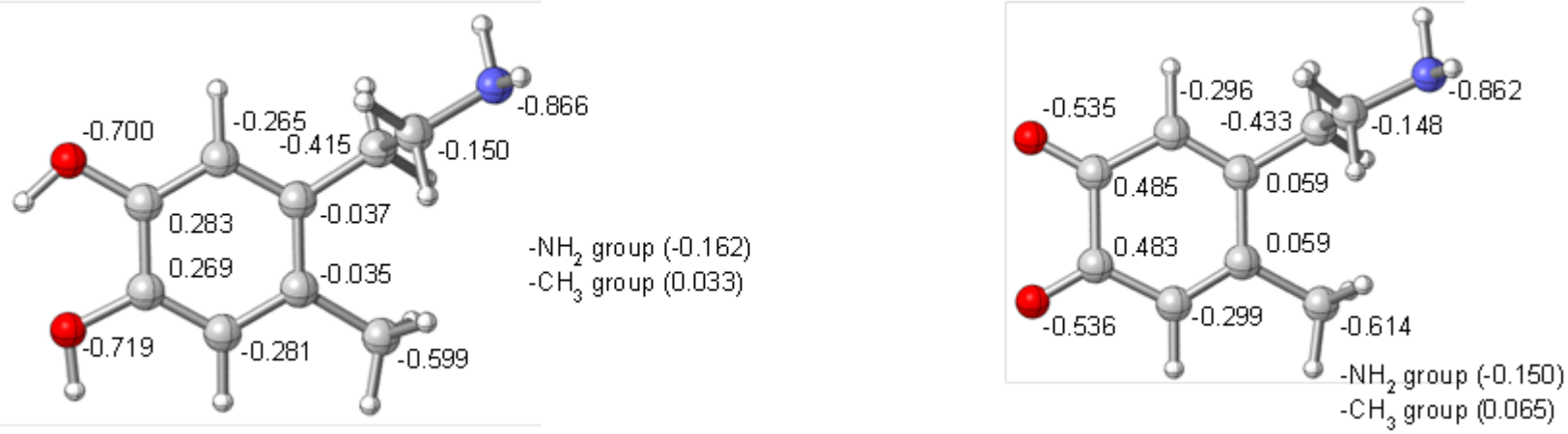

(A) (B)

Fig. 3.10. Natural charge of (A) 5-methyldopamine and (B) 5-methyldopamine o-quinone.

CHAPTER 4

DOPAMINE (DA) AND 5-METHYLDOPAMINE (5-MDA) INCORPORATED NAFION-MODIFIED ELECTRODES

4.1 Introduction

Nafion (Fig. 1.4 in Chapter 1, page 5) is an ion-exchange polymer that is highly permeable by cations but almost impermeable by anions. Nafion has been widely used to modify electrode surface in the in vitro or in vivo studies of DA since the Nafion coating strongly prevents the permeations of anionic compounds such as 3,4-dihydroxyphenylacetic acid (DOPAC) or 5-hydroxyindoleacetic acid (5-HIAA) through the Nafion film. This valuable property made the Nafion-modified electrode a good method to study DA, norepinephrine (NE) and 5-hydroxytryptamine (5-HT) which are cationic neurotransmitters [1]. This result in the increased sensitivity of the Nafion-modified electrode [2].

Besides that, with fast potential scan rate, Nafion could also prevent the oxidation products of the neurotransmitters from adsorbing on the electrode surface which leads to electrode fouling [3]. It is well known that DA undergoes intracyclization reaction which can lead to the formation of insoluble film on the electrode. This insoluble film will lead to decreased sensitivity of the electrode and the electrode can be used only for a limited time. Previous studies on the neurotransmitter's detection on electrode surface employed Nafion as an electrode modifier and the electrochemical behavior of DA on the Nafion-modified electrode was only studied in neutral pH due to the natural pH of the extracellular fluid of the brain.

Thus, in this chapter, we focused on studying electrochemistry of DA and 5-MDA in acidic and neutral pH solutions to study the electrochemical reaction of DA in acidic and neutral pH at Nafion-modified electrode. It is expected that due to the acidic pH, no intracyclization reaction will occur: the amino group of DA will be protonated and positively charged and it will be attracted to the negatively charged Nafion. Hence, the electrochemical behavior of DA at acidic pH will largely differ from that at neutral pH. The incorporation of DA and 5-MDA in the Nafion film during continuous potential cycles was studied in comparison between DA and 5-MDA since the methyl group of 5-MDA can affect its incorporation in the film. Different concentrations of buffer solution were employed to further understand the process of incorporation of DA and 5-MDA in the Nafion film during the continuous potential cycles.

4.2 Materials and methods

1 μL of Nafion® (5 wt. % solution, Sigma-Aldrich Co., USA) was dropped on GC electrode (diameter 3 mm) surface and left to dry for 30 min. The thickness of the Nafion film on the electrode surface was estimated from its density (1.98 g cm^{-3}) and it was approximately 3.6 μm. Then, cyclic voltammetry was carried out with the Nafion-modified GC electrode in Ar sat. 0.1 M NaCl solutions containing 5 or 50 mM universal buffers (pH 3 and 7) and 0.1 mM DA or 0.1 mM 5-MDA. Reference electrode used was Ag|AgCl|$KCl_{(sat)}$ and counter electrode used was platinum wire.

4.3 Results and discussions

4.3.1 Effect of pH and methyl group

DA and 5-MDA are more easily to be incorporated into the Nafion film at pH 3 compared to those at pH 7 (Figs. 4.1 to 4.8). This is due to the protonation of the amino group of DA and 5-MDA at pH 3 resulting to the attraction between the protonated amino group (NH_3^+) and the sulfonate group (SO_3^-) in Nafion. At pH 7, the amine group is neutrally charged and there is no interaction between the amino group of DA and 5-MDA with the sulfonate group making it difficult to incorporate the molecules into the Nafion film. Besides that, at pH 7, DA undergoes intracyclization forming leucodopaminechrome which may further decrease the interaction between DA and Nafion.

At pH 3 (Figs. 4.1, 4.2, 4.5 and 4.6), the cyclic voltammogram (CV) at 100^{th} cycle are bigger compared to the CV at 1^{st} cycle indicating that the DA and 5-MDA were incorporated in the Nafion film. This can be seen in Figs. 4.9 (A) and 4.10 (A), where approximately 111.34 x 10^{-10} mol cm^{-2} of DA and 116.98 x 10^{-10} mol cm^{-2} of 5-MDA were incorporated into the Nafion film. Due to the methyl group, it gave an extra hydrophobic effect to 5-MDA leading to the hydrophobic attraction between the 5-MDA and the polymer backbone of Nafion. Many studies have confirmed that interactions between Nafion and electroactive species are hydrophobic interaction and electrostatic attraction [4,5]. This leads to the higher amount of 5-MDA incorporated in the Nafion film compared to DA. At pH 7, approximately 23 x 10^{-10} mol cm^{-2} of DA and 38.8 x 10^{-10} mol cm^{-2} of 5-MDA were incorporated into the Nafion film.

4.3.2 Effect of buffer concentrations

The use of two different buffer concentrations (5 and 50 mM) gave significant impact on the DA and 5-MDA incorporation in Nafion film and the currents generated. For DA and 5-MDA in low buffer concentration (5 mM) at both acidic and neutral solutions, higher currents were observed compared to DA and 5-MDA at high concentration (50 mM) of buffer solutions. Anodic peak current (I_p^a) and cathodic peak current (I_p^c) values of DA and also those of 5-MDA at low concentration of buffer solutions are especially high which can be seen from the 1st to 20th potential cycles (Figs. 4.9 to 4.12). This means that DA and 5-MDA are more easily incorporated in the Nafion film at low buffer concentration (Figs. 4.9 to 4.12).

Comparing the currents observed at the 1st potential cycle, at pH 3 (Fig. 4.9(B)), low concentration (5 mM) of buffer gave higher value of I_p^a (33.69 µA) of DA compared to the high concentration (50 mM) of buffer (9.98 µA). The I_p^a value of 5-MDA (Fig. 4.10(B)) is also higher at low concentration (5 mM) of buffer (18.34 µA) compared to high concentration (50 mM) of buffer (6.4 µA). These different values indicate that at pH 3, currents generated by DA or 5-MDA depends on the concentration of buffer solution. Meanwhile at pH 7, the trend is also the same where higher I_p^a values can be observed at low concentration (5 mM) of buffer (11.32 µA for DA and 15.05 µA for 5-MDA) compared to high concentration (50 mM) of buffer (6.12 µA for DA nd 3.26 µA for 5-MDA) as shown in Figs. 4.11(B) and 4.12(B). Hence, we can conclude that low concentration of buffer leads to high current at any pH of solution.

The use of high buffer concentration proved to be a disadvantage since the quantities of DA and 5-MDA which can be incorporated into the Nafion film were limited due to several factors. First, the high concentration buffer may give some resistance to the diffusion of DA and

5-MDA from bulk solution to the Nafion film. Second, the cations in the buffer solution (Na^+) may compete with the cation groups (NH_3^+) of DA and 5-MDA (at pH 3) for the electrostatic binding at the anionic groups (SO_3^-) in the Nafion which leads to the slow incorporation into Nafion. Adams et al. (1985) observed the same phenomena where the electroinactive cationic species in the solution could occupy the anionic sites in the Nafion film [6]. This further reduced the sensitivities of the electrode which then lead to reduced current observed.

4.3.3 Effect of Nafion

The $E^{o'}$ values of DA at pH 3.2 and 7.1 are (0.39 ± 0.00) and (0.22 ± 0.01) respectively and it remained almost constant and from 1st to 100th potential cycles. Value of $E^{o'}$ of DA was not affected by the buffer concentrations. At pH 7, the $E^{o'}$ value of DA at Nafion-modified GC is the same as the $E^{o'}$ of DA at bare GC (0.22 V). However, at pH 3, the $E^{o'}$ of DA at Nafion-modified GC (0.39 V) shifted negatively compared to the $E^{o'}$ of DA at bare GC (0.43 V). This difference may be due to the effect of hydrophobic and electrostatic attraction between DA and Nafion at pH 3 that led to the negatively shifted of the $E^{o'}$ value. This means that due to the Nafion film, the DA has become more easily oxidized and/or more stable in the reduced form.

At pH 7, the $E^{o'}$ value of 5-MDA in 5 mM buffer solution changed from 0.15 V to 0.18 V (from 1st to 100th potential cycles) meanwhile $E^{o'}$ value of 5-MDA in 50 mM buffer solution at did not change significantly with average of 0.16 V. The reason why $E^{o'}$ value increased in 5 mM buffer solution may be due to the high concentration of 5-MDA incorporated in the Nafion film. We have observed from the results in previous chapter (Chapters 2 and 3) that high concentrations of DA (or 5-MDA) subsequently lead to positively shifted $E^{o'}$ values. The $E^{o'}$

value of 5-MDA in 50 mM buffer solution of pH 7 at Nafion-modified GC (0.16 V) is similar to the $E^{o'}$ value of 5-MDA in the same solution of pH 7 at bare GC (0.17 V). The $E^{o'}$ value of 5-MDA at pH 3 are quite similar at the different concentration of buffer solutions: 0.33 V (5 mM buffer) and 0.35 V (50 mM buffer). Both values are less positive compared to the $E^{o'}$ value of 5-MDA at bare GC (0.39 V). This means that redox reaction of 5-MDA is better at Nafion modified GC since 5-MDA is more easily oxidized and/or stable in the reduced form.

The ΔE_p values (Fig. 4.13(A) and (B)) for DA and 5-MDA at pH 7 are higher (0.3 to 0.5 V) compared to those at pH 3 (0.1 to 0.3 V). At both pH, reactions of DA and 5-MDA are irreversible. This may be due to the Nafion film on electrode surface increasing the length of electron transfer from the electrode surface to the DA or 5-MDA through the sulfonate chains. This further lead to slow electron transfer. Besides that, at pH 7, the uncharged amino groups of DA or 5-MDA are mostly repelled on the negatively charged Nafion film. Another reason may be due to the higher concentration of cation (Na^+) in the solution of pH 7 compared to that in the solutions of pH 3 that occupied the anionic sites and preventing reaction with DA and 5-MDA (Fig. 4.11).

This trend is the opposite for DA and 5-MDA at bare GC where ΔE_p values at pH 7 are smaller than that at pH 3. This also means that electrostatic attraction helps in the decreasing of the value of ΔE_p. It is worth to mention that the ΔE_p values from the first CVs of DA and 5-MDA at Nafion-modified GC in the solution of pH 3 are smaller (0.258 V for DA and 0.216 V for 5-MDA) compared to those at bare GC (0.415 V for DA and 0.310 V for 5-MDA). This further confirms that electrostatic attraction plays an important role in the decreased value of ΔE_p and increased in electron transfer.

4.3.4 Leaching of DA and 5-MDA from Nafion film

All of the DA and 5-MDA that were incorporated in the Nafion film leached out from the film when the electrode potential was scanned repeatedly in the absence of DA and 5-MDA at pH 7. DA and 5-MDA in high concentration buffer solution at pH 3 leached out slowly from the Nafion film (Figs. 4.14, 4.15, 4.16 and 4.17). This means that high concentration buffer gave some resistance effect in the solution to the mass transfer of DA and 5-MDA exiting from the Nafion film into the bulk solution. Besides that, the positively charged amine group of DA and 5-MDA at pH 3 electrostatically attracted with the negatively charged sulfonate group of the Nafion. The DA and 5-MDA did not attach strongly in the Nafion film meaning that Nafion modification of electrode is not suitable for a strong bonding of DA and 5-MDA in the Nafion film.

4.4 Conclusion

DA and 5-MDA are easily incorporated in the Nafion film in acidic solution due to the electrostatic attraction between the negatively charged sulfonate group (SO_3^-) in Nafion and positively charged amino group (NH_3^+) in DA and 5-MDA. However, the methyl group (CH_3) in 5-MDA contributed to higher current due to hydrophobic attraction compared to DA in both acidic and neutral pH solutions. The electrostatic attraction between the amino group and sulfonate group is relatively weak since the incorporated DA and 5-MDA in Nafion film eventually leached out from the film. Low buffer concentration used in the solutions leads to higher current observation during the incorporation period due to the less competition for anionic sites (SO_3^-) between the electroinactive cation (Na^+) and electroactive cation (NH_3^+) species in

the solution. The Nafion film increased the electron transfer of DA and 5-MDA at pH 3 but decreased the electron transfer at pH 7 when compared to the reaction without the Nafion film at bare electrode without modification of Nafion.

4.5 References

[1] G.A. Gerhardt, A.F. Oke, G. Nagy, B. Moghaddam and R.N. Adams, *Brain Research* **290** (1984) 390-395.

[2] M.P. Brazell, R.J. Kasser, K.J. Renner, J. Feng, B. Moghaddam and R.N. Adams, *J. Neuro. Met*. **22** (1987) 167-172.

[3] J.E. Baur, E.W. Kristensen, L.J. May, D.J. Wiedemann and R.M. Wightman, *Anal. Chem*. **60** (1988) 1268-1272.

[4] H.S. White, J. Leddy and A.J. Bard, *J. Am. Chem. Soc*. **104** (1982) 4811-4817.

[5] M.N. Szentirmay and C.R. Martin, *Anal. Chem*. **56** (1984) 1898-1902.

[6] G. Nagy, G.A. Gerhardt, A.F. Oke, M.E. Rice, R.N. Adams, R.B.Moore, M.N. Szentirmay and C.R. Martin, *J. Electroanal. Chem*. **188** (1985) 85-94.

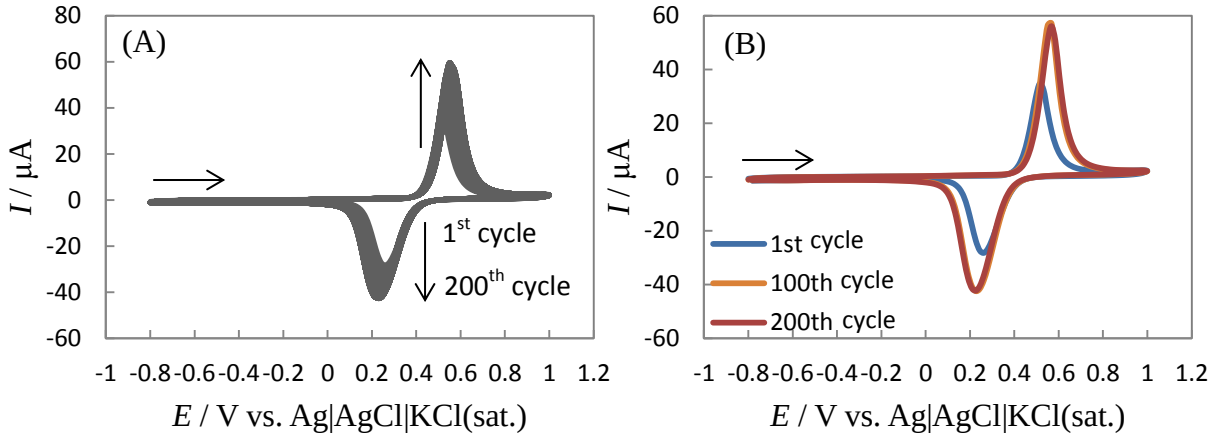

Fig. 4.1. (A) Continuously recorded and (B) selected cyclic voltammograms (CVs) of 0.1 mM DA at Nafion-modified GC electrode in 0.1 M NaCl containing 5 mM universal buffer solution (pH 3.20). Potential scan rate: 100 mVs^{-1}.

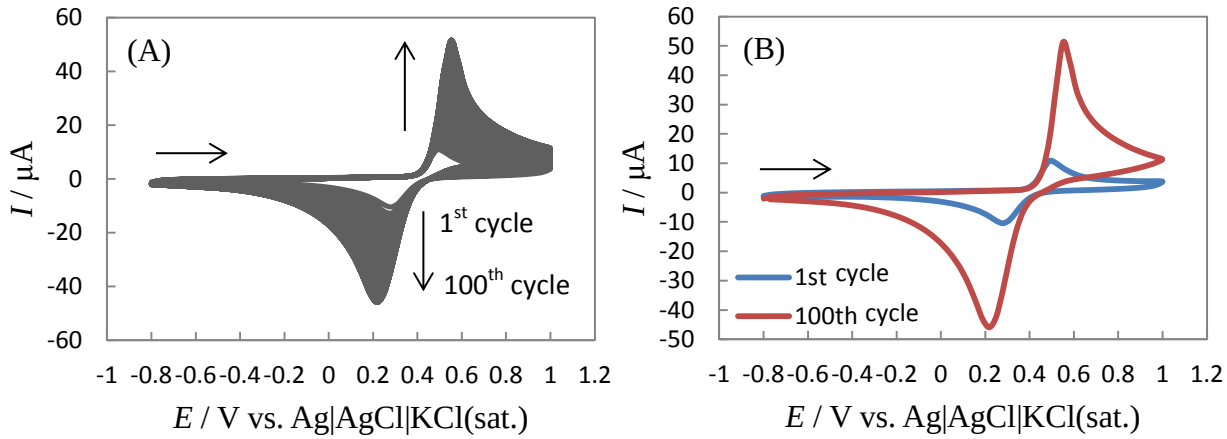

Fig. 4.2. (A) Continuously recorded and (B) selected CVs of 0.1 mM DA at Nafion-modified GC electrode in 0.1 M NaCl containing 50 mM universal buffer solution (pH 3.13). Potential scan rate: 100 mVs^{-1}.

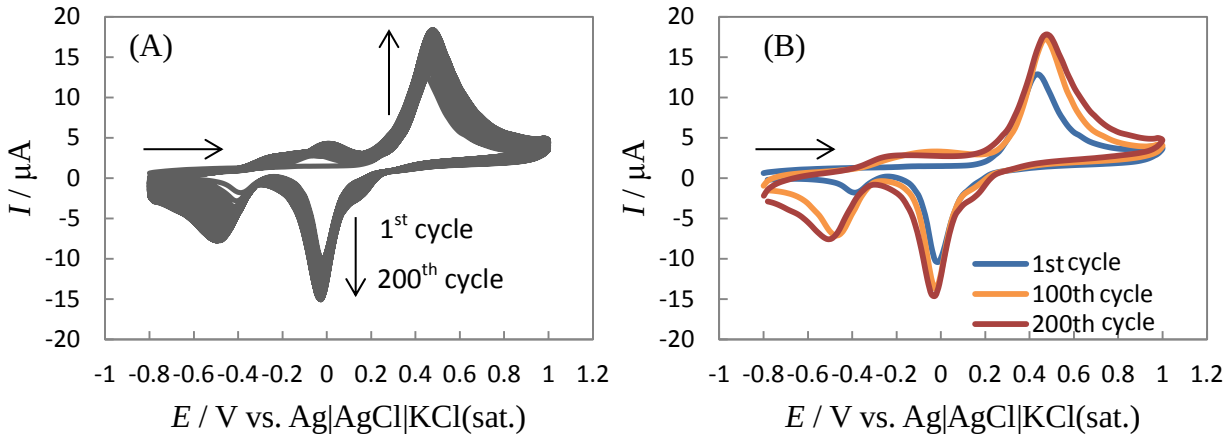

Fig. 4.3. (A) Continuously recorded and (B) selected CVs of 0.1 mM DA at Nafion-modified GC electrode in 0.1 M NaCl containing 5 mM universal buffer solution (pH 7.07). Potential scan rate: 100 mVs^{-1}.

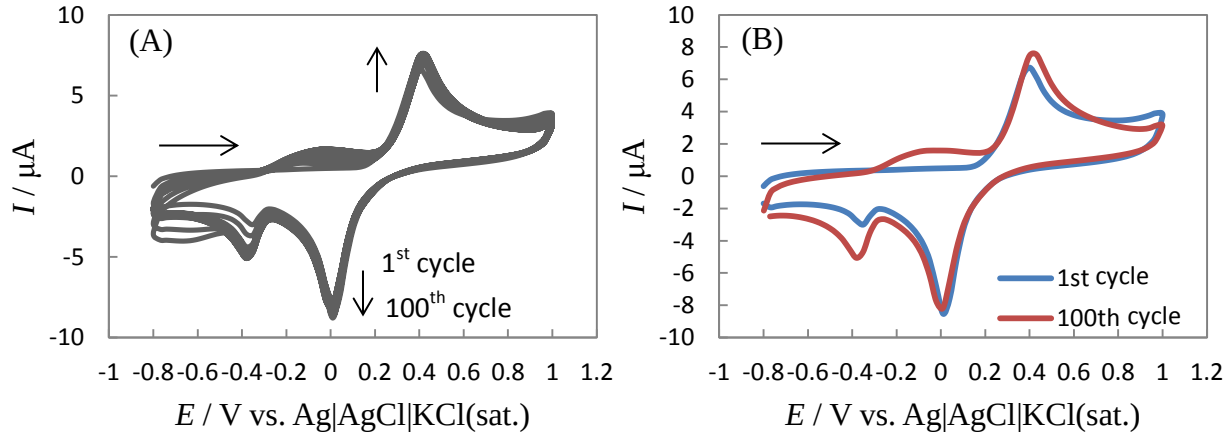

Fig. 4.4. (A) Continuously recorded and (B) selected CVs of 0.1 mM DA at Nafion-modified GC electrode in 0.1 M NaCl containing 50 mM universal buffer solution (pH 7.15). Potential scan rate: 100 mVs^{-1}.

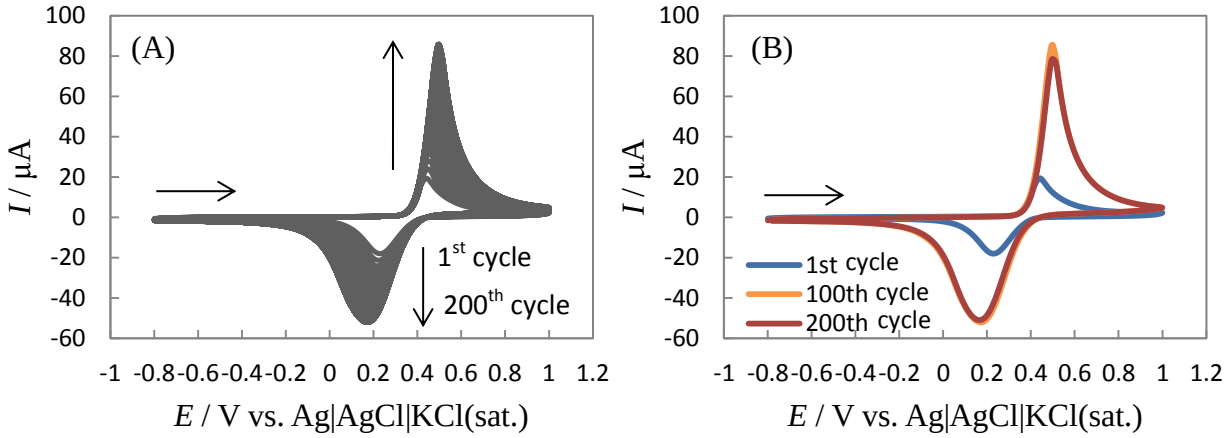

Fig. 4.5. (A) Continuously recorded and (B) selected CVs of 0.1 mM 5-MDA at Nafion-modifieed GC electrode in 0.1 M NaCl containing 5 mM universal buffer solution (pH 3.20). Potential scan rate: 100 mVs^{-1}.

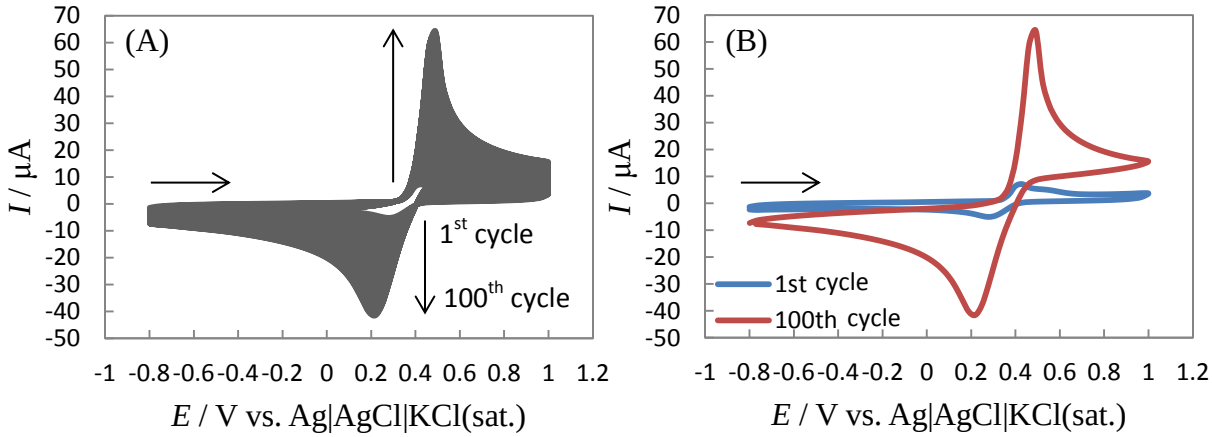

Fig. 4.6. (A) Continuously recorded and (B) selected CVs of 0.1 mM 5-MDA at Nafion-modified GC electrode in 0.1 M NaCl containing 50 mM universal buffer solution (pH 3.13). Potential scan rate: 100 mVs^{-1}.

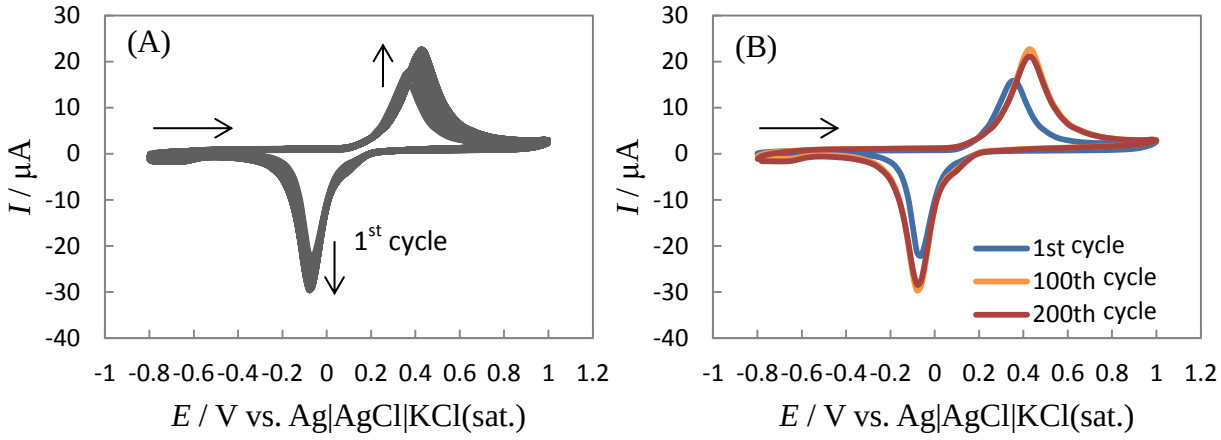

Fig. 4.7. (A) Continuously recorded and (B) selected CVs of 0.1 mM 5-MDA at Nafion-modified GC electrode in 0.1 M NaCl containing 5 mM universal buffer solution (pH 7.07). Potential scan rate: 100 mVs^{-1}.

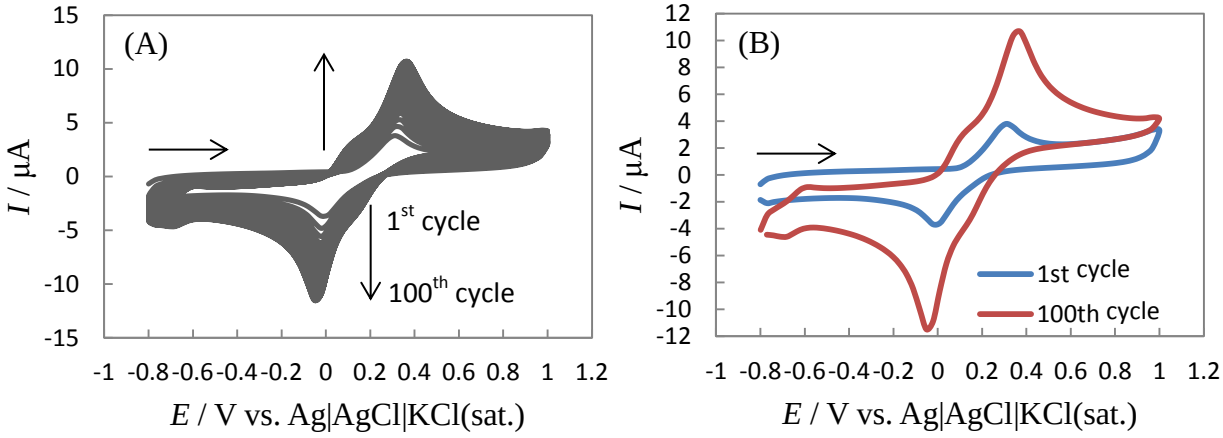

Fig. 4.8. (A) Continuous recorded and (B) selected CVs of 0.1 mM 5-MDA at Nafion-modified GC electrode in 0.1 M NaCl containing 50 mM universal buffer solution (pH 7.15). Potential scan rate: 100 mVs^{-1}.

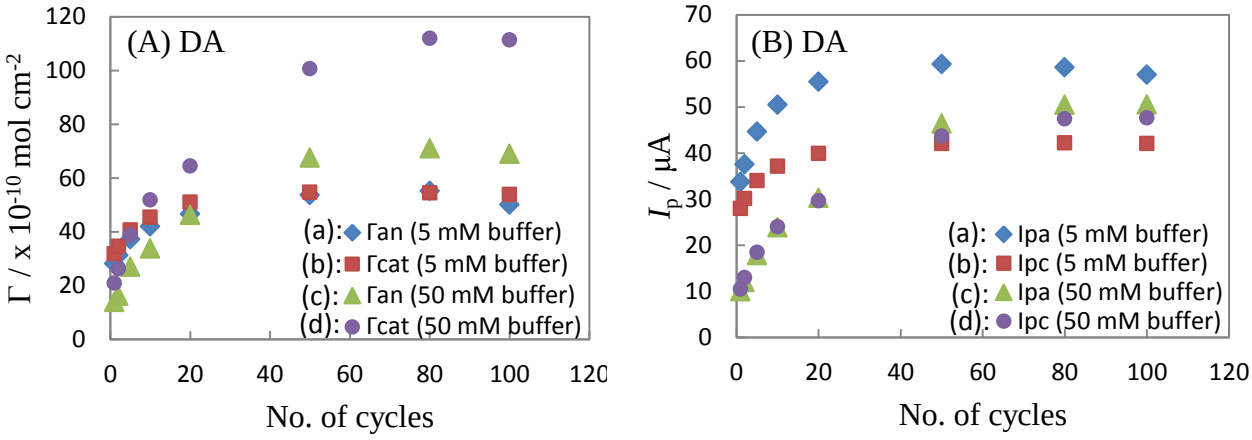

Fig. 4.9. Plots of (A) Surface concentration, Γ (an: anodic; cat: cathodic) and (B) I_p (a: anodic; c: cathodic) vs. No. of potential cycles. Data of (a) and (b) in (A) and (B) were taken from Fig. 4.1(A), and data of (c) and (d) in (A) and (B) were taken from Fig. 4.2(A).

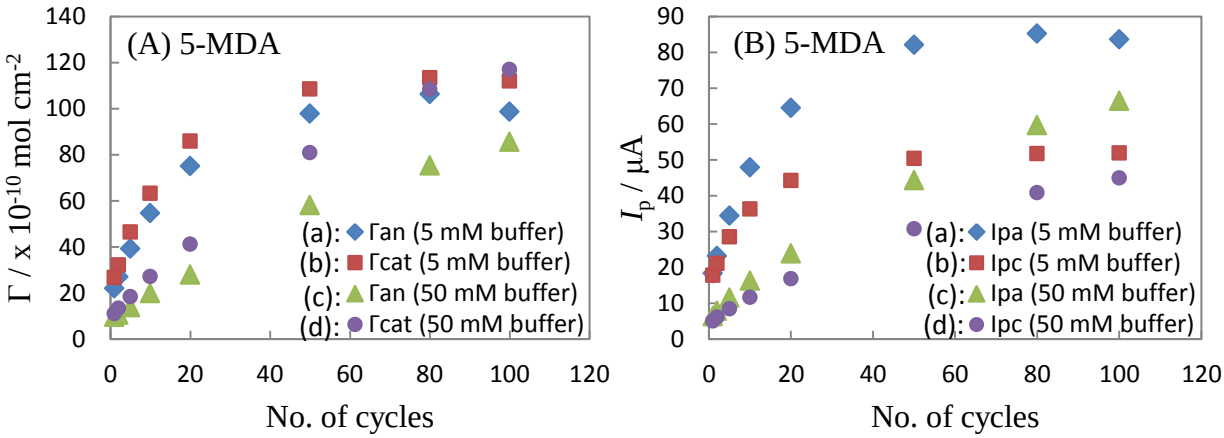

Fig. 4.10. Plots of (A) Surface concentration, Γ (an: anodic; cat: cathodic) and (B) I_p (a: anodic; c: cathodic) vs. No. of potential cycles. Data of (a) and (b) in (A) and (B) were taken from Fig. 4.5(A), and data of (c) and (d) in (A) and (B) were taken from Fig. 4.6(A).

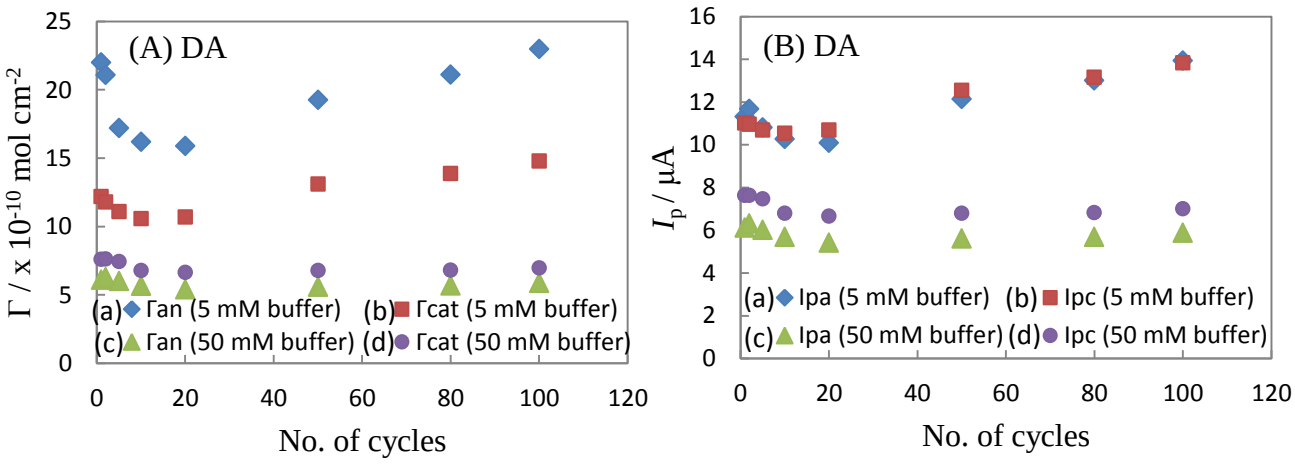

Fig. 4.11. Plots of (A) Γ (an: anodic; cat: cathodic) and (B) I_p (a: anodic; c: cathodic) vs. No. of potential cycles. Data of (a) and (b) in (A) and (B) were taken from Fig. 4.3(A), and data of (c) and (d) in (A) and (B) were taken from Fig. 4.4(A).

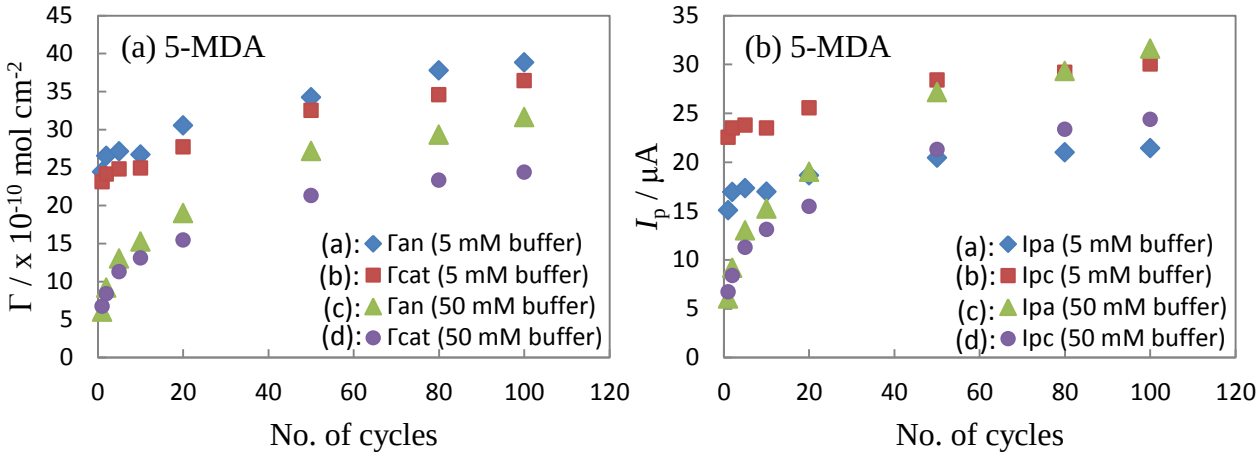

Fig. 4.12. Plots of (A) Γ (an: anodic; cat: cathodic) and (B) I_p (a: anodic; c: cathodic) vs. No. of cycles. Data of (a) and (b) in (A) and (B) were taken from Fig. 4.7(A), and data of (c) and (d) in (A) and (B) were taken from Fig. 4.8(A).

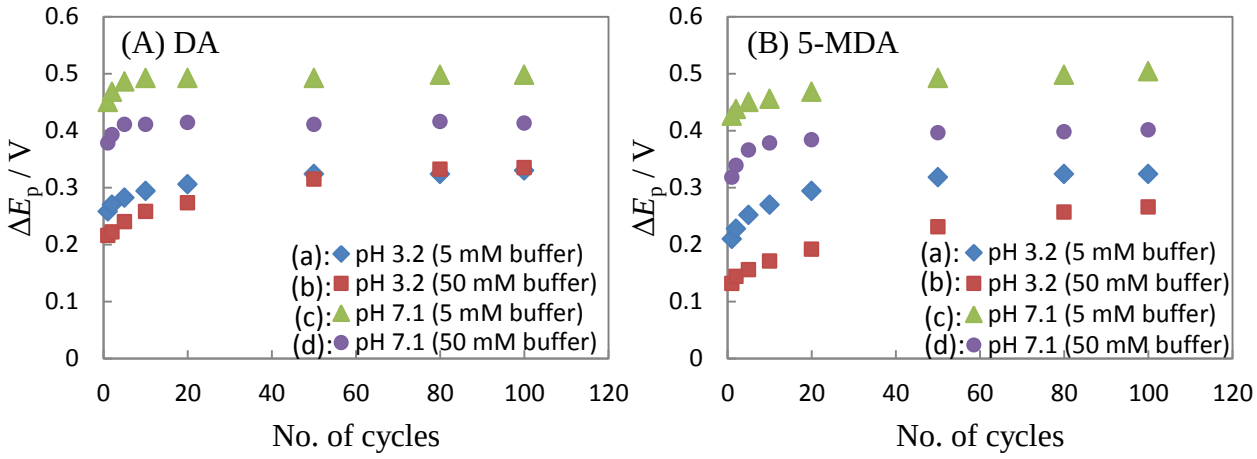

Fig. 4.13. Plots of ΔE_p in CVs of (A) DA and (B) 5-MDA vs. No. of potential cycles. Data of (a), (b), (c) and (d) in (A) were taken from Figs. 4.1(A), 4.2(A), 4.5(A) and 4.6(A), respectively, and data of (a), (b), (c) and (d) in (B) were taken from Figs. 4.3(A), 4.4(A), 4.7(A) and 4.8(A), respectively.

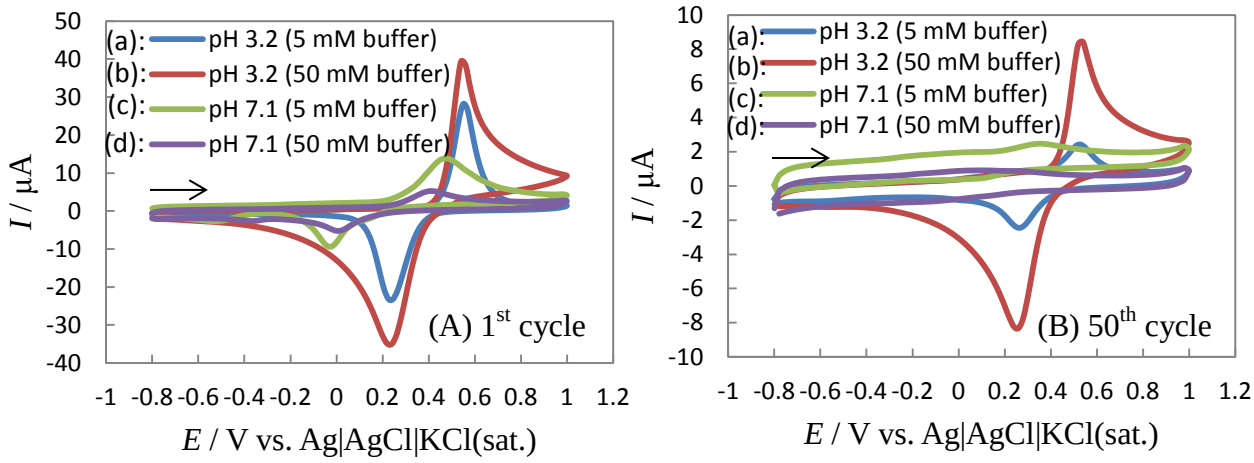

Fig. 4.14. Comparison of the 1st and 50th CVs obtained for DA adsorbed in Nafion-modified GC electrode during the 50 time-potential cycling in 0.1 M NaCl containing different buffer solutions ((a): 5 mM, pH 3.2; (b): 50 mM, pH 3.2; (c): 5 mM, pH 7.1; (d) 50 mM, pH 7.1). Potential scan rate: 100 mVs^{-1}.

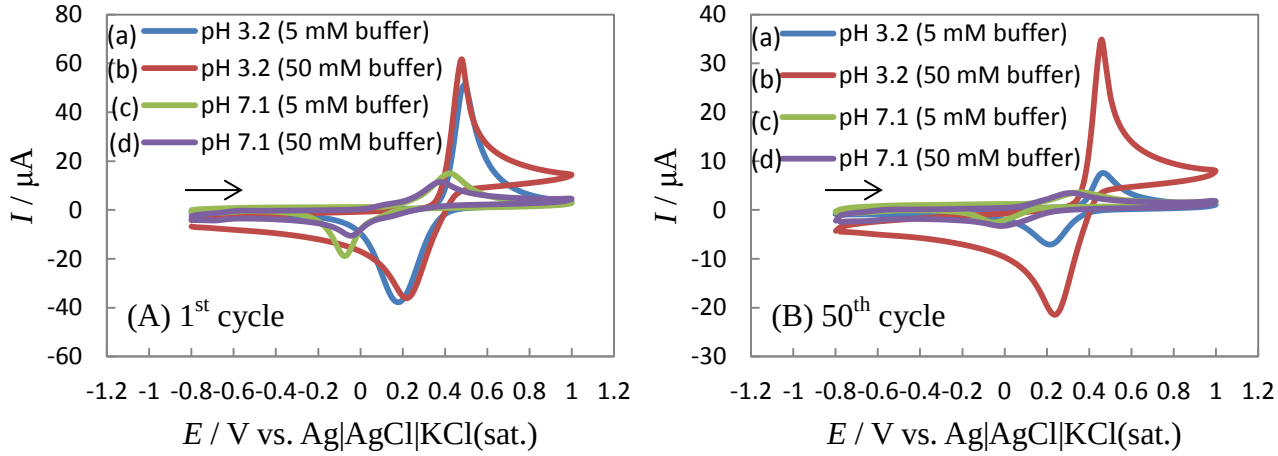

Fig. 4.15. Comparison of the 1st and 50th CVs obtained for 5-MDA adsorbed in Nafion-modified GC electrode during the 50 time-potential cycling in 0.1 M NaCl containing different buffer solutions ((a): 5 mM, pH 3.2; (b): 50 mM, pH 3.2; (c): 5 mM, pH 7.1; (d) 50 mM, pH 7.1). Potential scan rate: 100 mVs^{-1}.

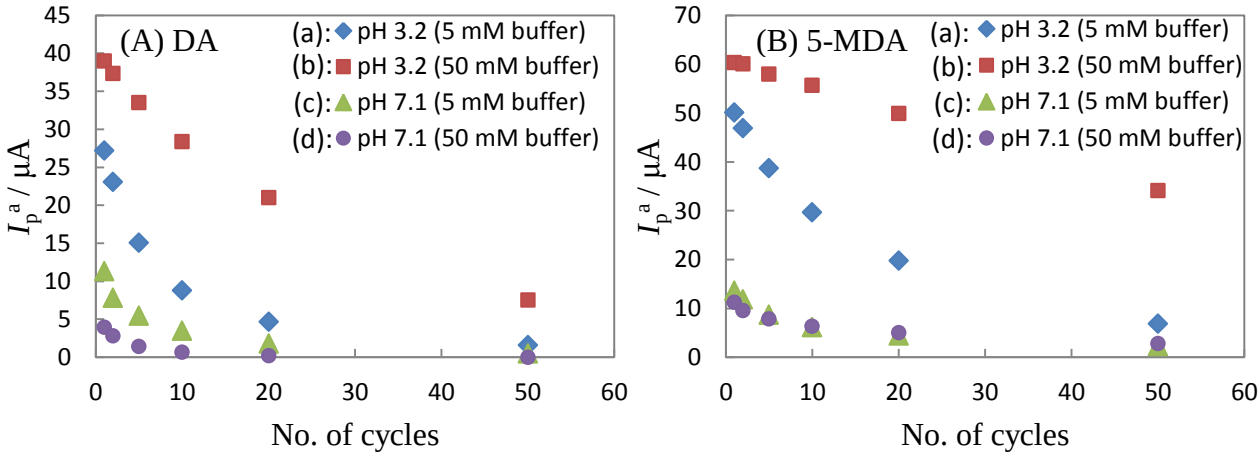

Fig. 4.16. Plots of I_p^a in CVs of (A) DA and (B) 5-MDA leaching out from Nafion film vs. No. of potential cycles. Data of (a), (b), (c) and (d) in (A) were taken from Figs. 4.14(A) and (B), respectively, and data of (a), (b), (c) and (d) in (B) were taken from Figs. 4.15(A) and (B), respectively.

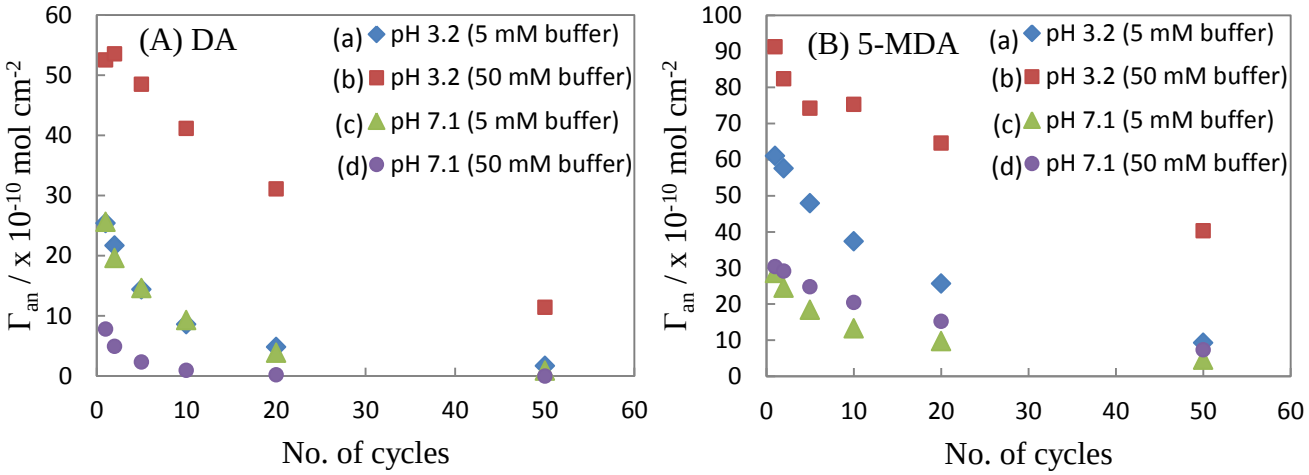

Fig. 4.17. Plots of Γ_{an} in CVs of (A) DA and (B) 5-MDA leaching out from Nafion film vs. No. of potential cycles. Data of (a), (b), (c) and (d) in (A) were taken from Figs. 4.14(A) and (B), respectively, and data of (a), (b), (c) and (d) in (B) were taken from Figs. 4.15(A) and (B), respectively.

CHAPTER 5

DOPAMINE (DA) and 5-METHYLDOPAMINE (5-MDA) COVALENTLY BONDED ON *p*-AMINOBENZOIC ACID (PABA)-MODIFIED ELECTRODE

5.1 Introduction

DA has been immobilized on the electrode surface through many techniques such as the binding of DA with self-assembled cysteamine monolayers on gold electrode [1], electrochemical oxidation of DA [2, 3] or a stepwise electrochemical grafting starting with the reduction of diazonium cation on electrode surface followed by immobilization of DA through amide bond coupling [3, 4]. In this study, the stepwise technique of immobilizing DA through diazonium reduction on electrode surface has been chosen because the distance between electrode surface and the bound DA is shorter compared to the bound DA in the self-assembled monolayer (SAM) technique. Besides that, the electrochemical oxidation technique will lead to surface roughening and large background currents [5].

Modification of surfaces with specific chemical functionalities has lots of possible applications such as in chemical and bio sensing, microelectronics and also protection from corrosion [6]. For example, redox mediators are covalently bound to the chemically modified electrode, which act as mediators for electron transport between the target redox species and the electrode. This leads to potential shift which is good for selective determination of the target redox species. These mediators could be the catechols, quinones, dyes and o-phenylenediamine [1].

Since DA in real biological sample coexists with other interference molecule such as ascorbic acid (AA), selective and sensitive detection of DA is important for accurate measurement. Many studies have been done on the redox reaction of DA and AA mixed solutions [7-10] and those chemically modified electrodes successfully separated the AA and DA peaks besides accurately determined their concentrations. In this chapter, the electrochemical grafting of diazonium on the electrode and the subsequent binding of DA will be employed for AA determination. It is also worth to mention that this study will not focus on the selective detection of DA and AA mixed solution.

The electrode modification method will be employed in 2 steps. In the first step, reduction of *p*-aminobenzoic acid (PABA) diazonium on the electrode surfaces. This will form a layer of phenyl with carboxyl (COOH) terminal group. Then, in the second step, DA will be bonded to this COOH group through amide bond coupling. The reduction of PABA will be done on GC and EPPG electrodes to determine the effect of electrode structure to the reduction's mechanism. Both DA and its analogue, 5-MDA will be used for the second step to compare the difference in molecular structures to the amide bond coupling. Electrochemistry of bound DA and 5-MDA will be compared to the free DA and 5-MDA from Chapter 2 and 3. Finally, the AA oxidation on the modified electrodes will be measured.

5.2 Materials and methods

5.2.1 Materials

Sodium nitrite ($NaNO_2$) was purchased from Kanto Chemical Co. Inc., Japan. Hydrochloric acid (HCl), *p*-aminobenzoic acid (PABA) and 2-[4-(2-Hydroxyethyl)-1-piper

azinyl]ethanesulfonic acid (HEPES) were supplied by Wako Pure Chmical Industries Ltd., Japan. N-Hydroxysulfosuccinimide (Sulfo-NHS) was obtained from Thermo Scientific, 1-(3-dimethylaminopropyl)-3-ethylcarbodiimide hydrochloride was supplied by Tokyo Chemical Industry Co. Ltd., Japan and L-ascorbic acid (AA) was purchased from Aldrich Chemical Company, Inc. The reagents used are all analytical grade. The aqueous solutions were prepared using water purified by Millipore Milli-Q system (Millipore, Japan).

5.2.2 DA and 5-MDA covalently bonded to PABA-modified EPPG

Two hundred microliter aliquots (200 µL) of chilled 0.1 M $NaNO_2$ solution (0 °C) was slowly dropped into Ar sat. 0.5 M HCl solution containing 1 mM PABA. Then, the solution was left for 5 min for reaction to take place (Scheme 5.1(a) and (b)) and electrochemical modification (Fig. 5.1(b) and (c)) was done on the roughened edge plane pyrolytic graphite (EPPG) electrode (Φ = 3 mm, the electrode surface was roughened using sandpaper 600 in advance) with potential scan between +0.7 and -0.5 V vs. Ag|AgCl|KCl(sat.) for 5 cycles at 50 mVs^{-1} [11]. PABA-modified electrode was obtained (Scheme 5.1). Then, the PABA-modified EPPG was soaked in Ar sat. 0.05M HEPES buffer solution (pH 7.5) containing coupling agents (i.e., 10 mM N-hydroxysulfosuccinimide (Sulfo-NHS) and 10 mM 1-ethyl-3-(3-dimethylaminopropyl)carbodiimide (WSC)) and 3 mM DA (or 5-MDA) for 1 hr. Thus obtained modified-electrode will have DA bound to the PABA as shown in Scheme 5.2.

5.2.3 Adsorption of DA and 5-MDA on bare EPPG

EPPG was soaked in Ar sat. 0.05M HEPES buffer solution (pH 7.5) containing 3 mM DA (or 5-MDA) for 100 sec.

5.2.4 Oxidation of ascorbic acid (AA) at modified electrodes

The modified electrodes were examined in Ar sat. 0.1M HEPES buffer solution (pH 7.5) in the absence and the presence of 2 mM AA by cyclic voltammetry which was performed at various scan rates.

5.3 Results and discussion

5.3.1 DA and 5-MDA covalently bonded on PABA-modified electrodes

PABA was successfully bound on the surface of EPPG as can be observed from Fig. 5.1. The 1st CV has a distinct reduction peak (at ~ 0.25 V) and higher current compared to the 5th CV. This shows that the PABA diazonium was largely reduced on the electrode surface in the first potential scan. At the 5th potential scan, the electrode surface is completely covered with the PABA and no PABA diazonium in the solution could be reduced or bind on the electrode surface since there is no reduction peak can be observed due to limited space for the reduction process. Even if the potential scan was continued up to ten cycles (not shown), the current remained the same as that in the 5th CV indicating that no PABA was being reduced on the electrode surface anymore. The CV of PABA-modified EPPG in HEPES buffer solution is shown in Fig. 5.2. PABA is an electroinactive compound. Hence, no redox peak can be detected.

DA was successfully bound to the PABA modified EPPG (Figs. 5.3 and 5.5). There is no leucodopaminechrome / dopaminechrome peak (-0.25 V) in the CVs indicating that intracyclization could not occur since the amine group of DA was bonded with PABA through amide bond. 5-MDA was also successfully bound to the PABA-modified EPPG as can be seen from Figs. 5.4 and 5.5. The lines in Fig. 5.5(A) show a linear relationship meaning that both DA and 5-MDA are confined on the electrode surface. The plot in Fig. 5.5(B) did not show linear relationship further confirming the fact that DA and 5-MDA are confined at the surface.

The surface concentrations of DA and 5-MDA or the amount of DA and 5-MDA bound to the PABA were estimated to be 0.6×10^{-10} and 1.2×10^{-10} mol cm^{-2}, respectively. These values were estimated from the CVs obtained at scan rate of100 mVs^{-1}. DA can be assumed to bind to the electrode in lesser amount compared to 5-MDA suggesting that the methyl group made the 5-MDA easier to bind to the PABA compared to DA. This could be due to the extra hydrophobic attraction given by the methyl group of 5-MDA making it more attracted towards the phenyl compound of the PABA bound on the electrode. Other than this, since the solution's pH used for amide bond coupling is pH 7.5, it is possible that DA in the solution may undergo intracyclization reaction, reducing the quantity of free amino group in the solution.

The peak current ratio (Fig. 5.6(A)) of both DA and 5-MDA redox reactions is near to unity (~1) at high scan (200 mVs^{-1}) rate. However, with decreasing scan rate, peak current ratio decreased too. At the lowest scan rate (10 mVs^{-1}), peak current ratio of DA decreased to 0.5 while peak current ratio of 5-MDA decreased to near 0.6. This could be due to the hydroxide attacked the quinone form of DA (or 5-MDA) at high pH which lead to the electroinactivity of DA and 5-MDA [1]. The low potential scan rate means that the DA and 5-MDA will be in the quinone form for a longer time which gives the hydroxide group more time for it to attack the

quinone forms of DA (or 5-MDA) compared to those at higher potential scan rate. The decreased peak current ratio of DA cannot be due to intracyclization since the amino group was being used for the formation of the amide bond between DA and PABA on the electrode, hence intracyclization could not occur and there is no leucodopaminechrome / dopaminechrome peak observed from the CV (Fig. 5.3).

There is no clear trend between the peak separation values of DA and 5-MDA bound on electrode surface and the potential scan rates (Fig. 5.6(B)). However, roughly we can say the trends are increase in peak separation values with increase of potential scan rate. The exception is only at 50 mVs^{-1} where at this scan rate, the peak separation values are similar for both DA and 5-MDA at 35 mV. At this scan rate, the different molecular structures of DA and 5-MDA attached on the surface of electrodes did not give any effect on the peak separation values.

We know that from Chapter 2 and 3, the peak separation values of 5-MDA (in solution) are always lower than DA (in solution) since 5-MDA is easily oxidized and/or stable in reduced form. Hence, the peak separation values trend from DA and 5-MDA dissolved in solutions cannot be used for DA and 5-MDA bound to chemically modified electrodes. Besides that, concentration also plays a major role in the peak separation value where at high concentration, peak separation value was shifted positively. So, the peak separation values from both dissolved and bound DA and 5-MDA cannot be compared easily.

5.3.2 Ascorbic acid oxidation on modified electrodes

The modified electrodes may electrochemically catalyze the AA oxidation since high oxidation current can be seen in presence of AA compared to in absence of AA (Fig. 5.7).

However, the oxidation current on bare electrode is much higher compared to the modified electrodes. In addition, the AA oxidation potential from bare electrode is more negative than the modified electrodes indicating that AA is more easily oxidized on bare electrode. This is due to the blocked electrode surface due to the PABA binding which prevented the AA to oxidize directly on the electrode surface.

The 5-MDA-modified EPPG gave higher oxidation current compared to DA-modified EPPG. This means that the higher amount of 5-MDA on the EPPG gave higher current compared to the lower amount of DA on the EPPG. The PABA-modified EPPG catalyzed the electrochemical oxidation of AA better than the DA- and 5-MDA-modified EPPGs but worse than the bare EPPG. The reason could be due to resistance or steric effect of the DA and 5-MDA blocking the AA from reaching the electrode surface directly. This leads to reduced AA oxidation current and positively shifted oxidation potential. From the figure, we can conclude that the more layers are on the surface, the less AA oxidation reaction can occur.

5.3.3 Effect of electrode material on the modification

Different electrode material gives different results on the reduction of PABA diazonium. The difference can be seen from the reduction current of PABA on GC surface (Fig. 5.8). In this figure, two broad peaks (at +0.3 and -0.15 V) can be observed from GC electrode compared to (only one peak at +0.25 V was observed) EPPG electrode (Fig. 5.1). Besides that, the PABA diazonium was reduced faster on GC electrode as can be seen from similar currents in 3^{rd}, 4^{th} and 5^{th} CVs meaning that the GC electrode surface has been completely covered with PABA after 2 reduction cycles. Baranton and Belanger (2005) also observed the same two peaks where the

second peak at negative potential (in this study; -0.15 V) is contributed by the reduction of the aryldiazonium cations into radicals [11]. Then, the radicals subsequently binds to the GC surface covalently. However, the origin of the first peak at positive potential (in this study; +0.3 V) is still not clearly understood and no explanation can be provided so far.

The DA bound covalently on PABA-modified GC can be seen from Figs. 5.9 and 5.10. The $E°'$ value of DA on modified GC and EPPG are quite similar at 0.18 and 0.19 V, respectively. The lines of anodic peak potential (I_p^a) vs potential scan rates (v) of DA on GC show linear relationship which is similar to the DA on EPPG. However, the I_p^a from the GC are higher compared to the EPPG. The plot of I_p^a vs $v^{1/2}$ show non-linear relationship indicating that the DA is bound on PABA modified GC.

The surface concentration of DA was estimated from the CV measured at100 mVs^{-1} and it was found to be 0.8 x 10^{-10} mol cm^{-2}. This value is a little bit higher compared to the value from modified EPPG (0.6 x 10^{-10} mol cm^{-2}). The current peak ratio of DA (Fig. 5.11(A)) on both GC and EPPG shows similar trends where at low potential scan rate, the current peak ratio decreased to near 0.5, and at high potential scan rate current peak ratio of DA is near to 1. The electron transfer on EPPG is slower compared to that on GC since the peaks separation (ΔE_p) value from EPPG are larger than that from GC (Fig. 5.11(B)) and the trends of ΔE_p value roughly increased as the potential scan rate increased. However, at 50 mVs^{-1}, the ΔE_p values are the same for both GC and EPPG electrodes.

The CVs comparison of GC and EPPG measured at selected scan rates is shown in Fig. 5.12. The current in CVs of modified GC are larger compared to that of modified EPPG. This is normal since the background response of bare GC is also larger compared to bare EPPG (not

shown). Fig. 5.13(A) further confirms that currents observed at bare GC are always larger compared to those at bare EPPG. However, the peak current observed from the AA oxidation on modified EPPG is higher compared to that at modified GC (Fig. 5.13(B)). The reason could be due to the compact structure of PABA layer formed on GC electrode, thus blocking AA from oxidizing directly on electrode surface. Hence, this is the reason why we use EPPG as the main electrode due to the good oxidation of AA.

5.3.4 Comparison of electrochemical behaviour between bound and free DA and 5-MDA

The electrochemical parameters of free DA (and 5-MDA) and bound DA (and 5-MDA) are shown in Table 5.1. The bound DA peak current ratio increased due to the amino group binds to the electrode surface preventing further DA oxidation pathway compared to the free DA. However, the ΔE_p value of free DA is smaller than that of bound DA. This difference could be due to the PABA layer on the electrode surface preventing DA to react directly on the electrode surface. This will lead to bigger ΔE_p value and slow electron transfer. Since DA redox reaction involves two electrons, the redox reaction of free DA is considered to be reversible (ΔE_p = 30 mV) while the redox reaction of bound DA is quasi-reversible (ΔE_p > 30 mV). Besides that, the value of $E^{\circ\prime}$ of free DA (0.16 V) is less positive compared to bound DA (0.19 V). The peak current ratio of free and bound 5-MDA are higher compared to DA. In free DA and 5-MDA form, the methyl group blocks the intracyclization reaction from occurring, thus the peak current ratio of 5-MDA is higher than DA. Even though the value of ΔE_p of 5-MDA is bigger compared to the DA, the $E^{\circ\prime}$ of 5-MDA is lower than DA. This means that the existing methyl group in 5-MDA shifted value of $E^{\circ\prime}$ negatively but increased the value of ΔE_p when comparing to DA.

5.4 Conclusion

The reduction of PABA diazonium on electrode surfaces is a simple technique to modify electrode surfaces. This technique could also serve as a method of studying the difference of electrochemical behaviour between free and bound DA or other catecholamines. Reduction of diazonium PABA on GC and EPPG electrodes gave the different results of the diazonium reduction which may be due to the interaction between the PABA diazonium and the GC and EPPG electrode surfaces. This lead to different behaviour of the PABA-modified GC and EPPG electrodes including the electrochemical oxidation of AA on the modified electrodes. AA was oxidized better at the modified EPPG compared to the modified GC.

5.5 References

[1] J. Sun, J. Xu, H. Fang and H. Chen, *Bioelectrochem. and Bioenerg*. **44** (1997) 45-50.

[2] R.S. Deinhammer, M. Ho, J.W. Anderegg and M.D. Porter, *Langmuir* **10** (1994) 1306-1313.

[3] J. Ghilane, F. Hauquier and J. Lacroix, *Anal. Chem*. **85** (2013) 11593-11601.

[4] B.D. Bath, H.B. Martin, R.M. Wightman and M.R. Anderson, *Langmuir* **17** (2001) 7032-7039.

[5] A.J. Downard, *Electroanal*. **12** (14) (2000) 1085-1096.

[6] J. Lyskawa and D. Belanger, *Chem. Mater*. **18** (2006) 4755-4763.

[7] C.R. Raj, K. Tokuda and T. Ohsaka, *Bioelectrochem*. **53** (2001) 183-191.

[8] C.R. Raj, T. Okajima and T.Ohsaka, *J. Electroanal. Chem*. **543** (2003) 127-133.

[9] P.R. Roy, T. Okajima and T. Ohsaka, *Bioelectrochem*. **59** (2003) 11-19.

[10] J. Huo, J. Li and Q. Li, *Mat. Sci. Eng*. **C33** (2013) 507-511.

[11] S. Baranton, D. Belanger, *J. Phys. Chem*. B. **109** (2005) 24401-24410.

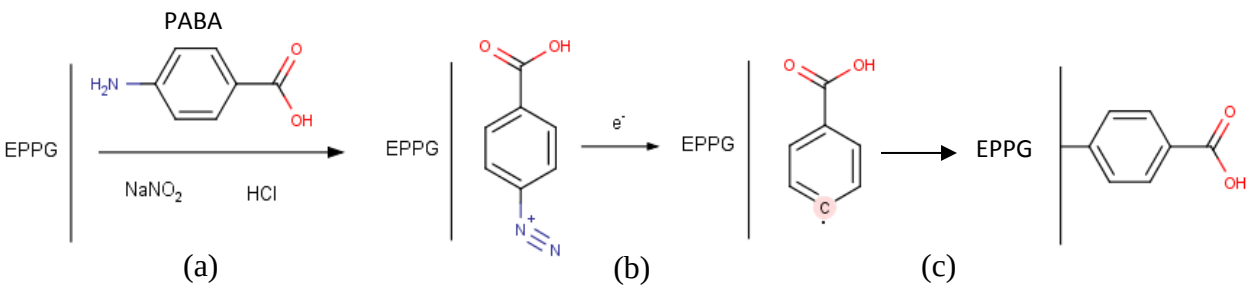

Scheme 5.1. Reduction of in situ generated diazonium cations on EPPG.

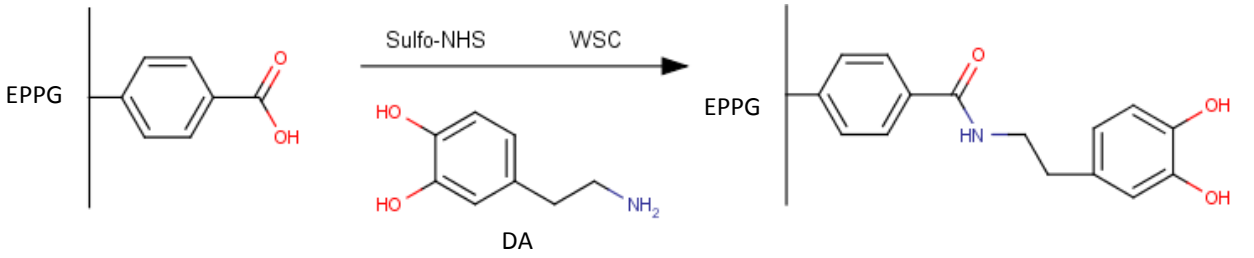

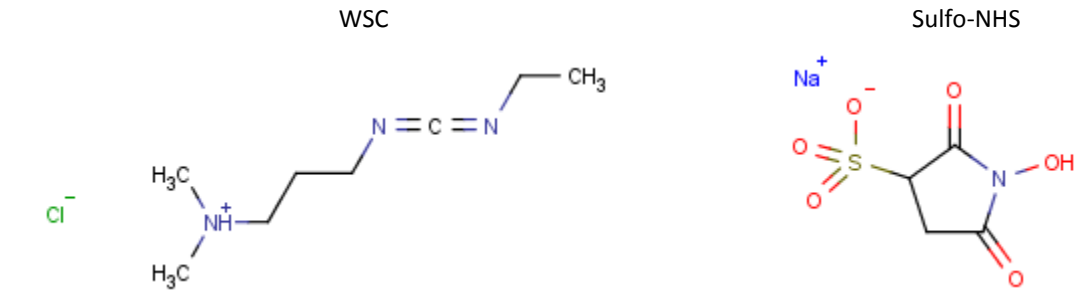

Scheme 5.2. DA covalently bound to PABA-modified EPPG through amide bond.

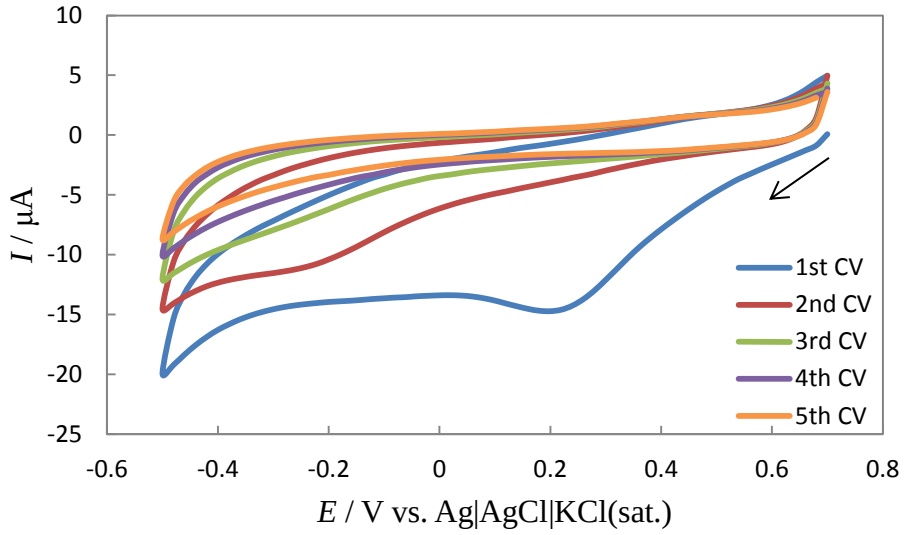

Fig. 5.1. Cyclic voltammograms (CVs) of diazonium cations reduction on EPPG in Ar sat. 0.5 M HCl solution containing 1 mM *p*-aminobenzoic acid and 2 mM $NaNO_2$ at 50 mVs^{-1}.

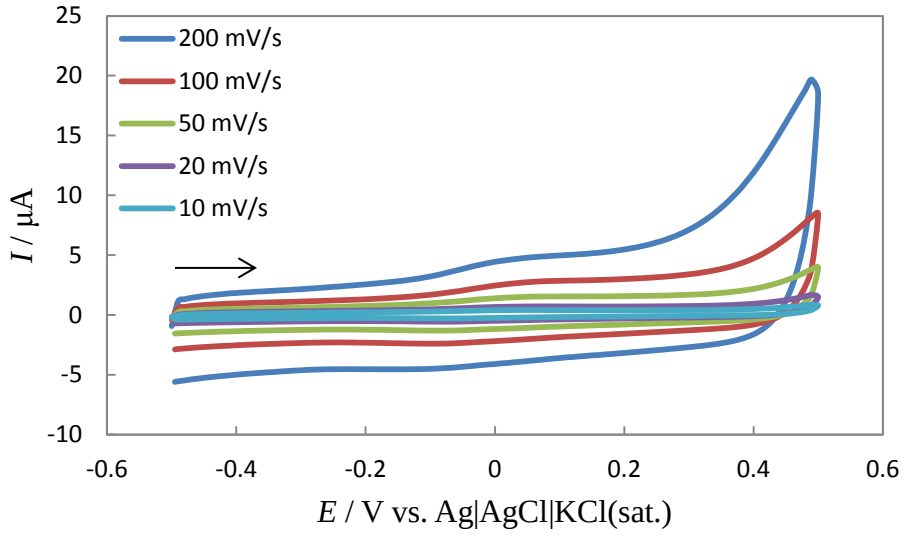

Fig. 5.2. CVs of PABA modified EPPG in Ar sat. 0.1M HEPES buffer solution (pH 7.5) at various scan rates.

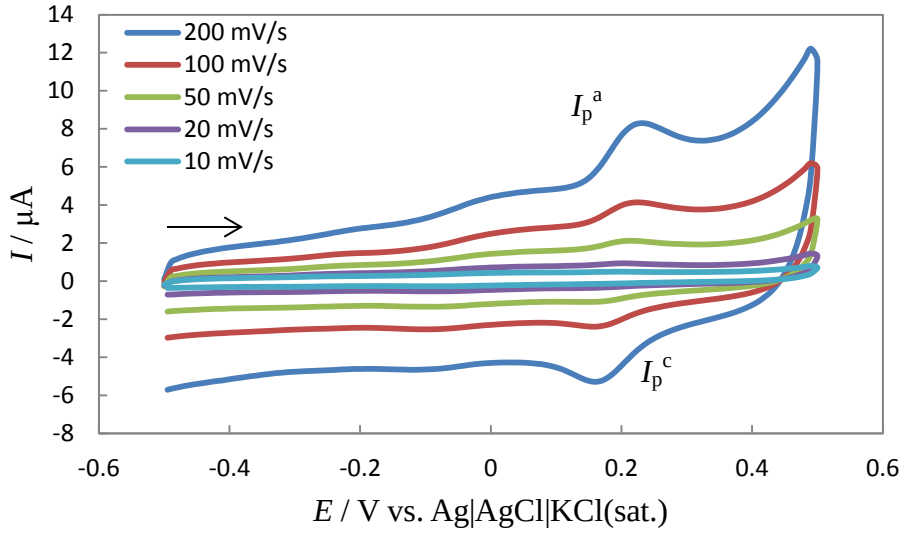

Fig. 5.3. CVs of DA/PABA modified-EPPG in Ar sat. 0.1M HEPES buffer solution (pH 7.5) at various scan rates.

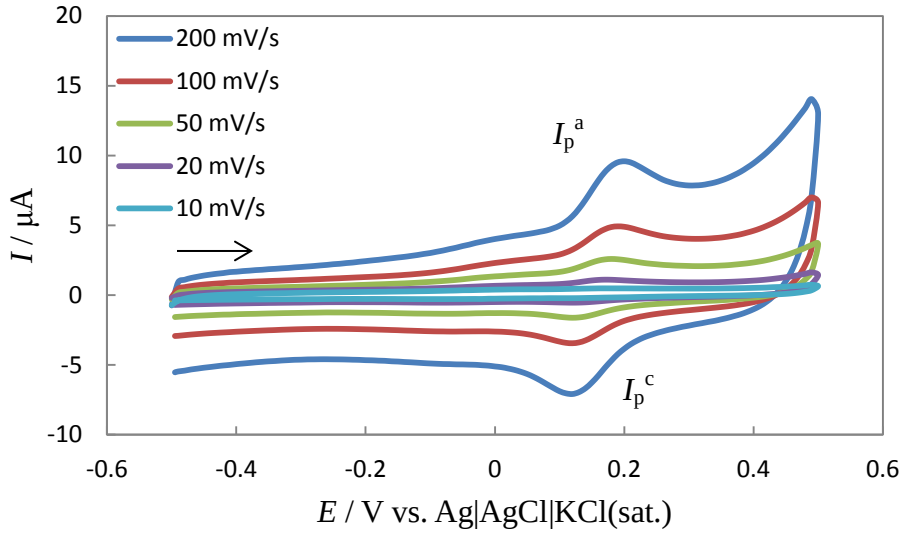

Fig. 5.4. CVs of 5-MDA/PABA modified EPPG in Ar sat. 0.1M HEPES buffer solution (pH 7.5) at various scan rates.

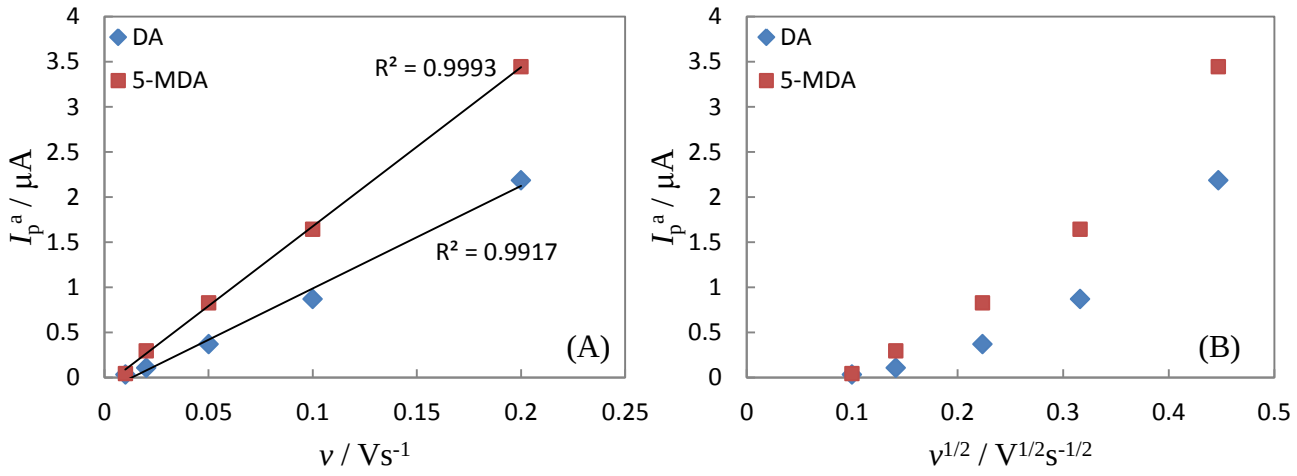

Fig. 5.5. Plots of (A) I_p^a vs. v and (B) I_p^a vs. $v^{1/2}$. Data were taken from Fig. 5.3 and 5.4.

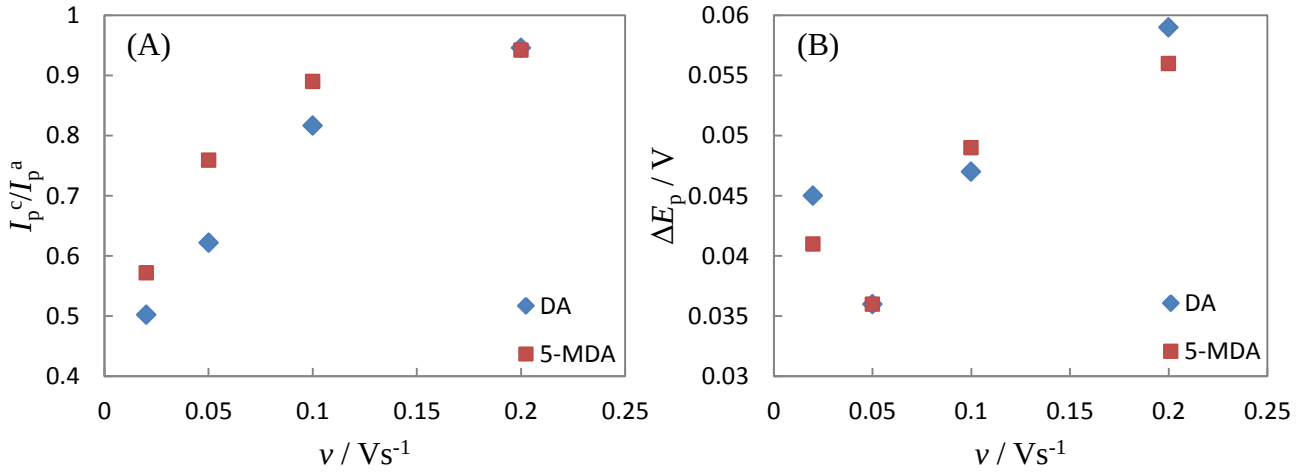

Fig. 5.6. Plots of (A) I_p^c / I_p^a and vs. v (B) ΔE_p vs. v. Data were taken from Fig. 5.3 and 5.4.

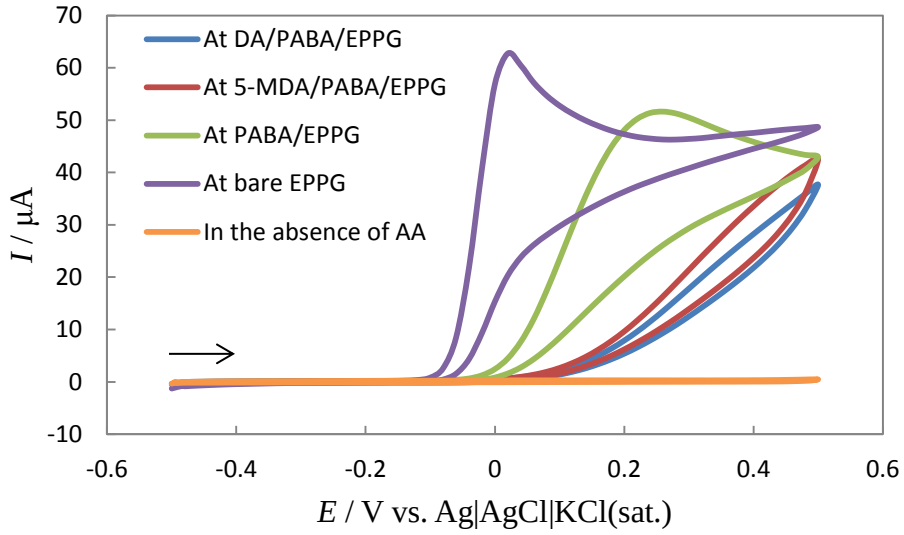

Fig. 5.7. CVs of various modified EPPGs in Ar sat. 0.1 M HEPES buffer solution (pH 7.5) containing 10 mM ascorbic acid at 5 mVs^{-1}.

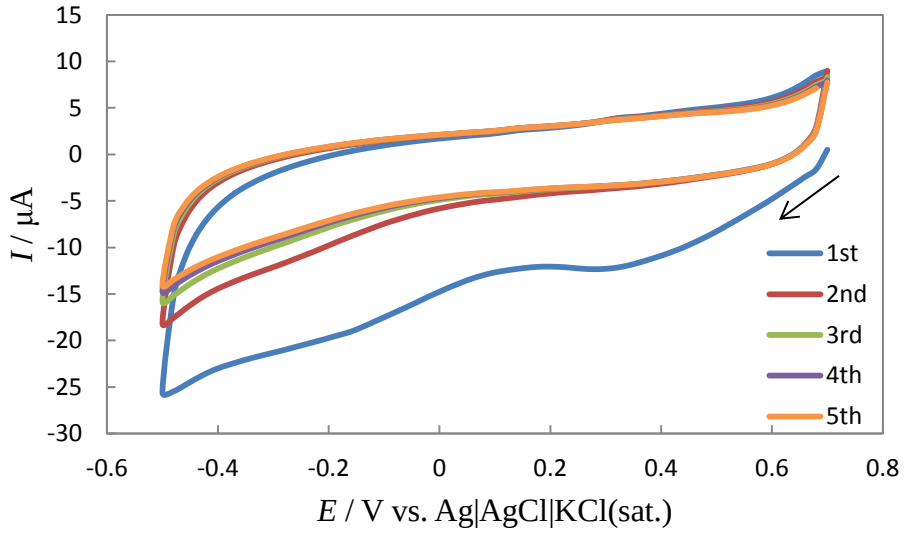

Fig. 5.8. CVs of diazonium cations reduction on GC in Ar sat. 0.5 M HCl solution containing 1 mM *p*-aminobenzoic acid and 2 mM $NaNO_2$ at 50 mVs^{-1}.

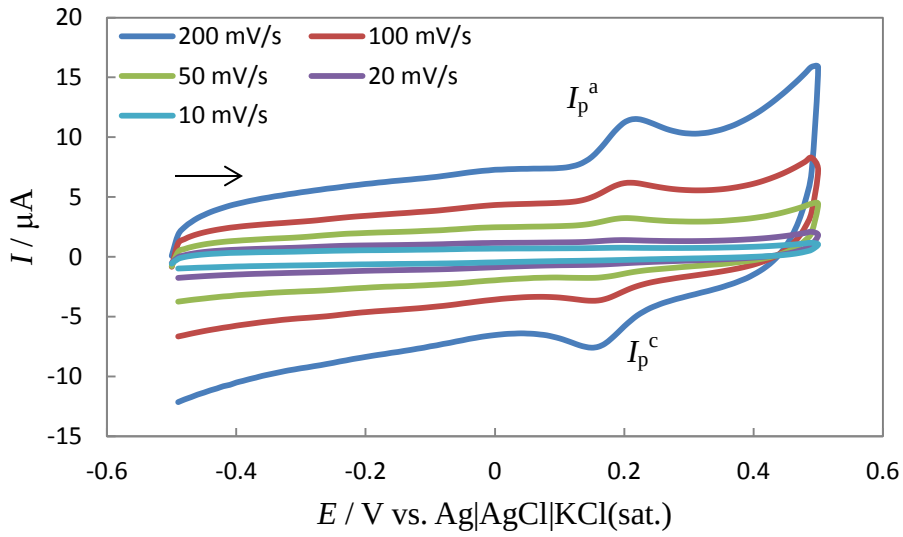

Fig. 5.9. CVs of DA/PABA modified GC in Ar sat. 0.1M HEPES buffer solution (pH 7.5) at various scan rates.

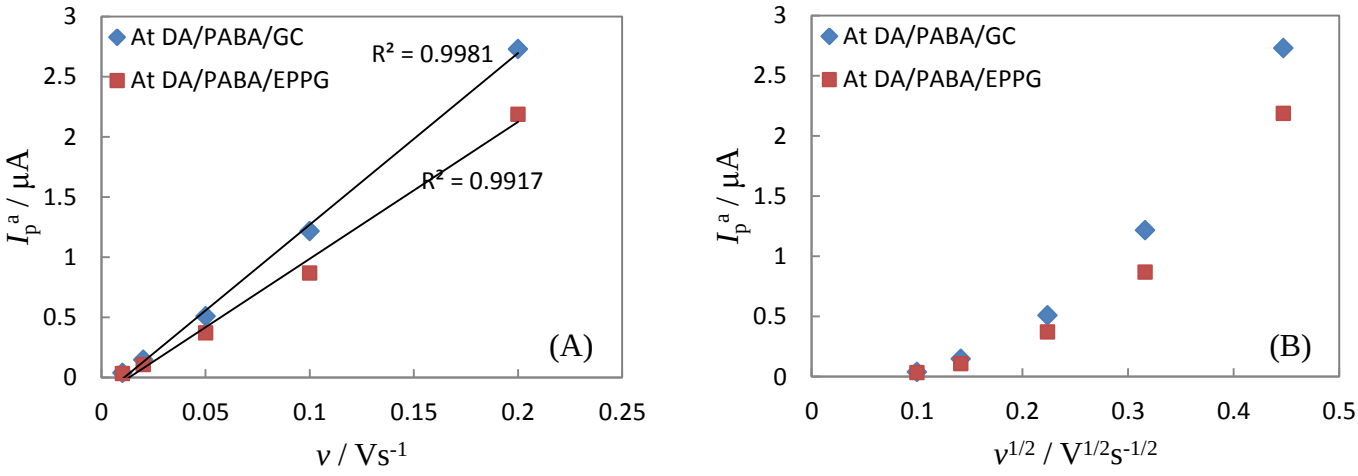

Fig. 5.10. Plots of (A) I_p^a vs. v and (B) I_p^a vs. $v^{1/2}$. Data were taken from Fig. 5.3 and 5.9.

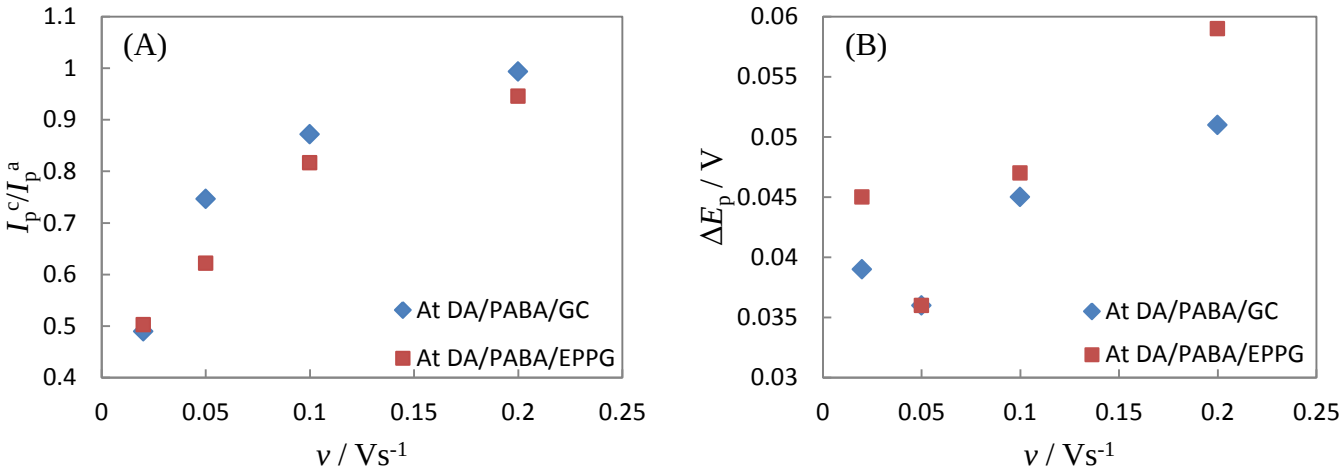

Fig. 5.11. Plots of (A) I_p^c / I_p^a vs. v and (B) ΔE_p vs. v. Data were taken from Fig. 5.3 and 5.9.

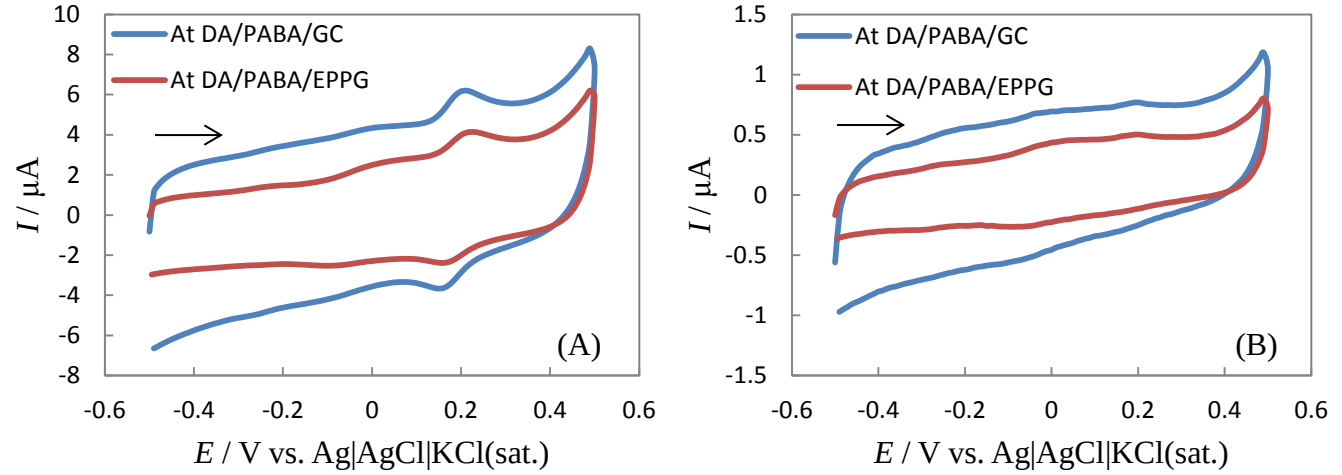

Fig. 5.12. CVs of DA/PABA modified electrodes in Ar sat. 0.1M HEPES buffer solution (pH 7.5) at (A) 100 mVs^{-1} and (B) 5 mVs^{-1}. Data were taken from Fig. 5.3 and 5.9.

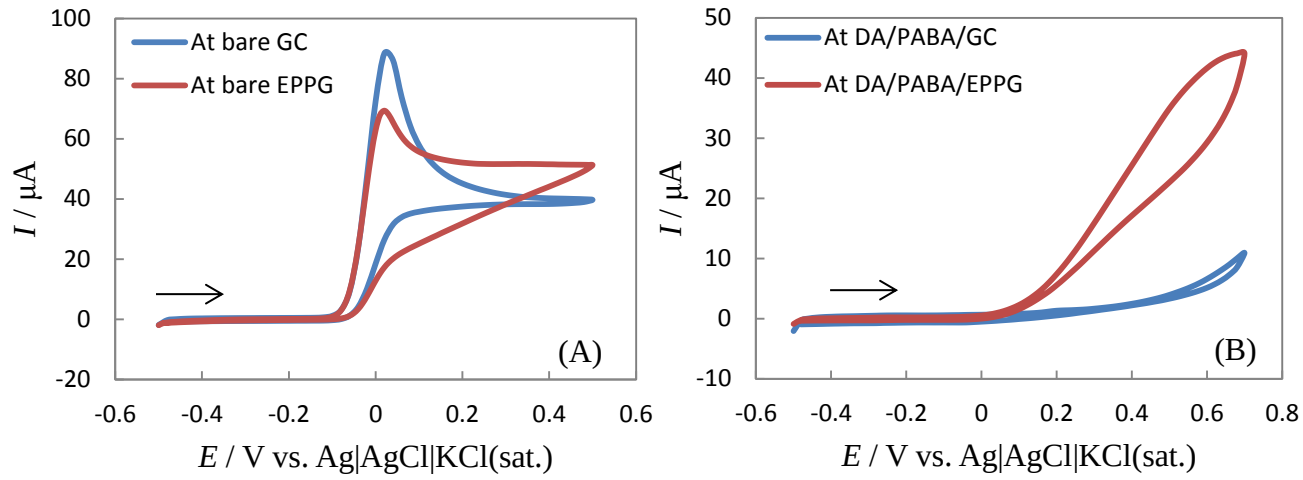

Fig. 5.13. CVs of (A) bare and (B) modified electrodes in Ar sat. 0.1M HEPES buffer solution (pH 7.5) containing 10 mM ascorbic acid at 5 mVs^{-1}.

Table 5.1. Comparison of electrochemical parameters in CVs obtained for the DA and 5-MDA redox reaction on EPPG.

Electrochemical parameters	**DA**		**5-MDA**	
	Adsorbed [a)]	**Covalently bound** [b)]	**Adsorbed** [c)]	**Covalently bound** [d)]
I_p^c **(µA)**	1.7	0.71	3.36	1.46
I_p^a **(µA)**	2.6	0.87	3.03	1.64
I_p^c/I_p^a	0.65	0.82	1.11	0.89
E_p^c **(V)**	0.15	0.17	0.11	0.12
E_p^a **(V)**	0.17	0.21	0.15	0.19
ΔE_p **(V)**	0.02	0.05	0.03	0.06
$E°'$ **(V)**	0.16	0.19	0.13	0.15

a) and c): CVs not shown in this chapter.
b) and d): Data were taken from Fig. 5.3 and 5.4 respectively.

CHAPTER 6

DOPAMINE (DA) AND PYRROLOQUINOLINE QUINONE (PQQ) COVALENTLY BOUND ON *p*-PHENYLENEDIAMINE (PDA) MODIFIED ELECTRODE

6.1 Introduction

PQQ is a redox cofactor and has a promising application in biosensor development. This is due to the PQQ enzymes ability to catalyze electron transfer from substrate to the electron acceptor. In addition, PQQ-dependent enzymes could transfer electrons directly to solid surfaces or to conducting polymers [1]. Many researches on application of PQQ modified electrode have been done [2-4]. However, these researches employed the PQQ adsorbed on specialized electrode, PQQ entrapped in the polypyrrole or electrostatic binding of PQQ methods, and PQQ was not covalently bound to the electrode.

Research on PQQ covalently bound to electrode surface has been done and extensive electrochemistry study of the modified electrode has been investigated [5-7]. In their researches, only PQQ molecule was employed in the fabrication of modified electrode. Hence, in this study a PQQ and DA bound covalently on the electrode surface will be done. A double redox active molecules covalently bound on chemically modified electrode will be employed rather than single redox active molecule.

The same technique (as in previous Chapter 5) of diazonium reduction and amide bond coupling will be employed in this chapter too. However, in this chapter, the electrode modification will be 3 steps: (1) *p*-phenylenediamine (PDA) diazonium reduced and bound to

electrode surface; (2) carboxyl group of PQQ form amide bond coupling with amino group of PDA; (3) amino group of DA form amide bond with another carboxyl group of PQQ. Since this modified electrode bears two redoxes active compounds, it will be interesting to study its electrochemical behaviour in various pH solutions, at various potential scan rates and also continuous potential cycles. The modified electrode will be used for ascorbic acid (AA) and uric acid (UA) determination to investigate possible application in analytical sensor. Finally, the stability or the reproducibility of the electrochemical behavior of the modified electrode will be determined.

6.2 Materials and methods

6.2.1 DA and PQQ covalently bound to PDA modified electrode

Two hundred microliter aliquots (200 µL) of chilled 0.1 M sodium nitrate ($NaNO_2$) aqueous solutionwas slowly dropped into Ar sat. acetonitrile containing 1 mM *p*-phenylenediamine (PDA) (Kanto Chemical Co. Inc., Japan) and 0.5 M perchloric acid ($HClO_4$) (60 %, Wako Pure Chemical Industries Ltd., Japan). The obtainedsolution was left for 5 min, and then used for electrochemical modification of roughened EPPG (Φ = 3 mm; The electrode surface was roughened using emery paper #600 before use) by scanning electrode potential between +0.5 and -0.7 V for 5 cycles at 20 mVs^{-1}. The preparation of PDA-modified EPPG electrodes is presented in Scheme 6.1.

Then, the PDA-modified EPPG was soaked in Ar sat. 0.01 M HEPES buffer solution (pH 7.5) containing coupling reagents (10 mM N-hydroxysulfosuccinimide (Sulfo-NHS) and 10 mM 1-ethyl-3-(3-dimethylaminopropyl)carbodiimide (WSC)) and 1 mM PQQ (Wako Pure Chemical

Industries Ltd., Japan) for 1 hr. The newly modified electrode will have the PQQ bound to the PABA as shown in Scheme 6.2. Furthermore, this PQQ bound PDA-modified electrode was soaked in Ar sat. 0.01M HEPES buffer solution (pH 7.5) containing coupling agents (10 mM N-hydroxysulfosuccinimide (Sulfo-NHS) and 10 mM 1-ethyl-3-(3-dimethylaminopropyl)carbodiimide (WSC)) and 2 mM DA for 1 hr as shown in Scheme 6.3. The final modified electrode is called DA/PQQ/PDA modifed electrode.

6.2.2 Electrochemical measurement of modified EPPG

Cyclic voltammetric measurements of modified electrodes were performed in Ar sat. 0.1M NaCl solution containing 50 mM buffer (pH range: 1 to 7) in the absence and the presence of 1 mM ascorbic acid (AA) and 1 mM uric acid (UA).

6.3 Results and discussions

6.3.1 DA and PQQ covalently bound to PDA modified electrode

PDA was covalently bonded on EPPG electrode as shown in Fig. 6.1. The PDA diazonium reduction current at the 1^{st} scan is bigger compared to that current at the 5^{th} scan. This indicates that the electrode surface is completely covered with the PDA at the 4^{th} to 5^{th} scan. This reduction peak shape cannot be compared to others since there is no research employing the same compound (PDA), electrode (EPPG) and solutions (acetonitrile, $HClO_4$). In previous Chapter 5, we already know that reduction *p*-aminobenzoic acid diazonium on different electrode materials gives different CVs (Figs. 5.1 and 5.8 (page 79 and 82 respectively).

Next, PQQ was bound to the PDA modified electrode as can be seen from Fig. 6.2. The clear redox peaks observed at approximately 0.1 to -0.2 V are the PQQ redox peaks. Then, the DA was bound to the PQQ bound PDA modified electrode (Fig. 6.3). We can observe two redox peaks couple at 0.1 to -0.2 V for PQQ and at 0.4 to 0.1 V for DA (Fig. 6.3(A) and (C)) at pH 6.9. At pH 3.01, the anodic peak of PQQ and DA shifted positively (Fig. 6.3(B) and (D)). The PQQ anodic peak are shifted from -0.02 (at pH 6.9) to 0.2 V while DA anodic peak shifted from 0.25 (at pH 6.9) to 0.44 V. Both redox peaks obtained at low scan rate are clearer (Fig. 6.3(A) and (B)) compared to those at higher scan rate (Fig. 6.3(C) and (D)).

The total surface concentrations (Γ_T) of PQQ and DA at pH 6.9 were estimated to be 0.97 and 0.49 x 10^{-10} mol cm^{-2}. This means that amount of PQQ confined on the electrode surface is twice compared to the amount of DA. This is not the case as expected from Scheme 6.3 where one PQQ molecule bound to at least one DA molecule. When a different experiment was done in a solution where the PQQ bound only to the DA (not confined on any electrode surfaces), it was found that one PQQ molecule bound to one DA molecule only. Thus, the binding orientation of PQQ on the PDA layer is also play an important factor in determining the binding of DA.

It is worth to compare between the DA bound to PABA in previous Chapter 5 (Fig. 5.3, page 80) and the DA bound to PQQ in this chapter. At pH 7.5, both DA have similar redox potentials (0.19 V and 0.2 V respectively) and similar surface concentrations (0.6 mol cm^{-2} and 0.5 mol cm^{-2} respectively). This means that the number of layers bonded on the surface do not affect the redox potential of these DA. The more layers on the electrode surface, the bigger the peak separation values. If we compare between the peak separation values at 20 mVs^{-1}, the less number of layer gave 45 mV (Fig 5.6(B)) while the more number of layers gave 108 mV (Fig. 6.5(B)). Hence, slower electron transfer at multiple layers due to longer time the electron will

take to travel from the bound DA to the electrode. In Ghilane and coworkers research [8], they also found that the length/thickness of the aryl layer used to modify the electrode for DA bonding did not affect the electroactivity of DA. Thus, the theory that electron tunnels through the layers towards the electrode is possible.

6.3.2 Effect of continuous potential scan and potential scan rates to DA and PQQ bound to PDA modified electrode

Continous potential scan did not give any big effect to the CVs of the modified electrode (Fig. 6.4). We can conclude that PDA is attached stably on the electrode surface and the amide bonds connecting DA to PQQ and PQQ to PDA do not break. We also have confirmed that the amide bond will only break if the modified electrode was dipped (for 1 min) in highly alkaline pH solution (pH >10) (data not shown). From Fig. 6.4, after 10 potential scans, only negligible peak currents for reduction can be observed.

The plot of I_p^a against scan rate (Fig. 6.5(A)) shows a linear relationship confirming that both PQQ and DA are covalently attached to the PDA layer. The I_p^a values of PQQ and DA were estimated with the same baseline (Fig. 6.3(A)) since the DA baseline is difficult to determine. Due to this factor, the difference between I_p^a values of PQQ and DA cannot be discuss accurately. Values of ΔE_p increased as potential scan rate increased (Fig. 6.5(B)). However, the peak separation of PQQ and DA at pH 6.9 is bigger compared to the peak separation at pH 3.01. This means that at acidic pH, electron transfer is faster than in neutral solution. This will be discussed in detail in the next section.

6.3.3 pH effect on DA and PQQ bound to PDA modified electrode

The effect of pH on the electrochemical behavior of the modified electrode was done. (Fig. 6.6). The plots of $E^{\circ\prime}$ values against pH show linear relationship with the slopes near 60 mV/pH indicating that both redox reactions of PQQ and DA involve 2e and $2H^+$ process (Fig. 6.7(A)). As pH increased, the values of ΔE_p of DA and PQQ increased (Fig. 6.7(B)). We can compare the trend of ΔE_p values of DA bound to PQQ to that of dissolved DA shown in Chapter 2 (Fig. 2.1). The electrochemical reaction difference between dissolved and bound DA at various pH will be compared.

From Chapter 2 (Fig. 2.1), the value of ΔE_p of dissolved DA decreased as pH increased is known. However, in this Chapter 6, the value of ΔE_p of bound DA increased as pH increased. Besides that, the anodic peak currents (I_p^a) of both PQQ and DA decreased as the pH increased (Fig. 6.7(C)). The baseline used to estimate the I_p^a values can be refer to Fig. 6.3(A). The decreasing trend of I_p^a of PQQ could be contributed by the decreasing trend of the surface concentration of PQQ, however since the baselines for PQQ anodic current (I_p^a) and surface concentration (Γ) are different (Fig. 6.3(A) and (B)), the relationship between the two properties is a difficult discussion. However, the interesting point is that I_p^a and Γ values of PQQ varies according to pH of the solutions (Fig. 6.7(C) and (D)).

The carboxylic acid group's pKa of PQQ varies from 1.6 to 4.5: pKa values are specifically different according to the COOH location in PQQ. However, at pH below pH 4.5, all of the COOH groups will be protonated. Hence, the larger values of I_p^a and Γ could be contributed by the protonated COOH groups in acidic pH. We also did an experiment where the PQQ is bound to DA through amide bond but they are not bound to any surfaces, and they are

dissolved in the solution. Similar results were obtained where larger I_p^a values of PQQ were observed at acidic pH compared to those at alkaline pH (data not shown). Since the DA baseline is difficult to estimate, the DA relation between anodic current and surface concentration will not be discuss.

6.3.4 Oxidation of ascorbic acid (AA) and uric acid (UA) on DA and PQQ bound to PDA modified EPPG

Oxidation of AA and UA on the modified electrode is shown in Fig. 6.8. Only small oxidation current can be observed. This means that the multilayers of the grafted compounds blocked the AA and UA from reacting directly on the electrode surface. In the presence of AA, high oxidation current can be observed. On the other hand, in the presence of UA, no oxidation current of UA can be seen. This means that the modified electrode catalyzed the AA oxidation reaction but not the UA oxidation reaction. Other explanation could be that the modified layer blocked UA from reacting with DA or PQQ. Hence, in the absence and the presence of UA, the CVs are similar.

The blocking effect of the modified layer can be originated from physical barrier of the grafted layer, electrostatic repulsion, hydrophobic nature or electron transfer limitation [9]. Due to the unknown real structure of the grafted layer and the various possible reasons, it is difficult to mention exactly why UA oxidation did not occur. When the two compounds (AA and UA) were mixed, higher oxidation current was obtained in comparison with that in the oxidation of AA alone

6.3.5 Reproducibility of the electrochemical behavior of DA and PQQ bound to PDA modified electrode

The freshly modified electrode was stored in the refrigerator (below 10 °C, Milli-Q water) for 5 days. The electrochemical behaviour of the stored modified electrode at pH 7.1 and 3.0 is shown in Fig. 6.9(A) and (B). The PQQ and DA redox peaks clearly decreased after 5 days. The bound compounds; PQQ and DA may be degenerated after storage. This means that the reproducibility of the modified electrode is low. At pH 3.01, the redox currents are higher compared to those at pH 7.1. This result is similar to that results obtained from freshly modified electrode. This indicates that the electrochemical behavior of the DA and PQQ bound to the PDA modified electrode are unchanged.

The PDA layer can be considered to be stable on the electrode surface because the bond between the diazonium-derived layer and the electrode surface is stable for months. Besides that, diazonium-derived layer has been known to withstand high temperature (at least 200 °C depending on the diazonium compounds) [10]. The amide bond between PQQ and DA is also stable because in a separate experiment, PQQ was still bound to DA even after 7 days of storage (in this experiment, PQQ was bound only with DA and they did not attach to any surface).

6.4 Conclusion

Two redox active compounds (PQQ and DA) were covalently bound to the PDA modified electrode through amide bond coupling between amino group of DA and carboxyl group of PQQ and another carboxyl group of PQQ and amino group of PDA. The modified electrode shows different behavior at different pH where anodic peak current of PQQ is highest

at pH 1.04 and peak separation value of PQQ is lowest meaning fastest electron transfer. However, at pH 6.9, the anodic peak current of PQQ is lowest and the peak separation value of PQQ is highest meaning slowest electron transfer. These trends are the opposite from the trend of free DA. The modified electrode blocked most of AA and all of UA from reacting on the electrode due to the multilayers of the grafted compound on electrode surface. Finally, reproducibility of the electrochemical behavior of modified electrode after storage.

6.5 References

[1] V. Laurinavicius, J. Razumiene, B. Kurtinaitiene, I. Lapenaite, I. Bachmatova, L. Marcinkeviciene, R. Meskys and A. Ramanavicius, *Bioelectrochemistry* **55** (2002) 29-32.

[2] V. Flexer, F. Durand, S. Tsujimura and N. Mano, *Anal. Chem*. **83** (2011) 5721-5727.

[3] Y. Kim, S.J. Park, D. Lee and H. Kim, *J. Appl. Electrochem*. **42** (2012) 383-390.

[4] J.A. Young, X. Jiang and J.R. Kirchoff, *Electroanal*. **25** (7) (2013) 1589-1593.

[5] E. Katz, D.D. Schlereth and H. Schmidt, *J. Electroanal. Chem*. **367** (1994) 59-70.

[6] E. Katz, T. Lotzbeyer, D.D. Schlereth, W. Shuhmann and H. Schmidt, *J. Electroanal. Chem*. **373** (1994) 189-200.

[7] E. Katz, M. Lion-Dagan and I. Willner, *J. Electroanal. Chem*. **408** (1996) 107-112.

[8] J. Ghilane, F. Hauquier and J. Lacroix, *Anal. Chem*. **85** (2013) 11593-11601.

[9] S. Baranton and D. Belanger, *J. Phys. Chem. B.* **109** (2005) 24401-24410.

[10] A.J. Bard and C.G. Zoski, *Electroanalytical Chemistry* **26** (2016) 132-133.

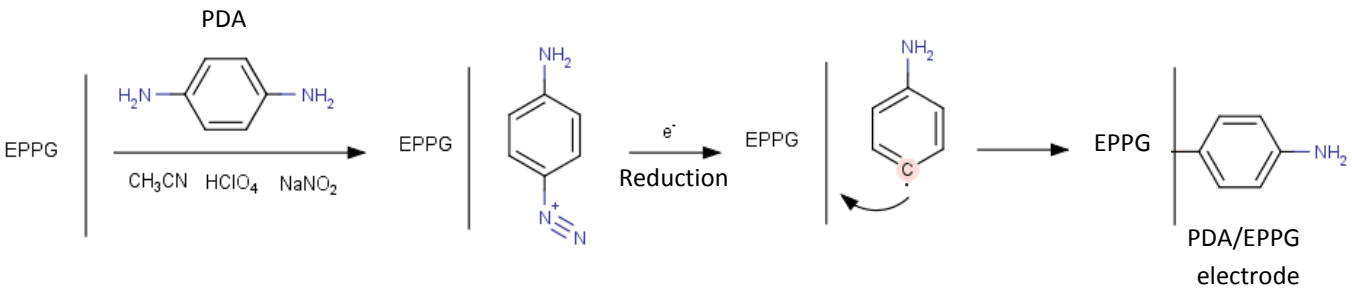

Scheme 6.1: Grafting amine functional groups on the EPPG electrode surface.

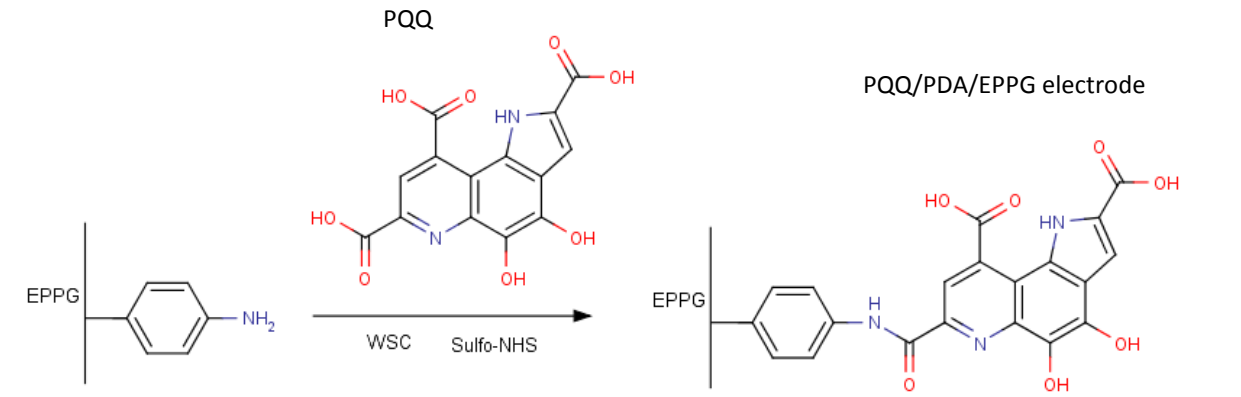

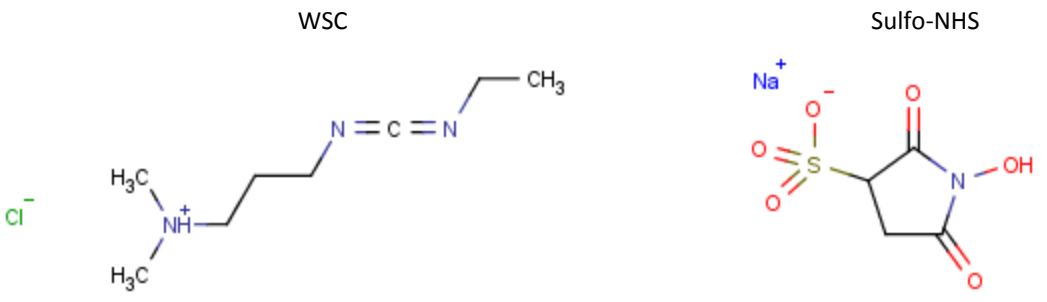

Scheme 6.2: Attachment of PQQ to the amine functional group of PDA/EPPG electrode.

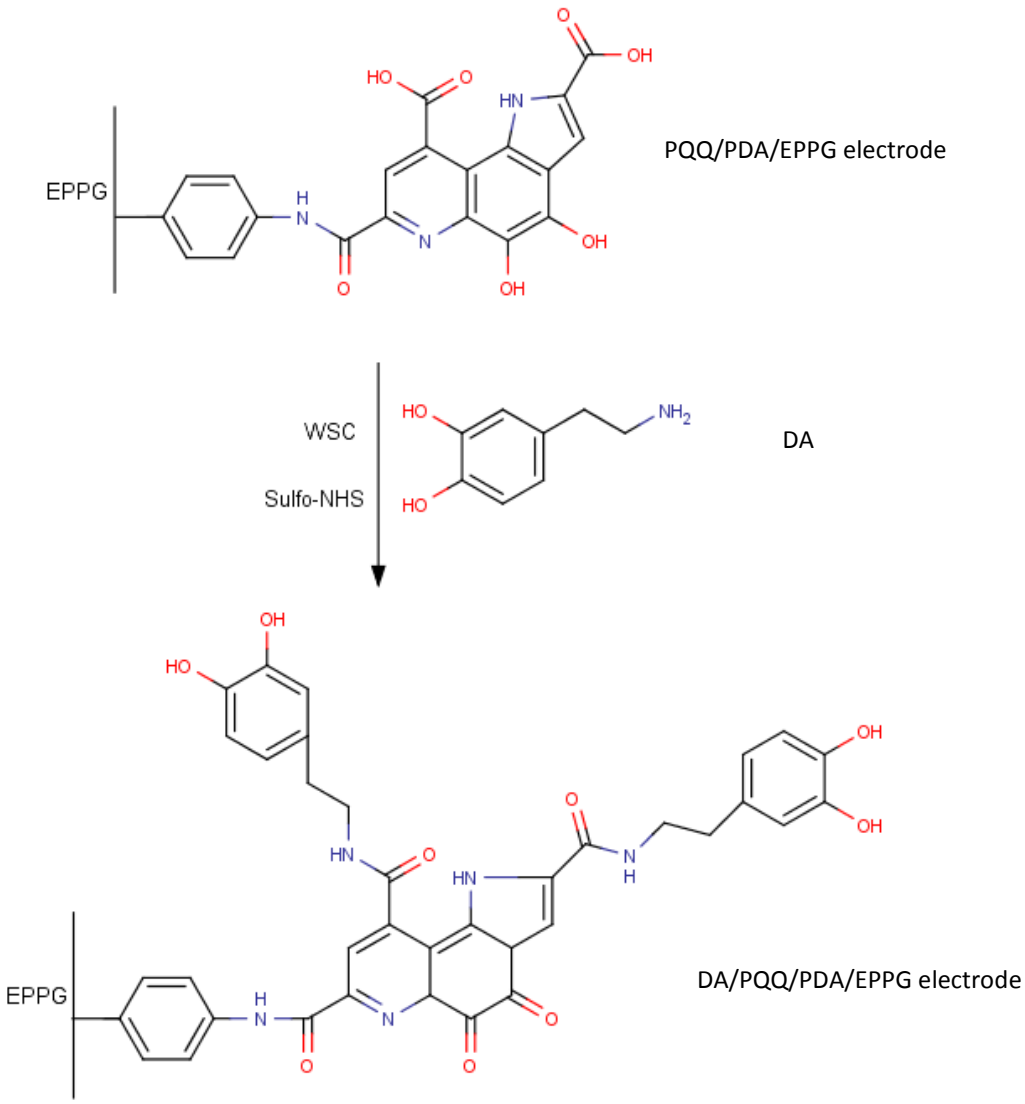

Scheme 6.3: Attachment of DA to the PQQ.

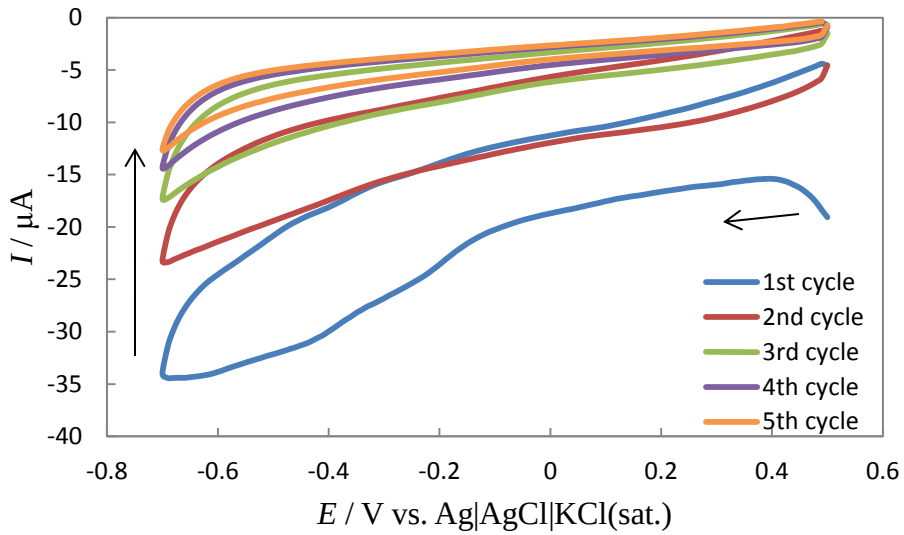

Fig. 6.1. Cyclic voltammograms (CVs) obtained at EPPG electrode in Ar saturated acetonitrile containing 0.5 M $HClO_4$, 2 mM $NaNO_2$ and 1 mM *p*-phenylenediamine.
Potential scan rate: 20 mVs^{-1}.

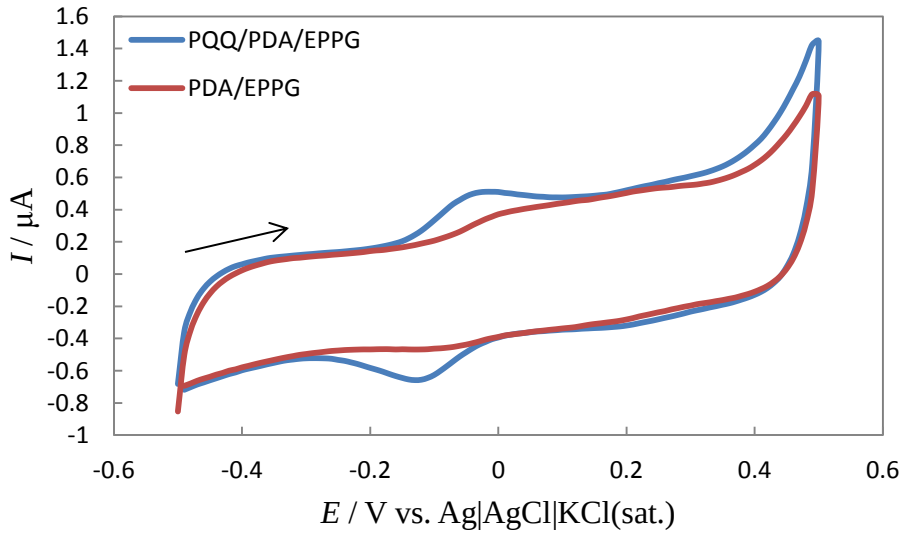

Fig. 6.2. CVs obtained at PQQ / PDA / EPPG and PDA/EPPG electrodes in Ar saturated 0.1 M NaCl solution containing 50 mM universal buffer (pH 6.9).
Potential scan rate: 10 mVs^{-1}.

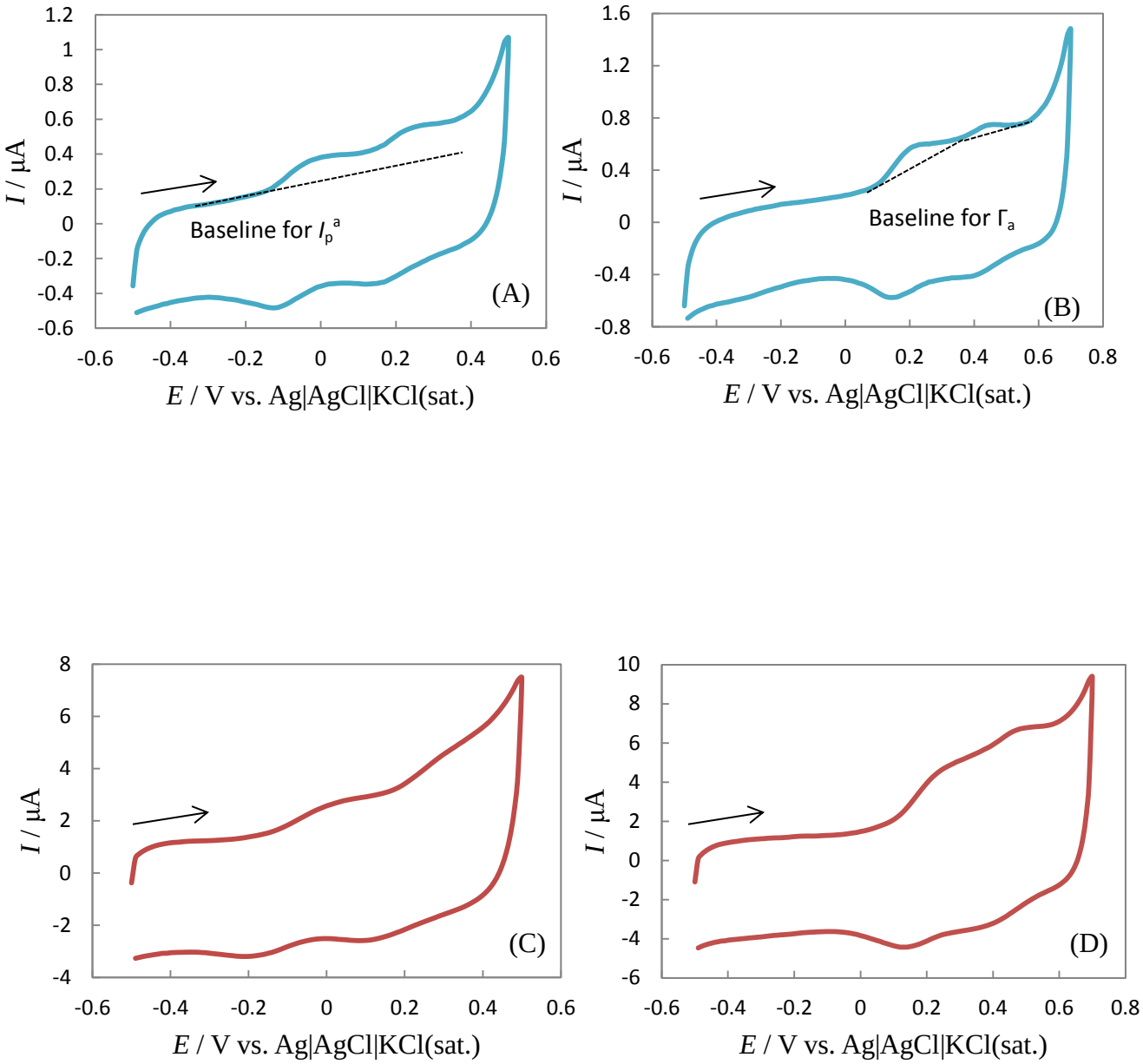

Fig. 6.3. CVs obtained at DA / PQQ / PDA / EPPG electrode in Ar saturated 0.1 M NaCl solution containing 50 mM universal buffers ((A and C) pH 6.9; (B and D) 3.01). Potential scan rate: (A and B) 10 mVs^{-1}; (C and D) 100 mVs^{-1}.

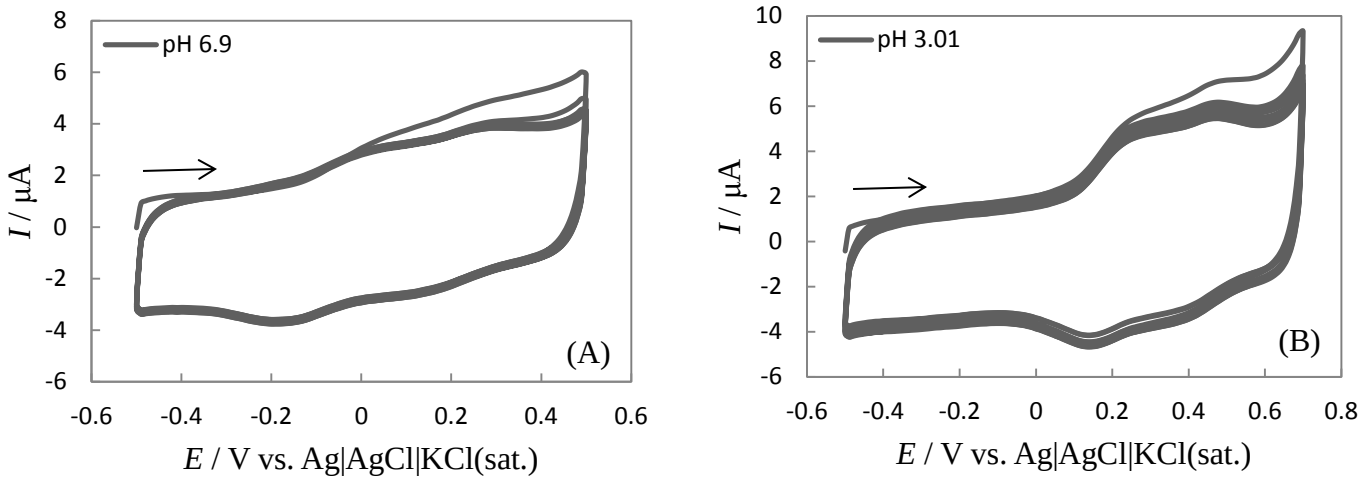

Fig. 6.4. Continuous CVs (10 cycles) obtained at DA / PQQ / PDA / EPPG electrodes in Ar saturated 0.1 M NaCl solution containing 50 mM universal buffers ((A) pH 6.9 and (B) 3.01). Potential scan rate: 100 mVs^{-1}.

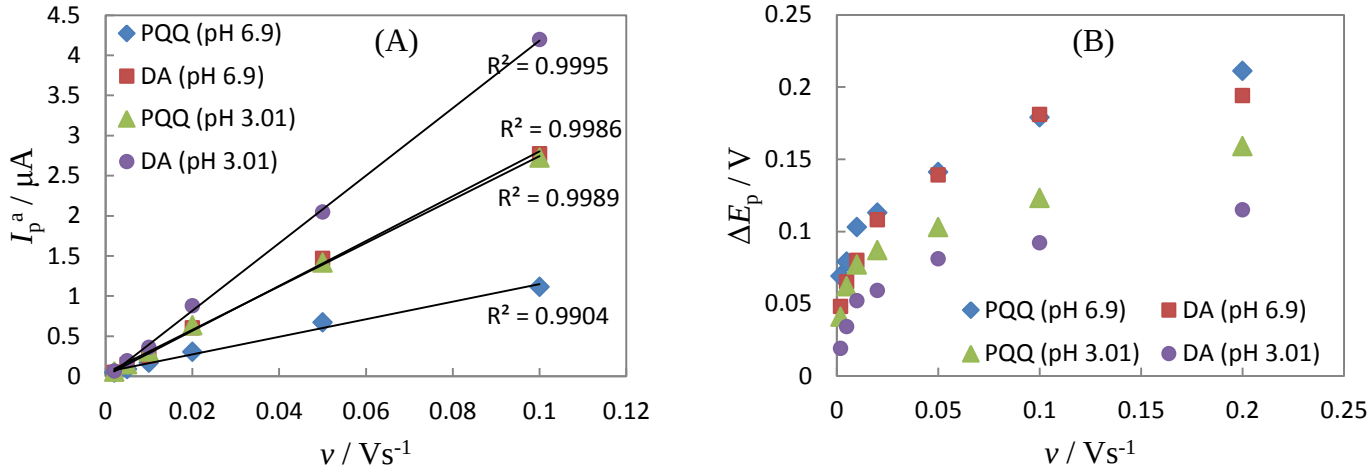

Fig. 6.5. Plots of (A) I_p^a vs. v and (B) ΔE_p vs. v. Data were taken from CVs obtained at DA / PQQ / PDA / EPPG electrodes.

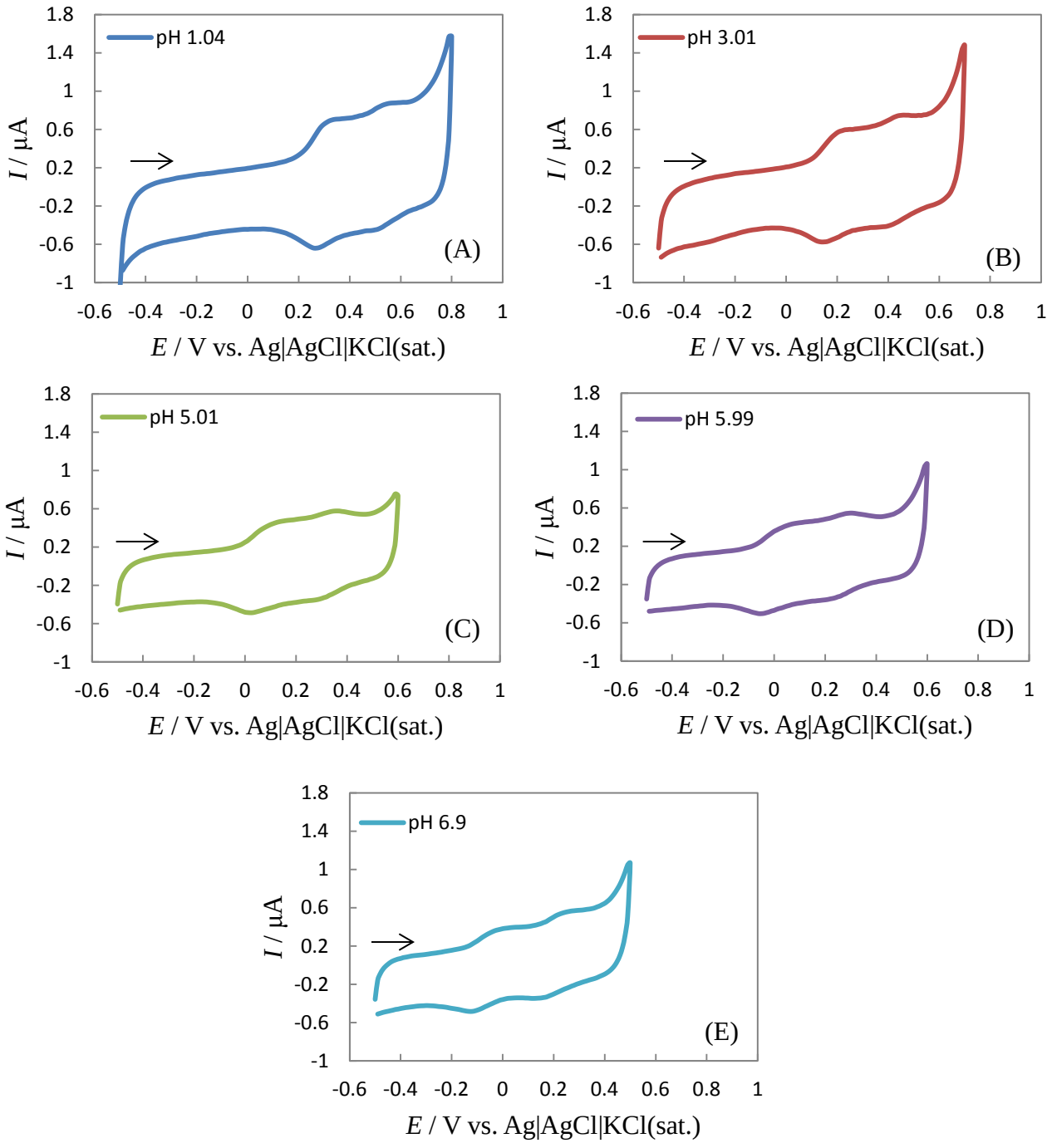

Fig. 6.6. CVs obtained at DA / PQQ / PDA / EPPG electrode in Ar saturated 0.1 M NaCl solution containing 50 mM universal buffers. ((A) pH 1.04; (B) pH 3.01; (C) pH 5.01; (D) pH 5.99; (E) pH 6.9.
Potential scan rate: 10 mVs^{-1}.

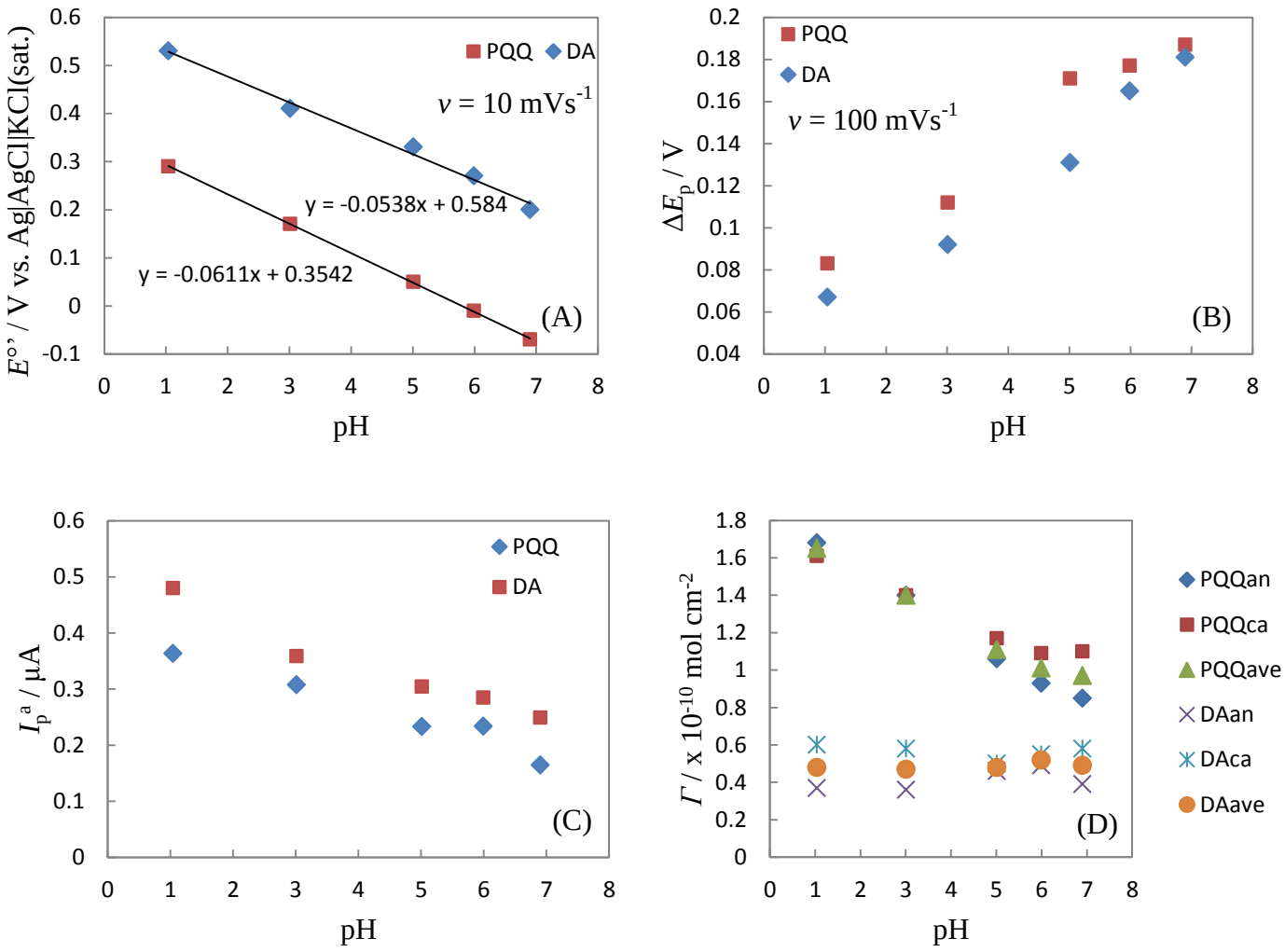

Fig. 6.7. Plots of (A) $E°'$ vs. pH, (B) ΔE_p vs. pH, (C) I_p^a vs. pH and (D) Γ vs pH. Data were taken from CVs shown in Fig. 6.6.

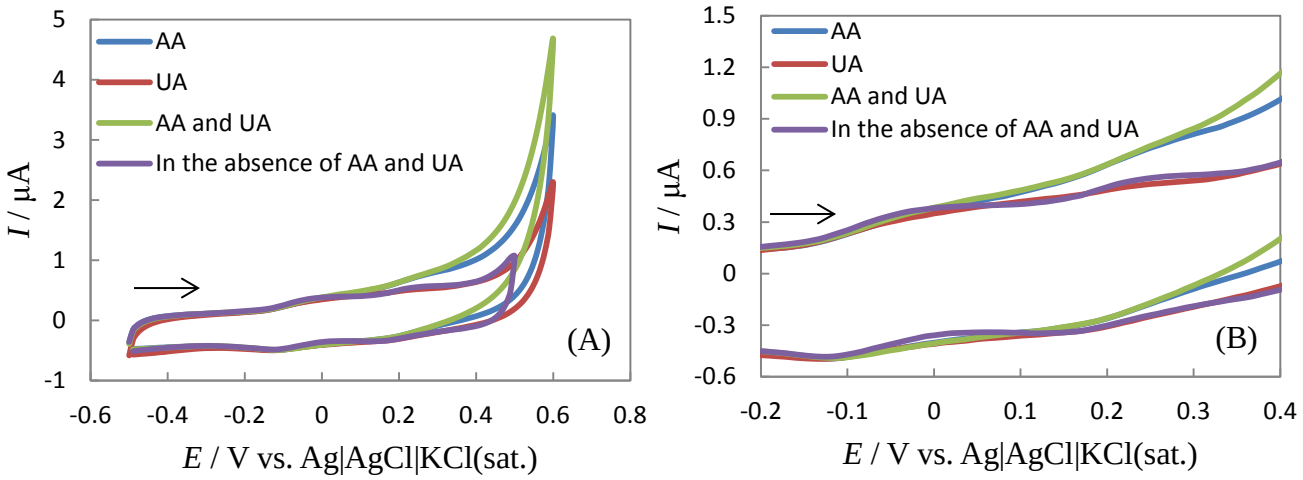

Fig. 6.8. (A) CVs obtained at DA / PQQ / PDA / EPPG electrode in Ar saturated saturated 0.1 M NaCl solution containing 50 mM universal buffers (pH 6.9) containing 1 mM AA only, 1 mM UA only, and 1 mM AA and 1 mM UA. (B) The voltammograms obtained in the narrow potential range -0.2 to 0.4 V, which were taken from Fig. 6.8(A).
Potential scan rate: 10 mVs^{-1}.

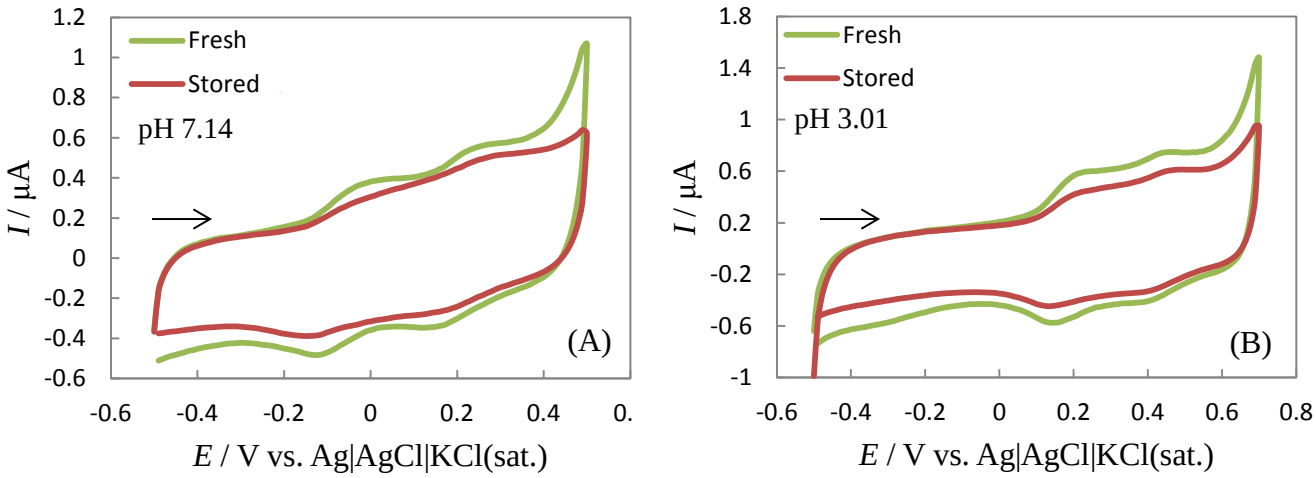

Fig. 6.9. CVs obtained at stored DA / PQQ / PDA / EPPG electrode in Ar saturated 0.1 M NaCl solution containing 50 mM universal buffers ((A) pH 7.14 and (B) pH 3.01).
Potential scan rate: 10 mVs^{-1}.

CHAPTER 7

GENERAL CONCLUSIONS

Electrochemical behaviour of DA depends on solution pH, its concentration, potential scan rate etc. which are closely associated with the intracyclization reaction (ICR) and polymerization. Electrochemical behaviour of DA has been studied experimentally and theoretically and the obtained results were used to support the proposed model of electrooxidation pathway of DA. DA-modified electrodes, in which DA is covalently bound to chemically modified electrodes, was successfully fabricated through simple stepwise technique of diazonium reduction on electrode surface and amide bond coupling.

In Chapter 2, electrochemical reaction of DA was investigated in detail. At acidic pH, ICR did not occur because of the protonated amino group. ICR leads to formation of leucodopaminechrome/dopaminechrome couple, and the redox peak of this couple was easily observed from the first potential cycle in solutions of pH 6 and above. At pH 5, the redox peak of leucodopaminechrome/dopaminechrome couple was observed after long time potential holding at oxidative potential (i.e, 0.8 V) or at low potential scan rates (i.e, 10, 20 mVs^{-1}). These indicate that ICR needs longer time to occur at pH 5. The electrochemical reaction of DA proceeds in an ECC mechanism at pH 9 and below. However, at pH above 10, ICR and the subsequent chemical reactions occur rapidly. Higher concentration of DA (i.e, 1 mM or more) led to faster polymerization reaction resulting in the polymerized DA adsorbed on electrode surface. A CEC mechanism proceeds at pH 10. The calculations of free Gibb's energies, HOMO/LUMO energies and natural charges of DA supported the results obtained from the experiment.

In Chapter 3, it was found that redox reaction of 5-MDA is simpler than that of DA. This is because the methyl group at C5 position of benzene ring prevents the amino group from nucleophilic attack at C5 position. ICR does not occur due to the methyl group. Electrochemistry of 5-MDA is quite similar at pH 9 and below. However, at pH above 10, 5-MDA was largely electroinactivated due to the attack by hydroxide group in the alkaline solution. 5-MDA is more easily oxidized due to the methyl group compared to DA. High concentration of 5-MDA led to faster polymerization of 5-MDA and subsequently they adsorbed on the electrode surface. The methyl group could not prevent the polymerization reaction from occurring. Comparison of HOMO/LUMO energies between DA and 5-MDA provided the explanation on the question of why 5-MDA was more easily oxidized. 5-MDA has higher HOMO energy compared to DA, meaning that 5-MDA more easily donates electron than DA.

In Chapter 4, it was found that the incorporation of DA and 5-MDA on Nafion-modified electrode is better at acidic pH compared to that at neutral pH. This is because the positively charged amino groups of DA and 5-MDA are electrostatically attracted to the negatively charged sulfonate group of Nafion. Comparing between DA and 5-MDA at acidic pH, 5-MDA was more easily incorporated into the Nafion film probably due to the hydrophobic attraction of the methyl group. The concentration of buffer solution affected the incorporation process where the higher the concentration of buffer solution, the slower the incorporation process due to the decreased electrostatic attraction. High concentration of cations in buffer solution led to the decrease in the peak currents of DA and 5-MDA due to the competition between electroactive and electroinactive cations in the buffer solution. At acidic pH, the redox reaction of DA (and 5-MDA) on Nafion-modified electrode is $E^{\circ\prime}$ value shifted

negatively compared to that on bare electrode due to hydrophobic interaction between the oxidized form of DA (and 5-MDA) and the hydrophobic moieties of Nafion. In this case, the ΔE_p value on the modified electrode is larger than that on bare electrode due to the larger IR drop effect. However at pH 7, redox reaction of DA (and 5-MDA) is better (smaller ΔE_p value) on bare electrode compared to reaction on Nafion-modified electrode which is due to Nafion repelled the DA (and 5-MDA).

Covalently bound DA to the *p*-aminobenzoic acid (PABA)-modified electrode was fabricated in two steps technique in Chapter 5. The first step is the reduction of PABA diazonium on the electrode surface. The PABA-modified electrode bears the carboxyl terminal group. In the second step, the carboxyl group was bound to the amino group of DA (and 5-MDA) through amide bond coupling. DA was found to be covalently bound to PABA since no redox peak of the leucodopamichrome/dopaminechrome couple could be observed. This indicated that ICR could not occur due to the amide bond binding between amino group of DA and carboxyl group of PABA. It was found that both DA and 5-MDA were confined on the electrode surface and that the amount of 5-MDA confined on the electrode surface was twice in comparison with that of DA. Hydrophobic attraction between methyl group of 5-MDA and the benzene ring of PABA could be the reason behind the high amount of 5-MDA. The peak current ratios of DA and 5-MDA are close to unity at high potential scan rate (i.e, $v \geq 200$ mVs^{-1}). However at low potential scan rate (i.e, $v \leq 20$ mVs^{-1}), the ratio reduced to nearly half because of the hydroxide group attacked the quinone forms of DA and 5-MDA. Ascorbic acid (AA) cannot be easily oxidized on the modified electrode surface because PABA and DA (and 5-MDA) blocked the AA from oxidizing directly on the electrode surface . Hence, only small peak current can be observed and the oxidation potential was shifted positively.

Two redox molecules were covalently bound to the chemically modified electrode in Chapter 6. The redox molecules were pyrolloquinoline quinone (PQQ) and DA. Similar technique of electrode modification as shown in Chapter 5 was employed with a little modification where (in the new technique) three steps were involved. The first step is reduction of *p*-phenylenediamine (PDA) diazonium on the electrode surface. The PDA-modified electrode bears the amino terminal group. The second step is the amide bonding between the amino group of PDA and carboxyl group of PQQ. The final step is the binding of amino group of DA and another carboxyl group of PQQ. ICR did not occur due to this amide bonding formed in the final step. PQQ and DA molecules were stably confined on the electrode surface. The amount of PQQ confined on the electrode was twice that of DA. This is probably due to the orientation of PQQ on the electrode surface which blocked the DA from binding to the carboxyl group. It was found that DA can electrocatalyze the oxidization the oxidation of AA but PQQ cannot.

List of Publication

1. Studies on the early oxidation process of dopamine by electrochemical measurements and quantum chemical calculations.
   Iryane Ismail, Takeyoshi Okajima, Susumu Kawauchi and Takeo Ohsaka, *Electrochimica Acta* 211 (2016) 777-786.

List of presentations

1. Redox behavior of dopamine and its analogue in aqueous solution
   Iryane Ismail, Takeyoshi Okajima, Susumu Kawauchi and Takeo Ohsaka
   2015 Spring Meeting of the Electrochemical Society of Japan (March 15-17, 2015, Yokohama, Japan)

2. Electrochemistry of dopamine and its derivative in aqueous media
   Iryane Ismail, Takeyoshi Okajima, Susumu Kawauchi and Takeo Ohsaka
   2015 Autumn Meeting of the Electrochemical Society of Japan (September 11-12, 2015, Saitama, Japan)

Acknowledgements

I would like to express my sincerest and deepest heartfelt gratitude to Prof. Takeo Ohsaka for his continuous patience, support, constructive criticism and encouragement during my doctoral study.

I also wish to express my thanks to Dr Takeyoshi Okajima for his helpful assistance, support and advices throughout my research period.

I sincerely thanked Associate Professor Fusao Kitamura for his advises and discussion during the weekly seminar in the group.

I am much indebted to Associate Profesor Susumu Kawauchi for his contribution in the quantum chemical calculations in this work.

Special thanks to my lab members for always helping, supporting and encouraging me throughout my studies.

I greatly appreciate the MEXT scholarship provided by the Japanese Ministry of Education, Culture, Sports, Science and Technology.

Not forgotten, I wish to honor my parents, siblings and friends for their endless support, patience, love and encouragement during this 3 years.

Acknowledgements

I would like to express my sincerest and deepest heartfelt gratitude to Professor Takeo Ohsaka for his continuous patience, support, constructive criticism and encouragement during my doctoral study.

I also wish to express my thanks to Dr. Takeyoshi Okajima for his helpful assistance, support and advices throughout my research period.

I sincerely thanked Associate Professor Fusao Kitamura for his advises and discussion during the weekly seminar in the group.

I am much indebted to Associate Professor Susumu Kawauchi for his contribution in the quantum chemical calculations in this work.

Special thanks to my lab members for always helping, supporting and encouraging me throughout my studies.

I greatly appreciate the MEXT scholarship provided by the Japanese Ministry of Education, Culture, Sports, Science and Technology.

Not forgotten, I wish to honor my parents, siblings and friends for their endless support, patience, love and encouragement during my stay in Japan.